

1-1-2008

# The effects of steel reinforcement corrosion on the flexural capacity and stiffness of reinforced concrete beams

Timothy A. Joyce  
*Ryerson University*

Follow this and additional works at: <http://digitalcommons.ryerson.ca/dissertations>



Part of the [Civil Engineering Commons](#)

---

## Recommended Citation

Joyce, Timothy A., "The effects of steel reinforcement corrosion on the flexural capacity and stiffness of reinforced concrete beams" (2008). *Theses and dissertations*. Paper 296.

TA  
445.5  
.J69  
2008

# **THE EFFECTS OF STEEL REINFORCEMENT CORROSION ON THE FLEXURAL CAPACITY AND STIFFNESS OF REINFORCED CONCRETE BEAMS**

by

Timothy A. Joyce  
Bachelor of Engineering in Civil Engineering  
McGill University, Montreal, Canada  
2002

A thesis presented to Ryerson University  
in partial fulfillment of the requirements  
for the degree of Master of Applied Science  
in the program of Civil Engineering

Toronto, Ontario, Canada, 2008  
©Timothy A. Joyce 2008

PROPERTY OF  
RYERSON UNIVERSITY LIBRARY



I hereby declare that I am the sole author of this thesis.

I authorize Ryerson University to lend this thesis to other institutions or individuals for the purpose of scholarly research.

I further authorize Ryerson University to reproduce this thesis by photocopying or by other means, in total or in part, at the request of other institutions or individuals for the purpose of scholarly research.



# ABSTRACT

Thesis Title: The Effects of Steel Reinforcement Corrosion on the Flexural Capacity and Stiffness of Reinforced Concrete Beams

Degree: Master of Applied Science

Year of Convocation: 2008

Name: Timothy A. Joyce

Program: Civil Engineering

University: Ryerson University

This study is an attempt to derive a relationship between steel reinforcement corrosion and the coinciding loss of flexural strength. The corrosion of the steel was isolated in the flexural region in order to eliminate contributions from stirrup corrosion and loss of bond within the development length. It was determined that the flexural capacity of reinforced concrete beams decreased as the rate of corrosion increased. In addition to the study of flexural capacity, the prediction of the flexural behaviour of corroded beams was studied through stiffness effects of reinforcement corrosion. The stiffness study indicated a sharp drop in stiffness at relatively low degrees of corrosion, followed by a slower decline at increasing levels of corrosion. Mass loss, crack width and chloride ion content were examined as indicators of degree of corrosion. These relationships are an essential step in developing an effective model for the performance of corroded reinforced concrete beams in the future.



# ACKNOWLEDGEMENTS

The successful completion of this project would not have been possible without the love and support I have received from my wife, Alexandra, throughout the entire process. Thankyou to my loving parents, Anne and Andy, for their unending support of all kinds and to my sisters, Steph and Mem, for always believing in me. Special thanks to my advisor, Dr. Lamy Amleh, for her many hours of consultation and invaluable guidance. All the Ryerson professors deserve credit for making my time at Ryerson enjoyable and educational. Another thankyou to the Ryerson lab staff, Nidal and Mohamed, for all the extra hours they worked on my behalf. There are too many people to thank in this small space but I will always be appreciative of all the help and inspiration I received from everyone.



# TABLE OF CONTENTS

<b>AUTHOR'S DECLARATION</b>	iii
<b>ABSTRACT</b>	v
<b>ACKNOWLEDGEMENTS</b>	vii
<b>LIST OF TABLES</b>	xiii
<b>LIST OF FIGURES</b>	xv
<b>1 INTRODUCTION</b>	1
1.1 Background Information	1
1.2 Research Significance	4
1.3 Scope of Investigation	4
1.4 Outline of Thesis	5
<b>2 LITERATURE REVIEW</b>	7
2.1 Introduction	7
2.2 Mechanism of Corrosion of Steel Reinforcement in Concrete	9
2.2.1 Carbonation of Concrete	12
2.2.2 Chloride Attack	13
2.3 Effect of Reinforcement Corrosion on Material Properties	16
2.3.1 Overview of the Effects of Reinforcement Corrosion	16
2.3.2 Changes in Flexural Behaviour due to Corrosion	18
2.3.3 Changes in Bond due to Corrosion	19
2.3.4 Changes in Failure Mode due to Corrosion	21
2.4 Modelling of Corroded Concrete Elements	22
2.4.1 Introduction to Modelling Corroded Concrete	22
2.4.2 Li Model	24
2.4.3 Oh Model	25
2.4.4 Val Model	26
2.4.5 Coronelli Model	28
2.4.6 Rodriguez Model	29
2.4.7 Amleh and Ghosh Model	30
2.4.8 Previous Research at Ryerson University	31
2.4.9 Summary	31

2.5 Protection and Prevention against Reinforcement Corrosion	32
2.5.1 New Design Philosophy	32
2.5.2 High Performance Concrete	34
<b>3 EXPERIMENTAL PROCEDURE</b>	<b>37</b>
3.1 Phase One: Preparation of Beam Specimens	37
3.1.1 Reinforcing Steel: Material Properties	37
3.1.2 Concrete Mix & Beam Dimensions: Material Properties	39
3.1.3 Mixing Pouring and Curing Procedure	40
3.2 Phase Two: Accelerated Corrosion Process	42
3.2.1 Experimental Setup for Corrosion Process	42
3.2.2 Monitoring Accelerated Corrosion Process	44
3.2.3 Development of Corrosion Levels	46
3.3 Phase Three: Beam Mechanical Testing	48
3.4 Phase Four: Data Collection	50
3.4.1 Mass Loss	50
3.4.2 Chloride Ion Content	51
<b>4 RESULTS AND DISCUSSION</b>	<b>55</b>
4.1 Introduction	55
4.2 Preparation	57
4.2.1 Cylinder Compressive Strength	57
4.2.2 Accelerated Corrosion Monitoring Process	59
4.2.3 Crack Propagation and Corrosion Patterns	64
4.2.3.1 Lowest Level Corrosion Group	69
4.2.3.2 Mid-Level Corrosion Group	70
4.2.3.3 Highest Level Corrosion Group	71
4.3 Mechanical Testing	72
4.3.1 Effect of Corrosion on Load-Deflection Behaviour	73
4.3.1.1 Control Specimens Group	73
4.3.1.2 Corroded Specimens Group	74
4.3.1.2.1 Lowest Level Corrosion Group	75
4.3.1.2.2 Mid-Level Corrosion Group	78
4.3.1.2.3 Highest Level Corrosion Group	81
4.4 Collection and Interpretation of Data	84
4.4.1 Mass Loss	85
4.4.1.1 Ultimate Load versus Mass Loss: Figures & Discussion	88
4.4.1.2 Stiffness versus Mass Loss: Figures & Discussion	93
4.4.2 Chloride Ion Content (C. I. C.)	98
4.4.2.1 Ultimate Load versus C. I. C.: Figures & Discussion	101
4.4.2.2 Stiffness versus C. I. C.: Figures & Discussion	102

4.4.3 Crack Width	104
4.4.3.1 Ultimate Load versus Crack Width: Figures & Discussion	104
4.4.3.2 Stiffness versus Crack Width: Figures & Discussion	106
4.4.5 Parameter Comparison for Corroded Beam Performance	107
4.4.6 Discussion Summary	110
<b>5 CONCLUSIONS</b>	<b>113</b>
5.1 Summary and Conclusions	113
5.2 Suggestions for Future Research	116
<b>REFERENCES</b>	<b>119</b>



# LIST OF TABLES

Table 4.1: Visual descriptions of corroded beam specimens	69
Table 4.2: Ultimate Loads and Corresponding Midspan Deflections	73
Table 4.3: Mass Loss for Corroded Bars	86
Table 4.4: Visual Descriptions of Corroded Reinforcing Bars	87
Table 4.5: Relative Strength and Mass Loss for Each Beam	88
Table 4.6: Chloride Ion Content Results	100



# LIST OF FIGURES

Figure 2.1: The Tuutti model (Tuutti, 1982)	23
Figure 3.1: Reinforcing steel layout	39
Figure 3.2 Accelerated corrosion setup	43
Figure 3.3: Four-point loading setup	49
Figure 4.1: Cylinder compressive strength for each beam specimen	59
Figure 4.2: Summary of average current for each beam	60
Figure 4.3: Current summary for lowest level corrosion group	61
Figure 4.4: Current summary for mid-level corrosion group	62
Figure 4.5: Current summary for highest level corrosion group	63
Figure 4.6: Crack propagation for lowest level corrosion group	66
Figure 4.7: Crack propagation for mid-level corrosion group	67
Figure 4.8: Crack propagation for highest level corrosion group	68
Figure 4.9: Cracking on only Side B of Beam 11M	65
Figure 4.10: Bearing failure of Beam 7	72
Figure 4.11: Load deflection behaviour of control specimens	74
Figure 4.12: Load deflection behaviour for all beam specimens	75
Figure 4.13: Shear cracking on Beam 8L	77
Figure 4.14: Failure on bottom face of Beam 8L	77
Figure 4.15: Failure through corrosion cracks of Beam 11M	79
Figure 4.16: Failure cracking on bottom face of Beam 3M	81
Figure 4.17: Concrete spalling following testing of Beam 4H	82
Figure 4.18: Propagation of failure cracks of Beam 5H	83
Figure 4.19: Corrosion at midspan of Bar 5B	86
Figure 4.20: Ultimate load versus mass loss	89
Figure 4.21: Relative strength versus mass loss	92
Figure 4.22: Stiffness versus mass loss	94
Figure 4.23: Corrected stiffness versus mass loss	96
Figure 4.24: Relative deflection at $P = 80\text{kN}$ versus mass loss	97
Figure 4.25: Relative deflection at $P = 110\text{kN}$ versus mass loss	98
Figure 4.26: Ultimate load versus chloride ion content	101
Figure 4.27: Stiffness versus chloride ion content	102
Figure 4.28: Corrected stiffness versus chloride ion content	103
Figure 4.29: Ultimate load versus crack width	104
Figure 4.30: Stiffness versus crack width	106
Figure 4.31: Corrected stiffness versus crack width	107
Figure 4.32: Chloride ion content versus mass loss	109
Figure 4.33: Crack width versus mass loss	110
Figure 4.34: Summary of load deflection behaviour within the elastic range	112



# 1 INTRODUCTION

## 1.1 Background Information

It is well documented that a large proportion of our concrete infrastructure is approaching the end of its service life. In most cases, steel reinforcement corrosion has proved to be a major contributor to the shortened service life of our infrastructure, and the primary contributor to structural deterioration. The widespread problems with corrosion due to chloride ions are well documented, particularly in parking garages and bridges. It has been reported that the infrastructure deficit in Canada alone was CAN\$100 billion in 2005 when the municipal, provincial and federal jurisdictions were included (Mirza, 2006). It has also been estimated that 79% of the country's infrastructure has already reached the end of its service life (Canadian Society of Civil Engineering, 2003). In some cases the lack of identification of reinforcement corrosion has had severe consequences, such as the collapse of the Berlin Congress Hall as shown in (Isecke, 1982) and of a parking garage in Minnesota (Borgard et al, 1990).

It is the engineer's obligation to look for ways through which our infrastructure can be evaluated, through field inspections and laboratory testing, and determine where resources are best spent. Above all, it is imperative to determine how corroded structures behave, in order to avoid more catastrophic failures in the future. It is in this vein that the following research paper is presented.

The adequate or inadequate performance, and subsequent failure, of concrete beams is due to a combination of several factors. Concrete mix design, reinforcement layout and curing practices all play a role. These factors working together determine the performance and behaviour of a reinforced concrete element. Concrete beams with corroded reinforcement are no different from uncorroded beams, except that there is another degree of variability. This new variability is the degree of corrosion of the reinforcement, and can have a tremendous impact on the beam behaviour.

Corrosion of the reinforcing steel causes a decrease in the bar diameter which adversely affects the mechanical properties of the steel bar in terms of its ultimate strength, yield strength and ductility. Furthermore, when reinforcement corrodes, the corrosion process is accompanied by a large increase in volume, and eventually a large pressure is exerted on the surrounding concrete causing cracks. These cracks propagate slowly as corrosion continues and spalling of the concrete cover can follow as corrosion advances. Also, corrosion of the reinforcing steel causes changes in the surface conditions of the reinforcement steel, and the layer of the corrosion products causes a loss of cohesion and adhesion at the steel-concrete interface as well as changes in the profile of the bar rib. Eventually, all of the concrete around the steel bar is forced off by the growing corrosion products, and the reinforcement loses a significant part of the bond resistance to transfer the forces from the reinforcing steel to the surrounding concrete, and vice versa. With the concrete cover lost, the reinforcement also loses any remaining protection against further corrosion.

Steel reinforcement corrosion is especially serious in the case of post-tensioned prestressed concrete due to the fact that the reinforcement is deliberately stressed in tension prior to any loading on the

structure. In addition, the post-tensioning tendons are free to move within the concrete over the beam length as they may be anchored only at the ends; such movements are prevented in grouted tendons. Therefore, rusting of the tendons may take place without any visible signs on the concrete surface. This risks a sudden structural failure without any advance warning.

It should be emphasized that the reinforcing steel is provided in reinforced concrete to resist the tensile forces, and to control cracking within the tensile zone. However, corrosion not only deteriorates the steel bar and its ability to transfer the tensile stresses, it deteriorates the concrete by spalling of the cover. As corrosion of the reinforcing steel progresses, the bond strength between the reinforcing steel and concrete diminishes progressively, and major repair or replacement is required. While much has been written about the problem, and numerous reports have appeared which discuss how this corrosion can be controlled, only limited data is available concerning its influence on the flexural behaviour of reinforced concrete beams.

If the engineering community hopes to be able to predict the structural performance of existing corroded concrete beams, there must first be an understanding of how each of the changing variables affects the beams individually. Once there is a clear understanding of each parameter on its own, the interaction between each can be assessed. This research covers the effects of reinforcement corrosion on flexural behaviour and stiffness of reinforced concrete beams.

## **1.2 Research Significance**

A study of the influence of corrosion and cracking on the flexural behaviour of reinforced concrete would be quite useful in determining the progressive deterioration of reinforced beam capacity with increasing levels of corrosion. The correlation between corrosion, flexural strength and cracking of the reinforced concrete requires urgent attention.

It is anticipated that the findings of this research program and its application will result in a better understanding of the corrosion problem, the risks associated with the problem, as well as its influence on the flexural behaviour of reinforced concrete beams.

## **1.3 Scope of Investigation**

This study is an attempt to derive a relationship between reinforcement corrosion and the coinciding loss of flexural strength. Steps were taken to isolate the corrosion of the steel to the flexural region in order to eliminate contributions from stirrup corrosion or loss of bond within the development length. This relationship is an essential step in order to develop an effective model of how corroded concrete beams will perform in the future.

The prediction of the residual strength of corroded beams was studied through stiffness effects of corrosion and loss of bond. The parameters that are used to evaluate the degree of corrosion in each beam were mass loss, crack width and chloride ion content. As will be described below,

some researchers have already begun this process. This research is an effort to continue the evaluation process.

## **1.4 Outline of Thesis**

Chapter 1 introduces the corrosion problem and addresses the goals of this research program. Chapter 2 presents a description of the mechanisms responsible for steel reinforcement corrosion as well as a review of current research literature. It discusses how the concrete environment protects the embedded steel. The basic principles of reinforcement corrosion are presented and the relevant characteristics of concrete are discussed. Chapter 3 describes the experimental program from the casting of the beams through the accelerated corrosion process. Also, it describes the mechanical experimental program and setup of the load testing that was performed after achieving the required corrosion conditions for each specimen. This chapter also summarizes the program planned to study several parameters influenced by corrosion, used in this study to evaluate the deterioration of the flexural capacity of the beams. Chapter 4 reports the results obtained from each experimental program as well as the discussion and analysis of the results that were obtained from the experimental program. A brief summary of the experimental and analytical work as well as the conclusions are presented in Chapter 5, and recommendations for further research and development on the influence of corrosion on flexural behaviour are included.



## 2 LITERATURE REVIEW

The corrosion of steel reinforcement is of great concern with respect to the deterioration of the infrastructure around the world. This chapter will discuss the factors that cause and control the corrosion of steel in concrete, and conditions under which steel reinforcement corrosion is likely to occur. In addition, factors influencing the electrochemical process are also discussed, and some protective measures are presented.

### 2.1 Introduction

Through the years, the study of concrete from a materials standpoint has evolved considerably. It wasn't too long ago that it was presumed that concrete structures should last for an indefinite period of time, and engineers were caught unaware when they didn't. Not until the 1970's did materials scientists begin to understand the destructive mechanisms at work within hardened concrete (*Corrosion of steel in concrete: Prevention, diagnosis, repair*, 2004). While these destructive mechanisms can include sulphate attack, reactive aggregate reactions, and acid attack, it is the corrosion of the reinforcing steel that has become the most widespread in countries with colder climates, where the use of de-icing salts is widespread.

Corrosion is the process of the transformation of a metal towards its "natural" form, its ore state, generally oxides, chlorides or sulphates. This transformation occurs because compounds such as the

oxides contain less energy than pure metals, and hence they are more thermodynamically stable. The corrosion process does not take place directly but rather as a series of electrochemical reactions with the passage of an electric current. Corrosion also depends on the type and nature of the metal, the immediate environment, temperature and other related factors. The corrosion may be defined as the destructive attack of a metal by chemical or electrochemical reaction with its environment.

Steel in concrete is normally immune from corrosion because of the high alkalinity of the concrete; the pH of the pore water can be greater than 12.5, which protects the embedded steel against corrosion. This alkalinity of concrete induces passivation of the embedded reinforcing bars. A microscopic oxide layer known as the 'passive' film, forms on the steel surface due to the high pH. This prevents the breakdown of iron. Furthermore, concretes made using low water-cement ratios and good curing practices have a low permeability which minimizes the penetration of the corrosion inducing agents. In addition, low permeability is believed to increase the electrical resistivity of the concrete to some degree, helping reduce the flow of electrical currents within the concrete which accompany the electrochemical corrosion. Consequently, corrosion of the embedded steel requires the breakdown of its passivity.

The steel reinforcement in a majority of concrete structures or concrete elements does not corrode because of these inherent protective characteristics. This protection will exist as long as the concrete quality and design are appropriate for the environmental and mechanical exposure of the element over its entire service life. However, corrosion of the steel in the concrete may result when the conditions mentioned above are not met. In places of very severe exposure, such as pilings in sea water or bridge decks exposed to de-icing salts, the use of other protective measures is

recommended. These include corrosion inhibitors, coatings on steel, sealing of the concrete surface, and cathodic protection.

## **2.2 Mechanism of Corrosion of Steel Reinforcement in Concrete**

To illustrate the strides which researchers have made in the last 30 years one need only refer to Neville's 1975 edition of Properties of Concrete which states "The possibility of corrosion of reinforcing steel by calcium chloride is still a subject of controversy, but the United States Bureau of Reclamation...found no indication that the use of calcium chloride, applied in the correct proportions, results in corrosion of reinforcement" (Neville, 1975). At this time, in the British Concrete Code, the dosage of CaCl was limited to 2% by weight of dry cement. Ultimately, the practice of using calcium chloride as a set accelerator was banned in England in 1977. Today, it is known that mixed chlorides at any dosage are likely to have a long term deleterious effect on the concrete.

Understanding the corrosion mechanisms at work will lead to understanding the kinds of care and treatments that will mitigate the process. Corrosion is an electrochemical process. The factors which determine the corrosion rate of steel in concrete are: the presence of an ionic conducting aqueous phase in contact with the reinforcing steel, pore water, the existence of anodic and cathodic sites on the metal in contact with this electrolyte and the availability of oxygen to enable the reactions to proceed.

The following four criteria must be met in order for reinforcement corrosion to take place. If these four criteria are not met corrosion will not take place (*Corrosion in reinforced concrete structures*, 2005):

1. An anodic reaction must be possible

With respect to the corrosion of steel in concrete, the anodic reaction is characterized by:



This reaction is made possible by the breakdown of the passive layer that protects the steel at high alkalinities.

2. A cathodic reaction must be possible

The cathodic reaction is written as:



This reaction is possible only in the presence of oxygen.

3. A flux of ions is possible

Within concrete the electrolyte pore solution serves as the salt bridge for the transport of ions from cathode to anode

#### 4. A flux of electrons is possible

The reinforcement itself serves as the medium for the transport to electrons in the opposite direction.

Within reinforced concrete, there exists two major mechanisms that generate conditions where corrosion of the reinforcement can occur. They are chloride induced corrosion and corrosion due to carbonation of the concrete. In general, they occur independently of one another. That is, each does not require the other in order to initiate corrosion. In some rare cases, both mechanisms can work simultaneously to create an especially severe corrosive environment.

In general, concrete under normal conditions will not corrode (Mindess, 2003). This is because under normal conditions the alkalinity of the pore solution in concrete is very high. This allows for the formation of a passive layer surrounding the steel reinforcement which acts as protective layer (*Corrosion of steel in concrete: Prevention, diagnosis, repair*, 2004). This passive layer is formed when  $\text{Fe(OH)}_2$  oxidizes at high alkalinities, to form gamma-ferric hydroxide according to the equation:

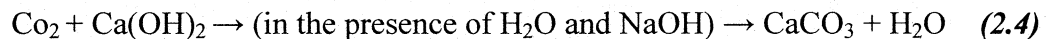


Gamma ferric hydroxide clings tightly to the reinforcing steel and allows for very little diffusion of oxygen, which as described above, is required for corrosion to occur. (Mindess, 2003).

Problems arise when certain factors cause a chemical change in the concrete pore solution that precipitates a drop in the alkalinity of the concrete. These factors influencing the chemistry inside the concrete can be generated internally, such as through the addition of CaCl to the initial mix, or more often, through foreign substances permeating into the concrete from the surrounding environment. If the alkalinity inside the concrete drops below a pH of 11.5 (Mindess, 2003), the passive film becomes unstable and can no longer protect the embedded steel from corrosion attack.

### **2.2.1 Carbonation of Concrete**

In carbonation, carbon dioxide present in the air penetrates into the concrete and reacts with the calcium hydroxide. Calcium hydroxide is a primary hydration product and reacts readily with the CO<sub>2</sub> according to the equation (*Corrosion of steel in concrete: Prevention, diagnosis, repair*, 2004):



Calcium hydroxide is also the component of the cement paste which provides the pore solution with its alkalinity. The above reaction results in the consumption of calcium hydroxide in solution and a corresponding reduction in alkalinity. In addition to this drop in pH, carbonation may also lead the release of bound chlorides in the concrete deteriorating an already dangerous situation (*Corrosion of steel in concrete: Prevention, diagnosis, repair*, 2004). It is interesting to

note that some experts believe that the pore solution will be maintained at a pH of about 12.5 until all the calcium hydroxide has reacted (*Corrosion in reinforced concrete structures*, 2005). Whether this is accurate or not, one can infer that the amount of calcium hydroxide present after hydration, while not important to the compressive strength, is a critical parameter in measuring a concrete's resistance to carbonation attack, and maintaining a highly alkaline pore solution.

Under normal exposure conditions, carbon dioxide will not penetrate more than 25mm into the concrete, and in higher exposure environments, no more than 50mm (Mindess, 2003). If the threat of carbonation is recognized, the concrete cover can be adjusted accordingly and a durable concrete can be achieved for the full course of its service life. As always, the key to ensuring a durable concrete starts with understanding the environment in which the concrete is to perform.

### **2.2.2 Chloride Attack**

The second mechanism by which the pore solution can lose its alkalinity is through the ingress of chlorides. Since the introduction of de-icing salts in the 1970's the incidences of corrosion of reinforcing steel have been rising dramatically (*Prediction of concrete durability: Proceedings of STATS 21st anniversary conference*, 1997). In northern countries, such as Canada, where the use of de-icing salts is commonplace, chloride induced corrosion is the most prominent mechanism of concrete deterioration. While de-icing salts prove to be the biggest problem in cooler climates similar to Canada, it is important to note that seawater and salt spray can have the same affect and makes the problem of chloride induced corrosion a truly global phenomenon (Higgins et al., 2006).

The structure of the passive film on the steel bar surface and the mechanism of its breakdown are not fully understood and considerable research on this subject is presently underway. It is generally agreed that the chloride ions replace some of the oxygen in the passive film, thereby increasing both its conductivity and solubility. This results in the loss of the protective nature of the film. In addition, the initial high potential difference across the film cannot be maintained, and this potential at the steel surfaces decreases considerably towards the value of an iron electrode.

Chlorides in solution can penetrate into the concrete through a number of transport processes. These processes include: Pressure induced water flow, water absorption, water vapour diffusion, wick action and ion diffusion. These mechanisms provide the means by which the chloride ions make their way towards the reinforcing steel. These are summarized well by N.R. Buenfeld (*Prediction of concrete durability: Proceedings of STATS 21st anniversary conference, 1997*).

The penetration of chlorides actually has a fourfold effect on the concrete matrix. Chlorides actively attack the passive film of the steel accelerating its breakdown. They cause a drop in pH by binding to calcium hydroxide and reducing its solubility as described above. They increase the moisture content by creating a concentration gradient and finally, they increase the electrical conductivity of the concrete (*Corrosion in reinforced concrete structures, 2005*).

The direct attack of the passive film, when compounded with the other effects, is what makes chloride induced corrosion so dangerous.  $\text{Cl}^-$  reacts with the passive film to form a soluble iron

chloride complex,  $[\text{FeCl}]^+$ . This complex then reacts further with the hydroxyl groups in solution resulting in the subsequent release of chloride ions per Eq. 2.5:



This characteristic release of  $\text{Cl}^-$  allows for the process to propagate itself, as well as simultaneously bonding free calcium hydroxide. The damage has been done and the chlorides are free to continue their attack on the passive layer.

Once depassivation of the steel has occurred all the criteria for corrosion have been met. At this stage the “initiation” phase is complete and the propagation phase begins, implying that corrosion will continue until action is taken to remedy the situation or the concrete structure has failed. Some researchers maintain that the service life has ended once depassivation of the steel has taken place. Other less conservative studies have used the appearance of cracks to the cover as the termination of service life (Alonso et al., 1998). At any rate depassivation marks the onset of corrosion and requirement for remedial action.

While understanding corrosion can help design engineers tailor their design to avoid corrosion, certain environments are so severe that corrosion is ultimately inevitable. In these cases there is the question of how to deal with existing corroded structures. Once corrosion has initiated it is important to understand the direct effects that corroded reinforcement has on the properties of the materials, and most importantly on the structural behaviour. This is addressed in the following section.

## **2.3 Effect of Reinforcement Corrosion on Material Properties**

### **2.3.1 Overview of Effects of Corrosion on Reinforced Concrete**

Corrosion of reinforcing steel can affect the properties of concrete in a variety of ways. Depending on the environment, concrete type and length of exposure, the resulting changes can vary significantly. Corrosion of reinforcement can lead to a loss in strength, loss of stiffness, loss of bond strength, loss of serviceability, as well as cracking and spalling. All of these factors can act individually or in combination with each other in order to provide a large variety of potential effects.

While research continues in all of these areas; the understanding of how each factor affects the other is still in its early stages. For example: cracking of concrete has an aesthetic effect, it results in a change in stiffness of the material, it also increases the permeability of the concrete and leads to more severe environmental effects. Quantification of these effects is necessary for the accurate prediction of behaviour.

When reinforcing steel corrodes, the formation of ferric hydroxide,  $\text{Fe}(\text{OH})_2$  is accompanied by a large expansion of volume. The expansion exerts an outward pressure on the concrete from inside and as the pressure builds, the ultimate result is cracking of the concrete, which in turns results in a loss of bond between steel and concrete. As mentioned above, this can lead to the further ingress of chlorides and the corrosion process can accelerate. Cracking also provides one of the most obvious signs that corrosion is taking place within the concrete. Its reliability as a corrosion indicator will be examined later in this study. Studies have shown that there is little

time between depassivation of the steel and the emergence of cracking of the cover (Alonso et al., 1998).

Another effect is the loss of steel area. As steel corrodes, and more and more ferric oxide is formed, naturally the remaining volume of original steel gets smaller. Since ferric oxide has no strength, corrosion will lead to a smaller cross sectional diameter of steel bars and subsequently, a loss in overall strength of the member. A loss in steel area also causes a loss in stiffness and can lead to excessive deflections. This is due mostly to the changes in sectional properties due to cracking and/or spalling.

In beams subjected to flexure, tensile steel is in place to take the majority of the load within the tensile region. In beams subjected to higher shear loading conditions, stirrups are placed to resist tension due to the shear forces. In both cases, a loss in cross-sectional area of the bars can have disastrous consequences. Loss of bond strength due to corrosion can also affect how well the load is transferred into the tensile steel. In this manner, we see how reinforcement corrosion can affect all structural reinforced concrete.

Rodriguez et al. (1997) succinctly summarized the effects of steel corrosion as follows:

1. The area of the steel reinforcement is reduced and correspondingly the mechanical properties are affected.
2. The area of concrete is reduced due to cracking and spalling, again leading to a loss of mechanical properties.

3. The concrete-steel interface is affected due to the loss of bond strength with corrosion

A brief review of several recent studies follows. Many have attempted to quantify the effects of the factors listed above.

### **2.3.2 Changes in Flexural Behaviour due to Corrosion**

Almusallam et al. (1996) studied the effect of corrosion on concrete slabs. Slab specimens were 305 x 711 x 63.5mm thick and were corroded using accelerated corrosion techniques. Constant current was used at a level of 2 Amps. It was remarked that flexural cracks were generated at lower loads in corroded slabs and that these cracks merged with corrosion cracks and caused a splitting failure in concrete slabs. In the highly corroded slabs, failure was characterized by a longitudinal splitting along the reinforcing steel, caused by a loss of bond. Reductions of 25% of ultimate strength were noted with 5% of steel mass loss. With 25% mass loss, the corresponding loss in strength was 60%. At mass loss values of 60% with respect to the original mass of steel, the ultimate strength of the slab was comparable to that of a plain concrete. This major loss of strength is a serious concern to design engineers.

Cabrera et al. (1996) tested beams of 125x160mm cross-section designed in two series, I and II, to fail in flexure and bond-slip respectively. Reinforcement was 12mm deformed bars corroded using accelerated corrosion under constant voltage. Results showed a significant increase in deflection with the corroded specimens; with a 9% level of corrosion inducing a deflection of 1.5

times that of the non-corroded samples. Caution must be exercised in the future by design engineers who wish to avoid serviceability failures in corrosive environments.

Using samples of comparable size, Mangat et al. (1999) conducted another investigation into the effect of reinforcement on load carrying capacity. Specimens were 100x150x910mm and reinforced with two No. 10 bars in tension. Stirrups (both embedded and external) were applied to avoid shear failure. Under a four-point loading they observed a 77% reduction in ultimate load with a corresponding loss of diameter of 10%. This result demonstrates that structural deterioration due to corrosion is not due to the loss of steel area alone.

It is imperative for engineers to identify potential problems in structures well before they reach such advanced stages of corrosion. Even small reductions in strength could have serious consequences in the future.

### **2.3.3 Changes in Bond due to Corrosion**

Almusallam et al. (1996) conducted an investigation to determine the effect of corrosion of reinforcement on bond strength on concrete. In order to better mirror real service conditions, a cantilever pullout test was used in lieu of the more widely used concentric test (ASTM C234). Specimens were 152x254x279mm and 12mm bars were selected. In order to reduce the risk of shear failure within the specimen, inverted stirrups were used in such a way that they did not affect the bond resistance of the specimens. Compressive reinforcement was added in a similar manner to prevent a crushing failure. Results indicated an initial increase in bond strength with

low levels of corrosion (up to 4% mass loss). This was attributed to an increased confinement with the expansive corrosion product, as well as an increase in roughness of the bar in the initial corrosion stages. This phenomenon has been observed by several other researchers as well (Bhargava et al., 2007; Cabrera, 1996). At higher stages of corrosion, the loss in bond strength was dramatic. At corroded mass losses of approximately 8%, the ultimate bond strength was less than 35% of that of the uncorroded specimens. This loss was attributed to increased crack width, a loss of confinement and the initiation of the loss of the rib profile. This kind of loss would severely impair the mechanical properties of reinforced concrete. At higher levels of corrosion, 12% mass loss, the mode of failure of the specimens switched from a splitting mechanism to a continuous slippage. This was attributed to the full loss of the rib profile, the lubricating effects of the corrosion layer as well as a loss of confinement.

Cabrera et al. (1996) conducted a comprehensive study including the effects of corrosion on both bond strength and beam deflection. In the bond strength portion of the study, pullout tests were performed under a monostatic load condition. A short embedment length was chosen to ensure a bond-slip failure instead of a splitting failure. At a mass loss of 12.6% the corresponding loss in bond strength was observed to be 23.8% for ordinary Portland cement pullout samples.

In a preliminary series of tests Amleh and Mirza (1999) studied the influence of level of corrosion on bond strength through consideration of both the transverse and the longitudinal cracks, and the relative bond effectiveness of the corroded bars was determined from the crack spacing. Different stages of the steel reinforcement corrosion were established to study their relative bond behaviour, ranging from no corrosion to "complete" corrosion at the steel-concrete

interface. The bond strength decreased rapidly with an increase in the corrosion level, especially in the case of any severe localized corrosion, or pitting. It was found that the first level of corrosion, which represented approximately 4 percent weight loss due to corrosion, resulted in a 9 percent decrease of the nominal bond strength, while the sixth level of corrosion with an approximate 17.5 percent weight loss (the case of very heavy corrosion) due to corrosion, resulted in a 92 percent loss of the nominal bond strength. The bond behaviour was influenced by the deterioration of the reinforcing bar ribs, and by the reduced adhesion, cohesion and loss of mechanical resistance of the reinforcing bar due to the widening of the longitudinal splitting cracks resulting from corrosion.

### **2.3.4 Changes in Failure Mode due to Corrosion**

In 1997, Rodriguez et al. studied the effect of varying degrees of corrosion on concrete beams. The beam specimens were 200mm by 150mm with a clear span of 2000mm. Beams had both tensile, compressive as well as shear reinforcement which was corroded using accelerated corrosion over a period of 101-190 days under a constant current density of  $100 \mu\text{A}/\text{cm}^2$ . It was determined that not only will there be a loss of strength in both shear and bending due to reinforcement corrosion, but also that corrosion can change the mode of failure as well. Failure in some beams shifted from bending to shear upon corrosion of reinforcement. This was prominent in beams with stirrup spacing close to the effective depth of the concrete sections, when combined with a high relative corrosion of the tensile bars. This change in failure mechanism was attributed to the reduction of the stirrup section due to pitting and the reduction of the concrete section due to spalling.

A shift in failure mode due to reinforcement corrosion was also observed by Uomoto et al. (1984) who observed a corroded concrete beams tended to exhibit a “shear-bond” failure while their non-corroded specimens failed in pure flexure. Beams were subjected to a four point loading to increase effects of the shear in this study. This conclusion corresponds well with that of Rodriguez et al. (1997) covered earlier.

## **2.4 Modelling of Corroded Concrete Elements**

### **2.4.1 Introduction to Modelling Corroded Reinforced Concrete**

Once there is an understanding of the mechanism at work and the effects upon the materials, a prediction of how reinforced concrete will behave when subjected to corrosive environments is possible. This is an important phase since it allows for a quantification of when serious dangers might be encountered. Often, it is not a ultimate failure, but a loss in serviceability that is enough to meet the failure criteria (Li et al., 2005).

In the following section proposed models of several researchers will be presented. Some examine the behaviour of whole members and some look at specific details with great focus. For accurate portrayals of realistic conditions, both must be effectively modelled.

Many models are based on the widely studied Tuutti model (Tuutti, 1982) which breaks the corrosion process into two phases, shown in Figure 2.1. The first phase is known as the initiation time. This is the time it takes from the beginning of the concrete's service life to the time of corrosion initiation. It encompasses the ingress of chlorides and the depassivation of the steel. The stage that follows the initiation time is called the propagation phase. This is the time from the initiation of corrosion to the end of the structure service life, or the time to failure. Considerable efforts have been made to model both of these stages.

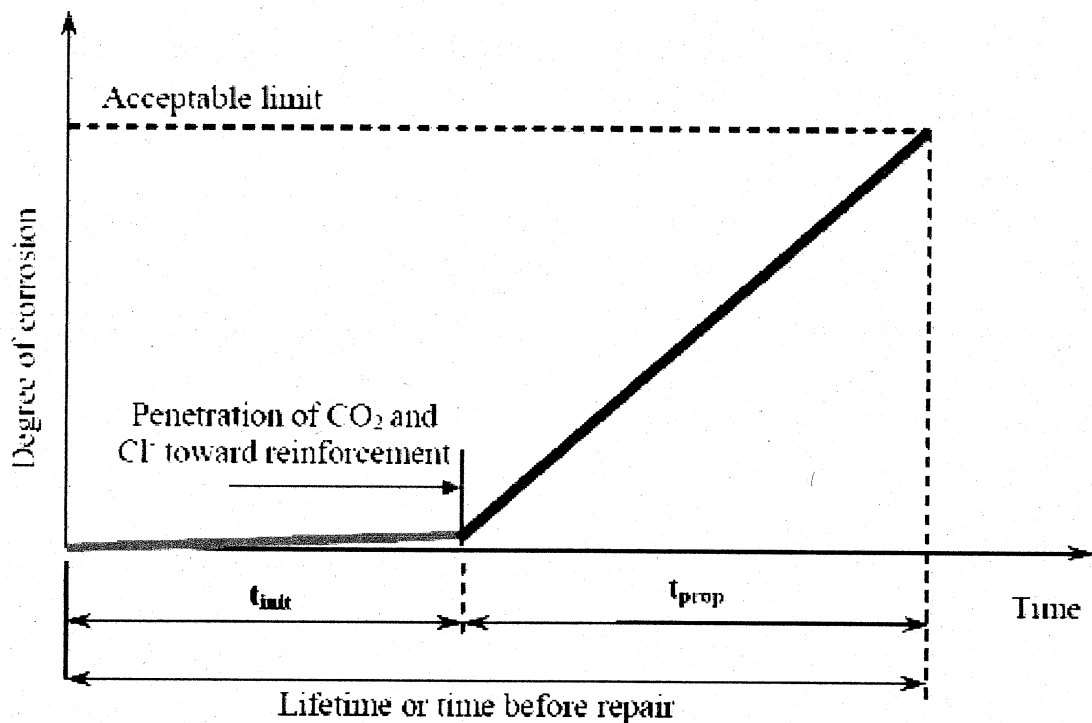


**Figure 2.1 The Tuutti Model (Tuutti, 1982)**

## 2.4.2 Li Model

Li (2003) suggests the following model for probability of corrosion at time,  $t$  :

$$p_i(t) = P[(C_i(t) \geq \delta_{cl}] \times P[\xi] \quad (2.6)$$

where  $P[\xi]$  is the probability of corrosion taking place for a given threshold value,  $\delta$ , and  $C_i(t)$  is the concentration at time,  $t$ .

For this relationship to be practical, however, it is necessary to define the threshold value as well the expected chloride content in greater detail. Li provides the following two relationships to define the ingress of chloride into cracked concrete as a stochastic process. The mean chloride content is written as:

$$\mu_c(t) = C_o \exp(at) \quad (2.7)$$

where  $C_o$  is the initial chloride content at the surface of the reinforcement. The coefficient of variation is written as:

$$V_c(t) = bt + 0.1433 \quad (2.8)$$

where  $a$  and  $b$  are coefficients determined through a regression analysis of experimental data.

With this information calculation of the probability of corrosion initiation for any time,  $t$ , becomes possible. It is also important to note that Li disregards the effect of concrete cover for the scenario of cracked concrete.

### 2.4.3 Oh Model

Oh et al. (2003) studied the relationship between the ingress of chlorides through concrete and the time to corrosion initiation. The following expression was derived for the corrosion initiation time to:

$$t_o = \frac{c^2}{4D_{cl}} \left\{ \frac{1}{\operatorname{erfc}^{-1}[(C_o - C_i)/(C_{thr} - C_i)]} \right\}^2 \quad (2.9)$$

where  $C_o$  is the surface chloride concentration,  $C_{thr}$  is the threshold value,  $C_i$  is the initial chloride concentration,  $D_c$  is the chloride diffusion constant, and  $c$  is the concrete cover depth.

Values for the probabilistic variables are provided in their earlier research.

The next phase of the Tuutti model, with respect to service life, is the propagation time. Many researchers have derived relationships based on the electrical current concentration and the diameter of the steel bars as well as a wide array of other parameters depending of the study.

These are well documented by Liang et al. (2002).

## 2.4.4 Val Model

Another aspect of corrosion which garners considerable attention from the modelling world is the reduction of cross-section area of the reinforcement that accompanies any corrosion activity. The problem is with chloride induced corrosion, there tends to be a high degree of pitting along the bar, whereas carbonation will cause a more general corrosion (Cairns & Millard, 1999). It is modeling the extent and effects due to pitting which proves to be the real trick, in each case.

Val (2007) defines the expected pit depth as follows:

$$p(t) = 0.0116i_{corr}tR \quad (2.10)$$

where  $i_{corr}$  is the measured corrosion current density,  $R$  is the ratio of maximum corrosion penetration to average corrosion penetration (usually about 4) and  $t$  is the time in years.

Using this relationship Val further defines the corresponding areas of the pits as:

$$A_p(t) = \begin{cases} A_1 + A_2, & p(t) \leq \frac{D_0}{\sqrt{2}} \\ \frac{\pi D_0^2}{4} - A_1 - A_2, & \frac{D_0}{\sqrt{2}} \leq p(t) \leq D_0 \\ \frac{\pi D_0^2}{4}, & p(t) \geq D_0 \end{cases} \quad (2.11)$$

where  $D_0$  is the uncorroded diameter of the bar, and  $A_1$  and  $A_2$  are defined below.

$$A_1 = \frac{1}{2} \left[ \theta_1 \left( \frac{D_o^2}{2} \right) - a \left| \frac{D_o}{2} - \frac{p(t)^2}{D_o} \right| \right] \quad (2.12)$$

$$A_2 = \frac{1}{2} \left[ \theta_2 p(t)^2 - a \frac{p(t)^2}{D_o} \right] \quad (2.13)$$

$$\text{where } a = 2p(t) \sqrt{1 - \left[ \frac{p(t)}{D_o} \right]^2} \quad (2.14)$$

Further, for a group of  $n$  reinforcing bars the remaining cross-section of steel after  $t$  years is written as:

$$A_s(t) = n \frac{\pi D_o^2}{4} - \sum_{i=1}^n A_{p,i}(t) \geq 0 \quad (2.15)$$

Together, these expressions provide a good basis for the estimation of steel loss at a given time of service life. It is important to test these models against real life scenarios, where possible, in order to strengthen the confidence we have in the models.

One can also examine the relationship between bond strength reduction and the corrosion process. It is known that bond plays an integral role in the development of mechanical properties in reinforced concrete so it is also important to have this relationship suitably modeled.

## 2.4.5 Coronelli Model

Coronelli (2002) defines the ultimate bond strength of a corroded bar according to the relationship:

$$\tau_{bu}(X_p) = \tau_{CP}(X_p) + \tau_{AD}(X_p) + \tau_{COR}(X_p) \quad (2.16)$$

where  $\tau_{CP}$ ,  $\tau_{AD}$ , and  $\tau_{COR}$  are the contributions in bond strength from the confining pressure at anchorage bond failure, adhesion between corroded steel and cracked concrete and radial corrosion pressure, respectively.

The anchorage bond and the radial corrosion pressure respectively and are defined under the following relationships:

$$\tau_{CP}(X_p) = \frac{nC_r \tan(\delta + \phi)(X_p)}{\pi} P_{\max}(X_p) \quad (2.17)$$

$$\tau_{COR}(X_p) = \mu(X_p) p_r(X_p) \quad (2.18)$$

$$\tau_{AD}(X_p) = \frac{nA_r(X_p)[\cot \delta(X_p) + \tan(\delta + \phi)(X_p)]}{\pi D_r(X_p) S_r} \quad (2.19)$$

where  $n$  is the number of transverse ribs at a section;  $C_r$  is a coefficient (0.8 for crescent shaped ribs);  $\delta$  is the rib angle;  $\phi$  is the friction angle between the steel and the concrete;  $P_{\max}$  is the maximum pressure at bond failure;  $\mu$  is the coefficient of friction between the corroded bar

and the cracked concrete;  $p_r$  is the radial corrosion pressure;  $A_r$  is the rib area at right angles to the bar axis;  $f_{coh}$  is the adhesion strength;  $D_r$  is the reduced diameter of the corroded bar;  $S_r$  is equal to  $0.6D_i$ .

The equation shown for  $\tau_{AD}$  (eq 2.19) has been modified by Bhargava (2007) in order to better account for the effects of the corrosion products.

#### 2.4.6 Rodriguez Model

An empirical model is proposed by Rodriguez et al. (1994):

$$\tau_{res}^{max} = \tau_{conc} + \tau_{tie} = 0.6(0.5 + C/d_b)f_{ct}(1 - \beta X^\mu) + kA_{tr}F_y/(sd_b) \quad (2.20)$$

where  $\tau_{res, max}$  is the residual bond strength;  $f_{ct}$  is the concrete tensile strength;  $\tau_{conc}$  is the concrete contribution to the bond;  $X$  is the corrosion attack penetration;  $C/d_b$  is the cover to bar diameter ratio;  $\beta$ ,  $\mu$ ,  $K$  are empirical constants;  $A_{tr}$  is the section of the tie;  $f_y$  is the yield stress of the ties;  $s$  is the spacing of the ties.

This equation has the benefit of including the contributions from the ties as well as those of the concrete. The relationship is based on empirical data from samples of uncorroded stirrups, assuming that the majority of the corrosion will be in the area of the flexural cracks, near midspan. Here, as with most empirical relationships, we must be careful to apply this equation

only in situations where the criteria being studied closely match those of Rodriguez et al. If members are similar in reinforcement ratio and bar arrangement then we can apply it.

#### **2.4.7 Amleh and Ghosh Model**

Amleh and Ghosh (2006) examined the basic influence of corrosion on bond at the steel-concrete interface and the associated slip and cracking. A non-linear finite element (FE) model is developed accounting for the effect of corrosion on deterioration of bond. It was found that the contact pressure normal to the steel-concrete interface is reduced when the concrete cracks, combined with the decrease of cross-sectional area of steel bar, and the decrease of the friction coefficient between the steel and the concrete. The losses of the contact pressure and the decrease in the friction coefficient with the mass loss of steel bars were evaluated using pull-out test specimens with different levels of corrosion of the rebar. Finally, the relationship between the loss of bond strength and the mass loss of the steel reinforcement was established. The results from the bond model compared well with the data from the pullout tests performed by Amleh et al. (2000). The FE analysis and the experimental results show that the loss of bond capacity is almost linear with reinforcement mass loss. These results show that, up to about 5% mass loss, the bond capacity loss is moderate, at 10 to 15 % mass loss, there is a significant loss in the bond capacity, and at about 20% mass loss, almost all of the bond capacity is lost. The computed results using the bond model are compared with the test results from the pullout tests, by Cabrera

and Ghoddoussi (1992) and Al-Sulaimani et al. (1990) and again good agreement in results is noted.

#### **2.4.8 Previous Research at Ryerson University**

Two detailed investigations dealing with accelerated electrochemical corrosion of reinforced concrete have been completed at Ryerson University [Hassan (2002) and Aldulaimy (2006)]. They developed a test set-up and a detailed procedure for accelerated corrosion testing using lollipop specimens, with the period to complete corrosion in most specimens not exceeding 45 days. The effects of the clear concrete cover thickness, deformed steel bars with and without an epoxy-coating, and the effectiveness of the surface sealants were studied. Smith (2006) has undertaken a similar study of the capacity of reinforced concrete beams subjected to a similar accelerated corrosion regime.

#### **2.4.9 Summary**

The research that has been conducted on modeling the effects of corrosion in concrete is extensive. Subjects of the mathematical models include the effects and prediction of concrete cracking (Vu & Stewart, 2005), variation of moments resistance (Oh et al., 2007), the tensile capacity of concrete cover (Li, 2004), as well as countless others pertaining to the models covered above. Only a few have been shown in detail mainly due to the pertinence to the subject for this paper as well as their ease of application for this data.

Modelling of corroded reinforced concrete behaviour will continue to grow until the point where there is reasonable consensus among the research community. The ultimate goal should be to formulate models that can be applied, using a reasonable amount of parameters, by the professional engineers and inspectors charged with the task of designing, building, inspecting and maintaining our infrastructure. It seems as though this possibility is still a fair ways off.

## **2.5 Protection and Prevention against Reinforcement Corrosion**

In many ways, the problem of corrosion has been thrust into the spotlight in recent years. Until then, there existed a state of ignorant bliss, in denial of the effects of de-icing salts on reinforcing steel and continuing to use calcium chloride as admixtures to delay early set. In the new millennium, it remains to clean up the problem, and prevent it from recurring in the future. How is this accomplished? This section will examine ways to prevent corrosion, both through changes in design philosophy and through physical means. These include corrosion inhibitors, high performance concrete, epoxy coated reinforcement, concrete toppings, non-metallic reinforcement, galvanized reinforcement and cathodic protection (Rostam, 2003).

### **2.5.1 New Design Philosophy**

One philosophy towards prevention is to consider the effectiveness of each reinforced concrete element over the course of its entire service life. Currently, design engineers rarely consider the life cycle implications of their material selections and subsequently many reinforced concrete

elements don't achieve their desired length of service. If better selection of materials can lead to a higher quality concrete, fewer repairs, and more value to an owner in its service life, is there any reason not to proceed in this fashion? Life cycle models don't have to be accurate down to the last dollar; they just have to give a clear indication of the best materials and methodology with which to proceed. It is the ratio of costs that is paramount to owners. While this philosophy does not represent a physical preventative measure, a shift towards more life cycle analysis would certainly have as big an impact on the industry as any new admixture or reinforcement coating. A higher quality concrete will reduce the cost of failure when it occurs (Trejo & Reinschmidt, 2007).

On the topic of life cycle costing, researchers are also investigating the effect of various maintenance schedules for infrastructure and comparing total costs associated to each schedule. Mirza et al. (2006) claims that an investment of as little as 2% annually of the total infrastructure costs would significantly delay the deterioration rate and future repair costs of infrastructure and create a better economic environment in Canada. Smaller investments would have less overall effect and allow the infrastructure deficit to continue to soar. With the huge infrastructure deficits facing us in the future, efforts to rebuild what is in need of repair would be a practical first step.

Many researchers support the probabilistic approach to design, using time dependant environmental and material models to predict life cycle performance (Mirza, 2006; Rostam, 2003). This could well be the way of the future, with engineers forgoing limit states and

examining acceptable probabilities of failure over structure life cycle. Akgul and Frangopol (2005) use deterministic parameters and random variable in their proposed methodology.

Another philosophy dictates that if we cannot always eliminate the effects of corrosion due to chlorides, at least we can determine how severe the damage is. In this vein we must continue to develop non-destructive testing and test their application in the field for reinforcement corrosion. Yoon et al. (2000) investigated the use of acoustic emission in determining the extent of damage caused by reinforcement corrosion. Corroded beams showed a much more varied response and failures such as micro-cracking and shear/bond cracking were effectively identified. However, as in many non-destructive techniques, the data required heavy analysis to be interpreted and was still ambiguous in some aspects. Further work needs to be done in order to make non-destructive techniques more user-friendly and a more viable tool in the field.

## **2.5.2 High Performance Concrete**

Another preventative measure is high performance concrete, in which exceedingly low permeabilities can significantly extend a reinforced concrete's service life. However, it is not without its drawbacks. Supplementary cementing materials included in the HPC mix have the effect of consuming a large portion of the calcium hydroxide typically present in a regular Portland cement concrete. Calcium hydroxide is the main contributor to the highly alkaline pore solution and any reduction in alkalinity results in a smaller 'buffer' capacity before the passive layer is susceptible to breakdown (Rostam, 2003).

Khedr et al. (1995) found that silica fume was less absorbent to water than their ordinary concrete mix, with their optimal results coming with a dosage of 15% silica fume, leading to a significant increase in resistivity as well. They also found that their experimental time to failure increases at these dosages when compared to the ordinary concrete mix. They concluded that the benefits of silica fume outweighed the danger of lowering the pH of the pore solution in this case. As always, one has to be conscious that there is no quick fix that cures all ills. Each situation must be looked at independently with each design catering to a specific environment (Mirza & Amleh, 2002).

In similar fashion, Al-Saadoun et al. (1993) investigated the potential benefits of fly ash blended concretes. Their study indicated a clear benefit of using fly ash in replacement for ordinary Portland cement. Using 30% replacement with Type C fly ash, they were able to delay the onset of corrosion three fold over ordinary Portland cement.

However, long term durability was difficult to gauge from this study and researchers warn that class selection of fly ash can play a significant role. Ahmed et al. (2006) found that fly ash, blast furnace slag and silica fume all helped reduce mass loss when subjected to the same current. Subjected to corrosion, fly ash beams at 50% replacement lost only 3% of their ultimate capacity, compared to 13% for ordinary Portland cement. Silica fume (10% replacement) gave the best results with respect to deflection, losing only 8% of capacity, compared with 16% for ordinary Portland cement beams.

In recent years, research into action against concrete reinforcement corrosion has begun picking up again. Unfortunately, it has taken some engineering failures in order to bring this issue back to light. If research continues at its present pace a comprehensive set of guidelines into dealing with corrosive environments and corroded structures should not be far behind.

# **3 EXPERIMENTAL PROCEDURE**

The experimental procedure consisted of four major phases. Phase One included the preparation of the beam specimens, 12 in total, from forming to the end of the curing process. Phase Two was the accelerated corrosion process. This consisted of the circuit setup and the steps taken to monitor the progression of the samples while they were undergoing corrosion. Phase Three was the mechanical testing phase of the research process. Corroded and uncorroded beams were tested in identical setups in order to effectively compare results. Phase Four was the collection of data from the failed beam specimens. This work consisted of the demolition of the beams to collect the corroded steel bars and the collection of dust samples from which the chloride ion concentration data was obtained.

## **3.1 Phase One: Preparation of Beam Specimens**

### **3.1.1 Reinforcing Steel: Material Properties**

The 15M size reinforcing bars used in the tests were obtained locally, and they conformed to the Canadian Standard Association (CSA) Standard G30.14-M83 (1983) which is equivalent to ASTM Standard A615-72 (1972).

Since the aim of this experiment was to investigate the effects of steel corrosion on flexural capacity, measures were taken to ensure that corrosion would be confined to the flexural region.

The tensile steel bars were epoxy painted in a manner that would concentrate the corrosion near midspan of the beam specimens. Standard 15M steel bars were used with nominal yield strength of 400MPa. The reinforcing bars were bent at 90 degrees at each end so that both bars exited vertically from the top of the concrete beam. The development length of the reinforcing bar, 300mm, was epoxy painted on each side, leaving 440mm unpainted at midspan. For the purposes of this experiment, the two tensile bars in each beam will be referred to as Bars A and B. Paint used was a typical spray-on white metal-adhering paint applied in three separate coats. The goal of painting the bars in this manner was to eliminate the contact of the pore solution and the steel surface, effectively eliminating the transfer of ions necessary to complete the oxidation-reduction reaction.

The stirrups used were deformed, double leg, 8mm nominal diameter with yield strength of 400MPa. The stirrups were spaced at 67mm within the shear span of the beam. In order to avoid severe corrosion in the stirrups they were also painted. They also were painted in three separate coats to ensure a uniform finish. Stirrups were held in place with 10M 400W bars that had been epoxy coated by the steel supplier. The fabricator had been unable to epoxy coat the stirrups the tensile bars due to equipment limitations for such a small scale. Figure 3.1 shows the layout of steel within the concrete beams, as well as the extent of the painted portions of the reinforcing steel.

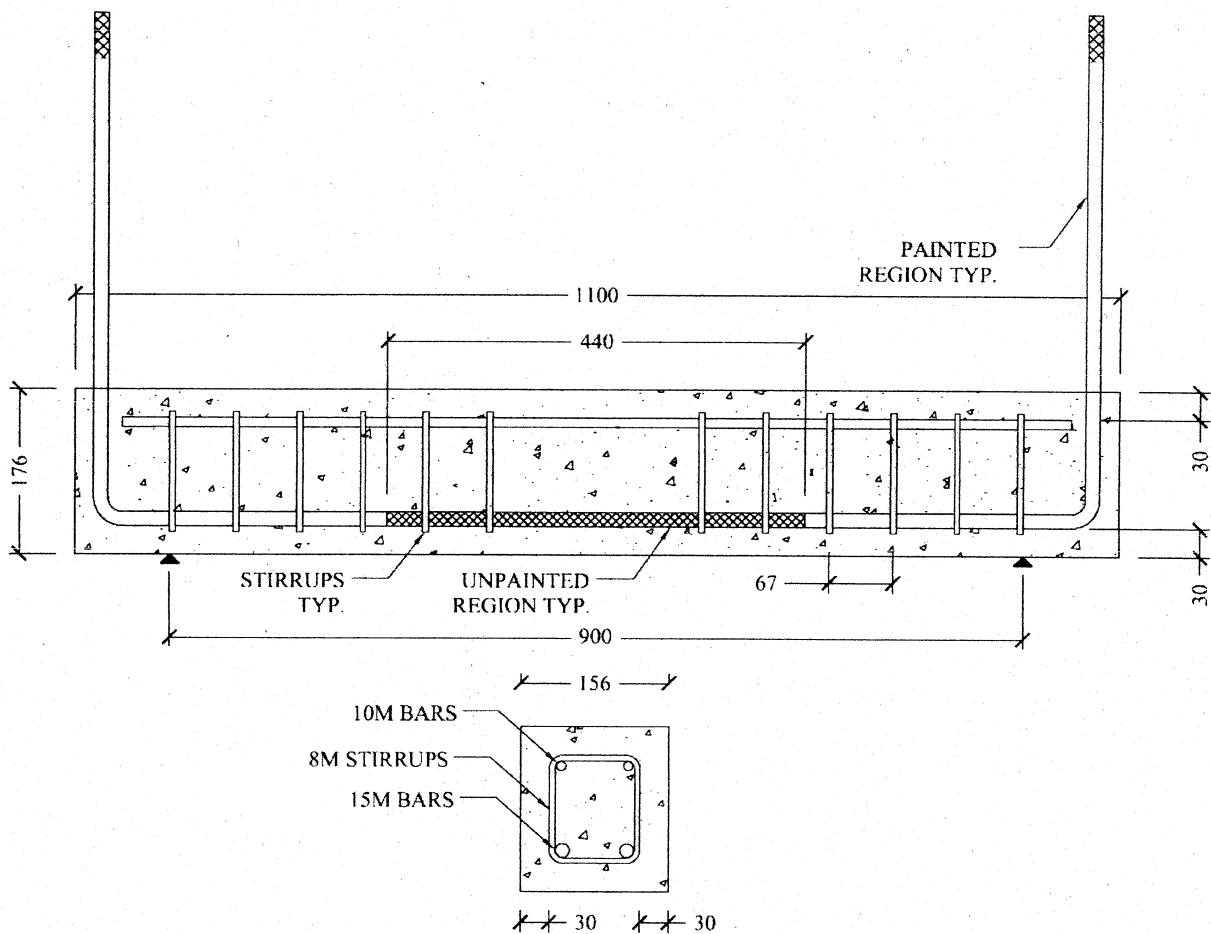


**Figure 3.1 Reinforcing Steel Layout**

### 3.1.2 Concrete Mix and Beam Dimensions: Material Properties

Beam specimens were 156mm in width by 176mm in height. This specific beam size was chosen in order to provide results that could be compared with similar studies; Rodriguez et al. (1997) used 200x150x2000mm specimens in one study. Huang et al. (1997) used specimens that were 150x150x500mm. Almusallam et al. (1996) selected specimens that were 152x254mm in cross section for his bond strength study. Smith (2007) used beam specimens of identical physical

dimensions. Tensile reinforcing steel was bent to allow for 30mm cover at the end faces of each beam. Steel reinforcing bars protruded vertically by 400mm. The top 50mm of each bar was left unpainted as well in order to make the electric connection that was required for the accelerated corrosion stage of the experiment.

To reflect what is generally practiced in concrete design, the beam section was under-reinforced. This would indicate that steel had yielded at first crushing of the concrete. This degree of ductility within the failing specimen is favourable to design engineers.

After fabrication of the forms and assembly of the steel cage according to the above specifications, the concrete was mixed and poured. Again, the concrete mix was designed to give results that could be easily compared with those of other researchers. Using a mix originally designed by Yoon et al. (2000), the mix ratio used was cement: coarse aggregate: fine aggregate: water = 2:4:4:1. This produced a concrete of high workability which was desirable due to the high volume of steel within the concrete beam. Fine aggregate used was sand and the coarse aggregate used was pea gravel, due to the high volume of steel. The targeted strength was estimated conservatively as 35 MPa (Mindess, 2003). No admixtures or salts were added the mix water during the mixing process.

### **3.1.3 Mixing, Pouring and Curing Procedure**

The mixing process followed the ASTM C685 / C685M – 07 for the 80L mixer used. Dry materials were mixed separately for 5 min. Water was added and the concrete was mixed for an

additional 5 min. The concrete was allowed to stand for 2 min. and the concrete was mixed for a final 5min. Following mixing the concrete was transferred immediately to the forms.

Concrete was vibrated in the forms using a rubber mallet, due to the absence of other available methods. The outside of the forms was hit several times with the mallet in order to lose any excess air in the concrete and ensure good contact between the concrete and the steel cage. Three concrete cylinder samples were also taken at this stage in order to test for strength at a later date. The concrete cylinders were taken in accordance with ASTM C943 - 02.

Following the pour, the concrete forms were covered with wet burlap to cure for 2 days. After 2 days the beams were removed from the forms and placed in the moist curing room for the next 26 days. Following the 28 day curing period described, the concrete beams were removed from the curing room and stored at low humidity, approximately 20%relative humidity, until they were scheduled to begin the accelerated corrosion process. Cylinder specimens were tested after the 28 day moist curing period outlined above, followed by a minimum 14 day curing period at low humidity, again approximately 20% relative humidity. The concrete cylinders were capped with a sulphur based compound and tested in pure compression using a hydraulic press.

Beams were numbered according to the order in which they were cast. With the first beam cast assigned number 1 and the last number 12 since 12 beams were cast in total. Tensile reinforcing bars were assigned as A or B, for each beam specimen. Beams 7, 9 and 10 were selected as control beams and the rest underwent the accelerated corrosion process. In order to avoid confusion a letter was assigned to each beam indicating the level of corrosion it underwent: C for

control, L for Lowest level corrosion, M for Mid-level corrosion and H for Highest level corrosion. For example: Beam 11M was the 11<sup>th</sup> beam cast and underwent mid-level corrosion. The lowest corrosion group underwent 5 days of accelerated corrosion, the mid-level group 22 days and the highest level group 39 days.

## **3.2 Phase Two: Accelerated Corrosion Process**

This section describes the test program undertaken to simulate the conditions of severe local corrosion conditions. This can result in significant changes in the surface conditions of the bar and the heights of the ribs.

### **3.2.1 Experimental Set-Up for Accelerated Corrosion**

In order to achieve the desired levels of corrosion within a reasonable period of time the corrosion process of the reinforcing steel was accelerated. Due to the same time constraints on the research schedule, a method of constant current corrosion was selected. As described previously, three detailed investigations dealing with accelerated electrochemical corrosion of reinforced concrete were completed at Ryerson University (Hassan 2002, Smith 2007, Aldulaimy 2007). They developed the test set-up and the detailed procedure for the accelerated corrosion testing using small lollipop and beam specimens. The same electrochemical method was adopted, and after a few trials, a corrosion cell was developed with some modifications due to the size of specimens.

Once the beam specimens were properly cast and cured, 9 specimens were placed in the tank. Figure 3.2 illustrates the schematic representation of the set-up. The tank was filled with an electrolytic solution [5% sodium chloride (NaCl) by weight of water]. The beam was placed in a 5% NaCl solution (by mass) up to a depth of 78mm or halfway up the height of the beam. Beams were allowed to soak for 24 hours in the NaCl solution prior to the current being applied. The electrolyte solution was changed on a weekly basis to eliminate any change in the concentration of the NaCl.

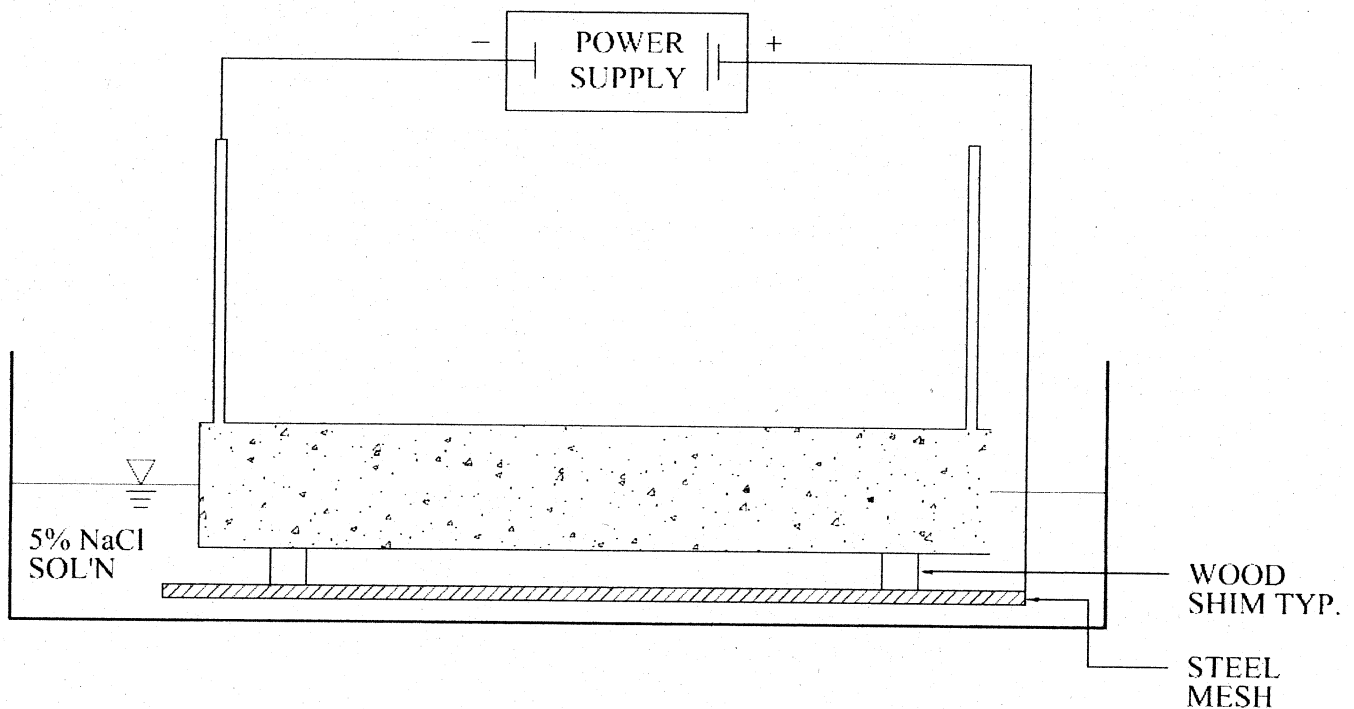


**Figure 3.2: Accelerated Corrosion Setup**

Through each bar an average of 0.3Amperes was induced. In some cases each power source was connected to a maximum of 4 total reinforcing bars in parallel. In this maximum case, the power

source was adjusted to output 1.2Amps in order to achieve the desired average of 0.3Amps/bar. In the case of four bars being hooked up in parallel, the setup resulted in some unequal sharing of the current. However, this was unavoidable due to the number of power sources available during the required time period.

As mentioned above, each power source was connected to a total of 2 or 4 reinforcing bars and the current was adjusted accordingly, in order to attain an average of 0.3Amp/bar. The electrical connection from the power source was made at the top of the reinforcement, where it protruded from the top of the beam as described. The top 50mm of the steel had been left unpainted in order to make this connection possible. Each beam was supported by a series of 4 - 50mmx50mm wood shims, which in turn rested upon the steel mesh which served as the cathode in the electrical circuit. The steel mesh was connected back to the original power source.

### **3.2.2 Monitoring Accelerated Corrosion Process**

The monitoring of the corroding samples was performed on a regular basis. Every 24h the current readings were recorded to discern if the current output was being split evenly or unevenly between the connected reinforcing bars. In addition, every other day the beams were lifted from their tanks in order to observe cracking and measure width propagation due to corrosion. Crack width was measured with a crackscope with minimum visible width of 0.5mm.

As mentioned earlier, a total of 12 beams were cast, making up 4 groups of 3 beams. While 3 beams were left uncorroded in order to serve as control beams, the remainder underwent the

corrosion process. Corrosion levels in the beams were established based on length of corrosion time, at constant current, which resulted in three groups of three beams of comparable corrosion level.

The time exposed to the accelerated corrosion process for the lowest level, mid-level and the highest level corrosion groups was 5 days, 22 days and 39 days, respectively. The 5 day period was selected since the first cracks were generally visible in approximately 4 days. The next groups, 22 and 39 days, were selected based on a desired crack width in the specimens. As mentioned above, while the average current through each reinforcing bar was 0.3Amperes, the actual current was recorded on a daily basis to accurately examine the data afterwards, and determine an average current through each bar and beam.

For the sake of simplicity as well equipment limitations, beams were not subjected to any load during the corrosion process, in this respect the conditions encountered did not mirror actual service life conditions. Some research has shown that crack width will propagate 22% faster in loaded conditions (El Maaddawy & Topper, 2005). For the same study, in terms of mass loss, loaded beams exhibited an increased mass loss of 8-9%. The difference was attributed to wider cracks allowing for faster diffusion of oxygen and moisture to the steel.

### 3.2.3 Development of Corrosion Levels

The levels of corrosion achieved in the various specimens varied from no corrosion (control specimens) to severe corrosion. One important aspect was the organization of experimental data by longitudinal crack width so that the levels of corrosion could be defined for a given specimen under a given set of environmental conditions. While the example cited in this chapter uses the longitudinal cracking as the basis for the level of corrosion achieved, other methods such as the definition of current readings can also be used to define the level of corrosion. It must be noted that this approach can be combined with other methods of defining the levels of corrosion.

Evaluation of the corrosion attack after exposure of the beam specimens was undertaken by inspection of corrosion damage with respect to crack width. However, the evaluation was ultimately carried out by determination of the weight loss after the corrosion products had been removed by cleaning the bar with dilute hydrochloric acid.

In summary, two criteria were used to determine the corrosion levels during the course of accelerated corrosion:

- (1) The width and the propagation of the longitudinal concrete crack width is the result of the formation of expansive corrosion products on the steel bar. The onset of cracking in the concrete cover and the increase of the crack width were monitored through visual observations of the specimens and recorded as this formed a reference for selecting subsequent post-cracking levels of corrosion. In order to achieve a good indicator of corrosion for the entire beam, the longitudinal cracks on every face were summed in order to

obtain a 'total' crack width for each beam specimen. Thus, a threshold total longitudinal crack width of 0.3mm was defined to be the first stage of corrosion, while the last level of corrosion was that associated with a major 2.0mm threshold total longitudinal crack. Following the corrosion process it was necessary to map the cracks due to corrosion to assess the effect of corrosion on failure capacity and failure mode. For this step, each crack was traced on the beam using a permanent marker. Each crack was measured using the crackscope at intervals of approximately 5cm in the longitudinal direction. After the complete mapping of the cracking pattern of all 6 sides of the beams, photographs were taken to document the pattern. These photographs were used to create scale sketches of the corrosion cracks on each face. Once cracks due to corrosion had been mapped, the beams were ready to be mechanically tested.

- (2) Loss of metal relative to the original reinforcing steel bar weight. The weight loss of the steel reinforcing bar was obtained as the difference between the weight of the corroded bar (after the removal of the loose corrosion products) from its weight before corrosion. For this purpose, the specimens were broken open for the retrieval of the reinforcing bar after the completion of the test. The reinforcing bar, for each specimen was cleaned and scrubbed with a stiff metal brush to ensure that the bar was free from any adhering corrosion products. The reinforcing bar was then carefully examined for its general condition as a result of the corrosion effects in terms of pitting, rib degradation, and then weighed for the determination of the weight loss. The percentage weight loss was determined as follows:

$$\text{Percentage weight loss} = \frac{[(\text{uncorroded weight}) - (\text{corroded weight})]}{(\text{uncorroded weight})} \times 100\%$$

(3.1)

Although attempts were made to confine the corrosion to the unpainted zone towards the middle of the reinforcing bars, some corrosion was observed outside it. Reasons for the extension of the corrosion will be discussed in Chapter 4. To accommodate the increased corrosion area, the length of the corroded zone was taken as 740mm, which corresponded to the extent of corrosion for the most corroded bar specimens. This assured that virtually 100% of the mass loss took place within this region. The uncorroded weight was calculated using the weight per unit width over this length. This method also allowed the corroded beams to be easily compared to one another.

The results obtained for the three criteria (mass loss, crack width and chloride ion content) are compared for the assurance of the appropriate corrosion level. Chloride ion content data was extracted as described later in Section 3.4.2.

### **3.3 Phase Three: Beam Mechanical Testing**

After the beams had reached the desired levels of corrosion and the cracks had been mapped, they were allowed to dry prior to being tested in flexure. Drying period was a minimum of 24 hours. The setup used for loading was a typical four-point loading was shown in Figure 3.3. In

order to create a favourable bearing condition a small bearing plate was inserted above the rollers, as shown.

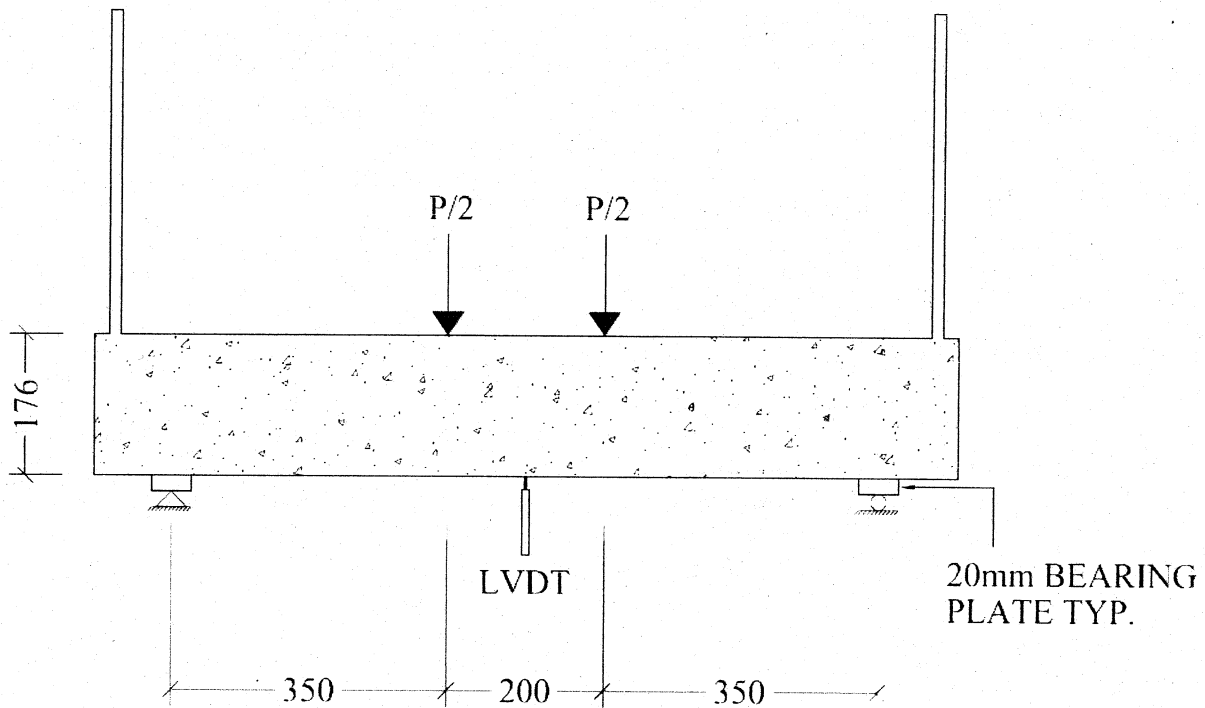


**Figure 3.3 Four point loading setup**

The beams were loaded to failure with a hydraulic hand jack. The load and midspan deflection for each beam specimen was recorded using a data acquisition system at predetermined intervals. In order to achieve a smooth load-deflection curve using the hydraulic hand jack, beams were loaded continuously to failure, and loading was continued to crushing of the concrete. In order to examine the propagation of the cracking pattern 2 digital DV video cameras were used, on each side of the beam.

The beams were loaded to a final deflection of 25mm. At this point the deflection equalled more than 5 times the allowable deflection the beams were deemed unserviceable. For the purposes of this experiment failure was defined as the load deflection started to decline following reaching the ultimate load. In order to examine the behaviour of the beam immediately following ultimate load the load deflection curves show an additional 1.0mm deflection. This will be reflected when the load deflection curves are presented in Chapter 4.

Mapping of the cracks was performed in a very similar manner to the corrosion cracks. The new cracks were traced onto the beams, crack widths were measured and then photographed. Later, sketches were made for the crack patterns of each beam. These sketches, along with visual observation were used to assess the influence of the corrosion cracks on the mechanical testing failure.

## **3.4 Phase Four: Data Collection**

### **3.4.1 Mass Loss**

After testing, the tensile reinforcement was extracted from each specimen to determine the amount of mass loss and the extent of corrosion. Special consideration had to be given to the concrete within the flexural area since testing would later be performed in order to determine the chloride content. For this reason, special efforts were made to remove the concrete within the flexural region. Using a small sledge hammer and chisel was effective in this respect. Portions of the concrete around the reinforcement were removed and labelled for the dust collection process

later. Once the concrete samples for testing had been obtained a small jackhammer was used to remove the remainder of the concrete surrounding the reinforcing steel.

The cleaning of the reinforcing steel was done in two phases. First, a steel wire brush attachment was used with an electric drill to remove all remaining concrete. Then, the bars were soaked in dilute hydrochloric acid for 1.0h to achieve a thorough cleaning (Du et al., 2007). Following cleaning, the bars were weighed in order to obtain the corroded mass. This mass was used to determine the percent mass loss in each beam specimen.

### **3.4.2 Chloride Ion Content**

The chloride ion content of concrete is critical to the life of the reinforcement, because small amounts of chloride can disrupt the passive layer that protects the steel from corrosion. This was examined in detail in Chapter 2. Therefore, to assess the condition of the deteriorating concrete, it is essential to determine the chloride concentration in the concrete. A chloride ion selective probe was used to determine the chloride ion profile for each specimen according to ASTM standard C1152-90 method.

In the field it isn't practical to demolish the beams, remove the corroded steel, and measure the mass loss of the steel due to corrosion. For this reason, investigators must look at different ways to evaluate concrete beams that do not require demolition. One such method is the measurement of the chloride ion content of the concrete. Higher chloride ion contents near the reinforcing steel will indicate a higher state of corrosion within the steel. This test can be performed in the field

by obtaining a dust sample from the hardened concrete. Previous research has shown that there is a strong relationship between mass loss and the chloride ion content at the steel level (Amleh & Mirza, 2004).

Samples were obtained from each specimen at three different locations by drilling three holes in the concrete and collecting the dust produced across the diameter of a specified location. The concrete powder was collected from three different depths (surface, 15mm and 30mm/bar depth), to determine how the chloride content changed with depth from the surface. The concrete powder was collected at each location in small plastic bags, sealed and marked.

As stated above, the first step in the test was to obtain a dust sample from the hardened concrete. The concrete dust was then dissolved in a test liquid, provided with the testing equipment. Following dissolution, an electrode was used to measure the electric potential of the solution. The measured voltage was then plotted against a calibration curve to obtain the chloride content for each dust sample. A chloride ion meter is used. The reagents for determining chloride content are as follows:

1. Digestive solution (prepared by mixing 60g of glacial acetic acid, 50g of isopropyl alcohol, and 940g of distilled water).
2. Stabilization solution: (3.75ppm of chloride ions in distilled water).
3. Calibration solutions (3, 9, 90, 180, and 374ppm of chloride ions in distilled water).

The ASTM Standard C 1152-90 and SHRP-S-328, and the probe/voltmeter combination manual's (Phoenix Model CL01502 and Gilson Model HH-344) procedure was used:

The chloride probe was calibrated against five standard chloride solutions. The daily calibration data was regressed linearly to obtain the slope and the intercept of the millivolt readings versus the log of chloride concentration ( $\text{Cl}^-$  ppm):

$$\log_{10}(\text{Cl ppm}) = a.(mV) + b \quad (3.2)$$

where  $a$  = slope

$b$  = intercept

$mV$  = millivolt reading



# 4 RESULTS AND DISCUSSION

This Chapter summarizes the results of the complete responses of 12 beam specimens from the initiation of loading up to failure. The results are subsequently analysed and discussed. For this study, the area of particular interest was the ultimate flexural load carrying capacity of corroded beams. The main variables in the experimental test series were the effect of the level of corrosion on the degree of flexural strength and capacity. Ultimate load has been studied in terms of the three parameters discussed earlier; mass loss, crack width and chloride ion content. Furthermore, the parameters of mass loss, crack width and chloride ion content will be used to evaluate the effects of reinforcement corrosion on beam stiffness as well as evaluated against each other to determine each parameter's effectiveness as an indicator of degree of corrosion.

## 4.1 Introduction

As was mentioned in Chapter 3, the experimental process has been divided into four major phases. They are Phase One: Beam Specimens, Phase Two: Accelerated Corrosion, Phase Three: Mechanical Testing and Phase Four: Data Collection. In order to clearly present the relevant data, the results and discussion will be presented in a similar manner.

- The preparation phase consisted of testing and reporting cylinder strengths, collecting and reporting the data from the corrosion monitoring process as well as describing the cracking patterns and measured crack widths prior to mechanical testing.
- The accelerated corrosion phase consisted of the accelerated corrosion procedure undertaken in order to simulate the effects of localized reinforcement corrosion on flexural behaviour of reinforced concrete beams.
- The mechanical testing phase consisted of a description of the failure mode of each beam specimen under the loading conditions as well as analysis of the load deflection behaviour observed in each specimen.
- The final phase consisted of the collection and presentation of all the data following the mechanical testing. This included the calculation of mass loss for each specimen, the measurement of the chloride ion content in each beam as well as the charts and figures associated with the data. Analysis of the data is included with each section. Summaries of the findings are available in the sections to follow.

As described in Chapter 3, twelve beam specimens were prepared and tested. Three specimens were used as control specimens. Aside from the three control beams, the remaining 9 specimens were subjected to different levels of corrosion using the accelerated corrosion technique summarized in Chapter 3.

After completion of the beam tests the specimens were tested for their chloride ion content at three depths of concrete cover, including at the steel level. Following the chloride ion content evaluation, the reinforcing bars were removed and processed to determine their percentage mass loss. The observed responses of the uncorroded and corroded specimens were compared using the load deflection behaviour of the beam specimens and the information on the crack widths. This information was used to derive the relative beam capacity at different levels of corrosion. Ultimately, the experimental results are analyzed and quantified for the influence of the level of corrosion on beam capacity, residual strength and stiffness.

## **4.2 Preparation**

Different stages of the steel reinforcement corrosion were established to study their effect on the flexural behaviour, ranging from no corrosion at all to severe corrosion at the steel-concrete interface. An electrochemical method was used to accelerate the corrosion within the specimens. Direct current was applied to the reinforcing bar embedded in the beam specimens for increasing periods of time. Beams were immersed in a concentrated sodium chloride solution (5% NaCl by weight of water). The lengths were 0 days (control specimens), 5, 17 and 39 days. In each group there were three beams studied in order to achieve a more comprehensive analysis.

### **4.2.1 Cylinder Compressive Strength**

Results from the concrete cylinder compressive strength testing showed an average strength of 40.2 MPa, which was close to the expected value for the mix design. The mix was estimated

conservatively to have a compressive strength of 35MPa based on the water to cement ratio (Mindess, 2003). The maximum cylinder strength was observed in Beam 7, at 45.70MPa. This corresponded to an average increase of 13.7% from the mean. The minimum strength was observed in Beam 2L, with an average strength of 35.04 MPa. This corresponded to a decrease of 12.8% from the mean. While the average strength was as expected, the deviation from the average was slightly higher than anticipated. This is likely due to the fact that each beam was cast from a separate mix. The mixer available was 80L and only one beam could be cast from each batch. It is much more favourable to cast all specimens from one large batch, but due to the small mixer this was not possible. A large batch from a concrete truck might have been possible but the small forms would have posed a problem. Since concrete is a composite material some deviation is always expected, in this case it was compounded by the fact that each batch was so small, and each beam was cast from a different batch. Figure 4.1 summarizes the average cylinder strength of each batch.

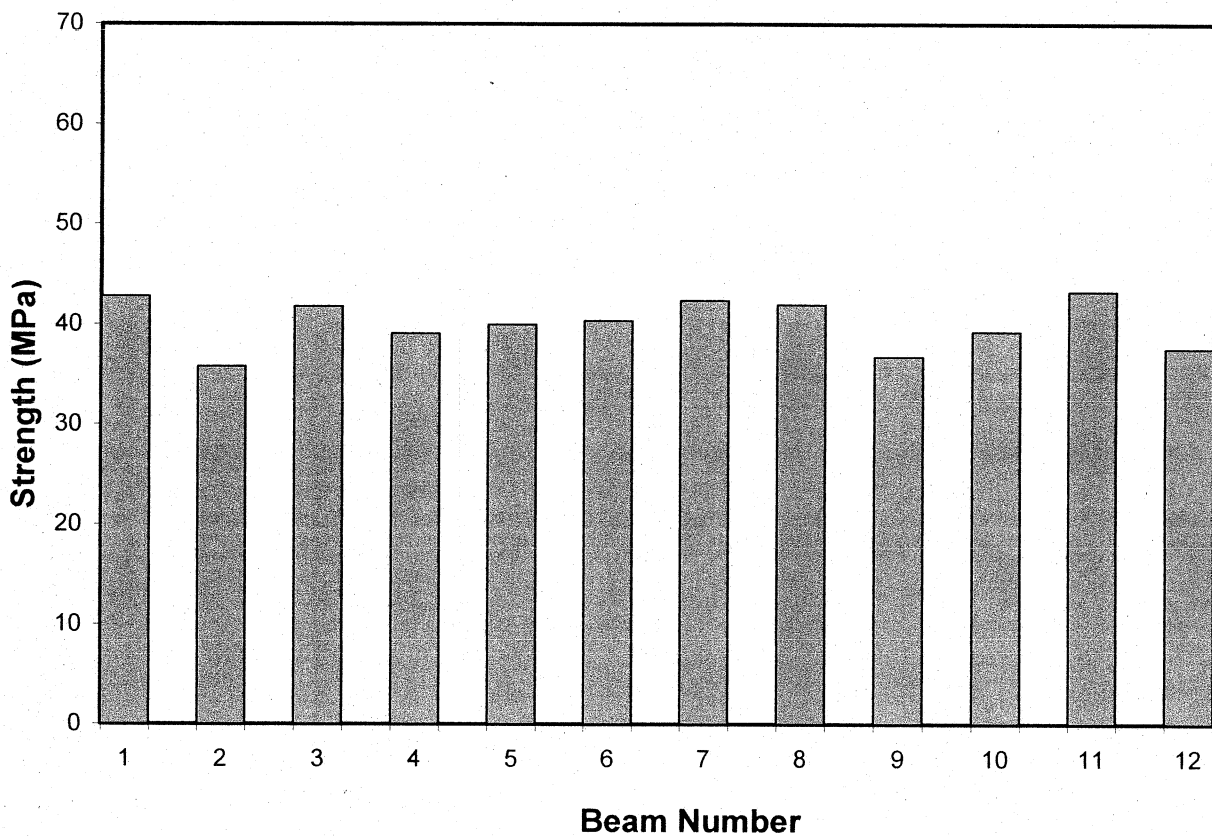


**Figure 4.1: Cylinder compressive strength for each beam specimen**

#### **4.2.2 Accelerated Corrosion Monitoring Process**

As discussed in Chapter 3, the current measurements for each specimen were recorded every 24 hours by means of a SMART Digital Multimeter that read both the current and the voltage. Circuits were connected in parallel to allow for constant current through each bar. However, due to the need to split and share current the result was slightly unequal sharing, as shown in Figure 4.2.

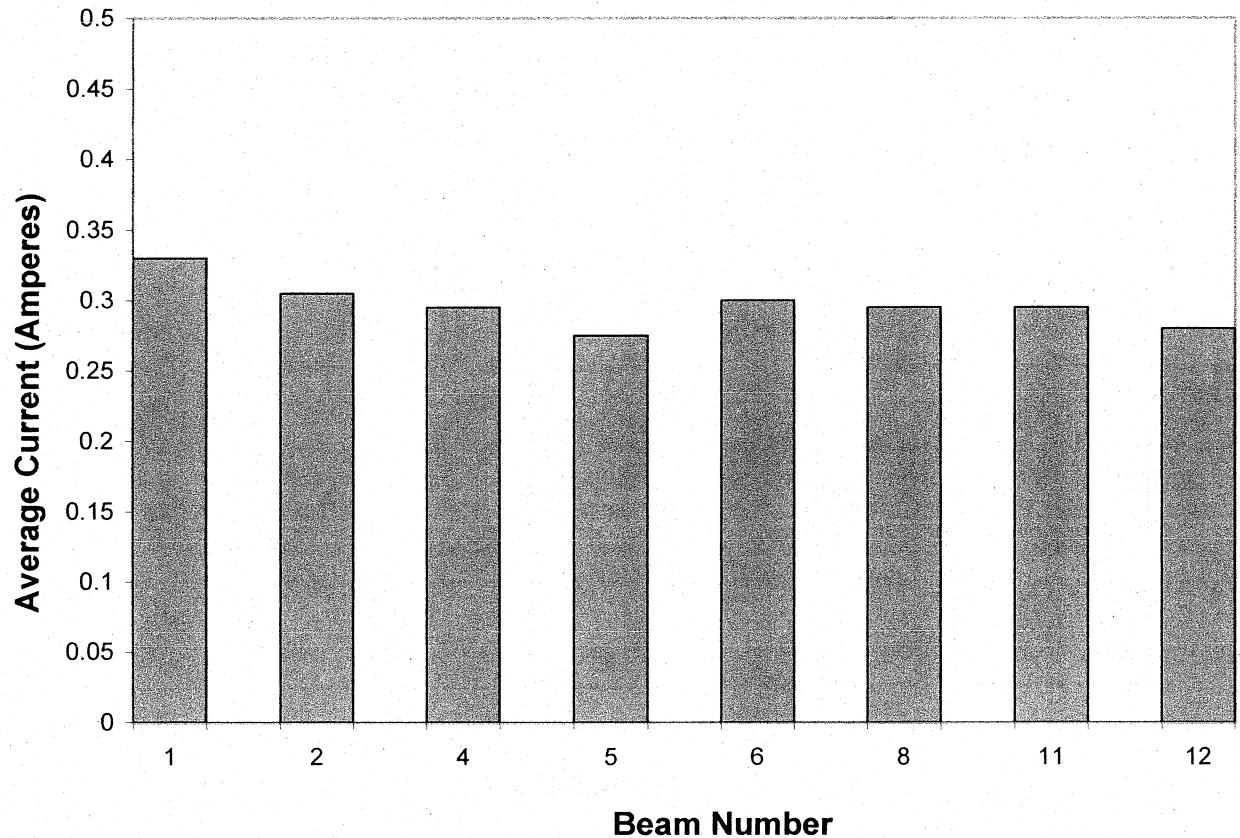


**Figure 4.2 Summary of average current for each beam**

The average current through each bar was equal to 0.30mA. This corresponded to an initial current density, the measure of intensity of accelerated corrosion, was approximately 4000  $\mu\text{A}/\text{cm}^2$ . With respect to the literature reviewed in Section 2 of this report, this is relatively high level current density for the purposes of reinforcement corrosion (ElMaaddawy & Soudki, 2003). However, this current density was selected due to time constraints on the project.

In general, the initial current levels corresponded well to the expected 0.3mA. However, as the resistivity of the reinforced concrete specimens changed due to the corrosion, the current constantly adjusted accordingly. For example, if the resistance for one reinforcing bar dropped at

a higher rate than that of the resistance of another bar connected in parallel, then the reinforcing bar with the lower resistance would take a correspondingly larger portion of the current.

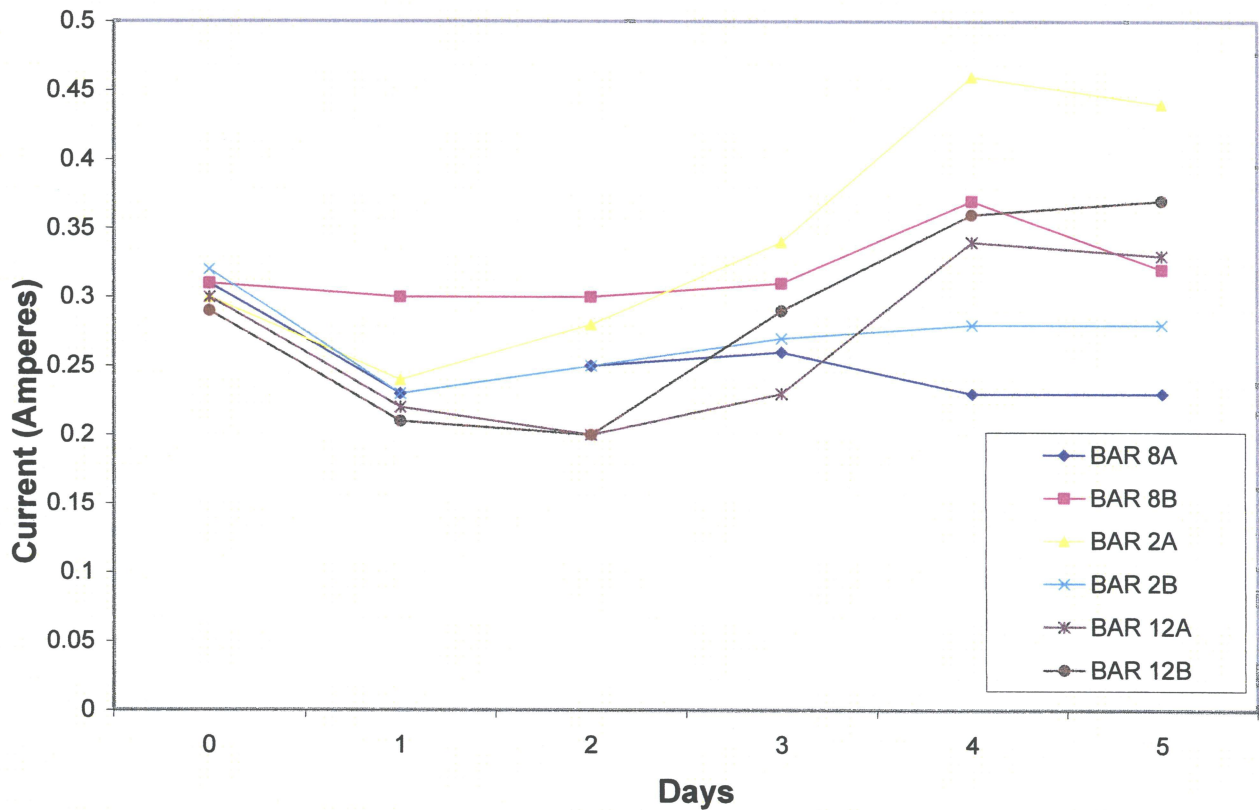


**Figure 4.3: Current summary for lowest level corrosion group**

Monitoring the changing current over time revealed the following results:

*Lowest Level Corrosion Group:* In the lowest level corrosion group, it is observed that Bar 2A received the highest average current at 0.34mA, 0.04mA above the average of 0.30mA (recall that Bar 2A specifies Bar A from Beam 2), corresponding to an increase of 13%. Bar 8A received the lowest current levels with an average current of 0.25mA, corresponding to a decrease of 17%. Figure 4.3 summarizes the changing current levels of the lowest level corrosion group.

*Mid-Level Corrosion Group:* In the mid-level corrosion group, it was observed that Bar 1B had the highest current average at 0.36mA, corresponding to an increase of 20%. The bar with the lowest current average was 3B with an average current of 0.26, corresponding to a decrease of 13%. Figure 4.4 summarizes the changing current levels of the mid-level corrosion group.

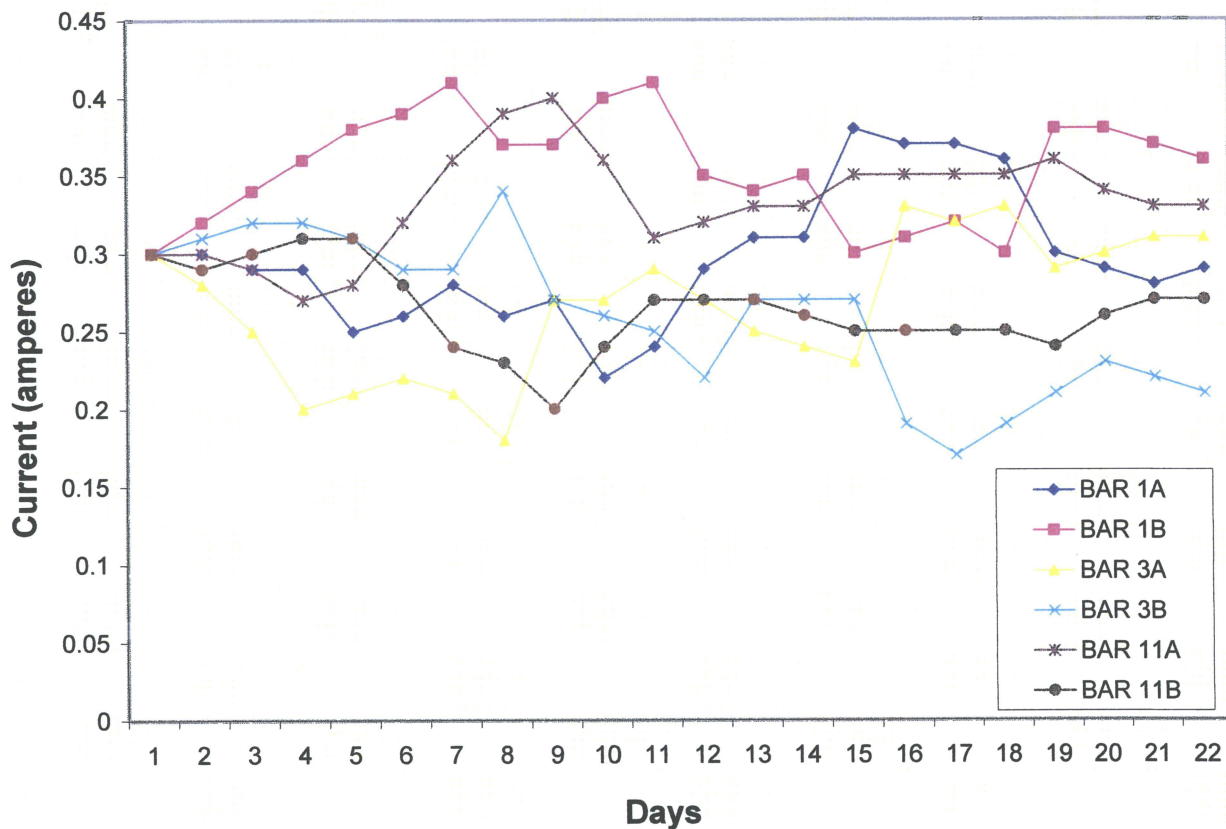


**Figure 4.4: Current summary for mid-level corrosion group**

*Highest Level Corrosion Group:* For the highest level corrosion group, the bar with the highest average corrosion was 4A. It had an average current of 0.33mA, corresponding to an increase of 10%. The lowest observed average current was in Bar 4B with an average current of 0.26mA. This corresponds to a decrease of 13%. Figure 4.5 summarizes the changing current levels of the highest level corrosion group.

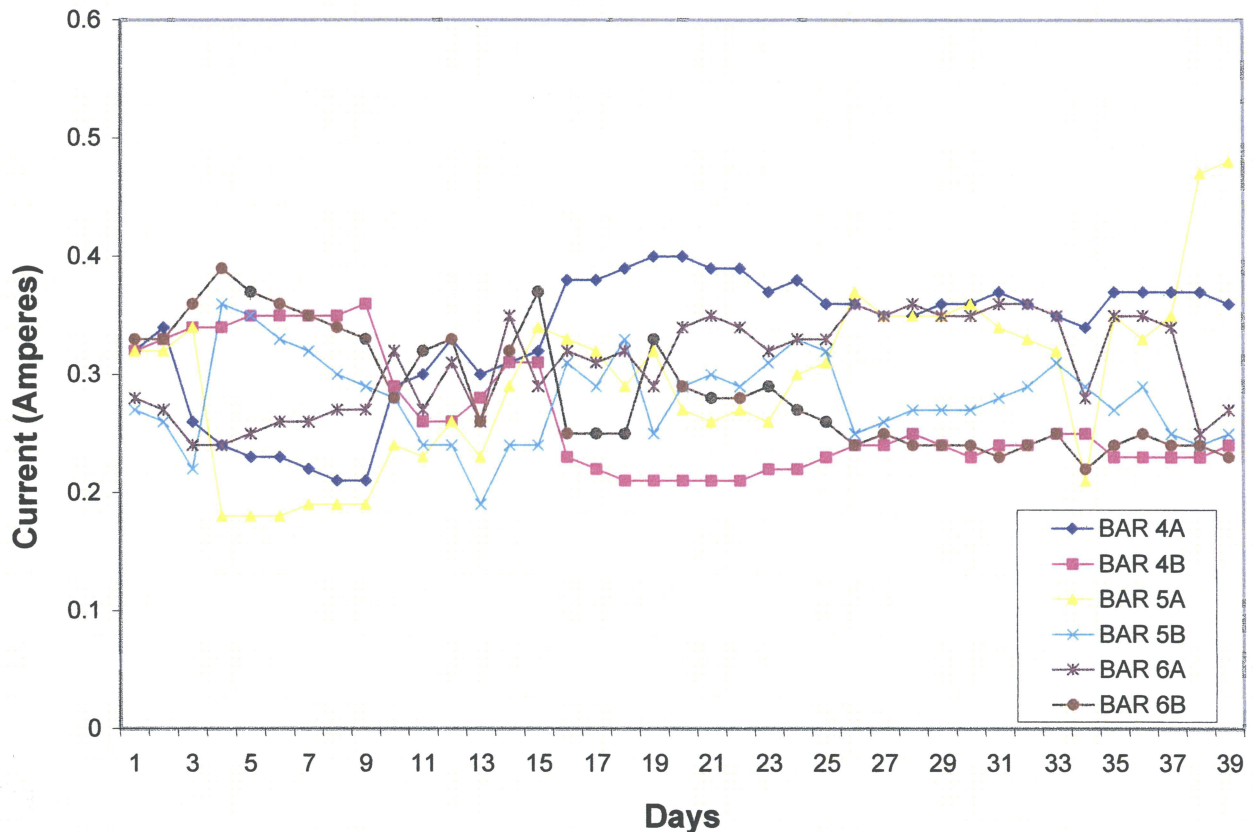


**Figure 4.5: Current level for highest level corrosion group**

It was observed that wherever one bar was receiving the majority of the current, most often the adjacent bar in the same beam generally received less of the current. This creates an unequal degree of corrosion within the beam itself, with one bar corroding at a higher rate than the other. However, this unequal sharing was not detrimental to the study. It has been shown that varying degrees of corrosion between reinforcing bars has little effect on the load deflection behaviour of the corroded beams. (Mangat & Elgarf, 1999). It should be noted that the variation in current increased with time as the specimens changed electrical resistances.

The current data was also analyzed with respect to average current per beam, since the reinforcing bars act in tandem. Observation showed that Beam 1 received the highest average

current value over its accelerated corrosion process, with an average current value of 0.33mA. Beam 5 received the lowest average current value, averaging only 0.28mA of current for each of its two bars over the duration of its accelerated corrosion process.

The unequal sharing of current was not of paramount importance for this study, it was simply an effect of the corrosion process. It is unlikely that field investigations would reveal identical corrosion among reinforcing steel bars of in-service structures. It also created a broader range of corrosion stages within the beams studied. For example, if the current had been equally shared between all reinforcing bars, the resulting mass loss for each bar would be very similar for each corrosion group. By the unequal sharing of current the resulting mass losses were varied and as a result it was possible to study a more varied set of corrosion stages, since beams within the same corrosion group received different amounts of current. In this respect it was beneficial to this study.

### **4.2.3 Crack Propagation and Corrosion Patterns**

In general the crack propagation patterns observed were similar in each specimen. The first recognizable cracking was observed on day 4 of the corrosion process for each beam with the one exception, Beam 11M, where first cracking was observed on day 5. This was likely due to the fact that Beam 11M did not receive as much current as Beam 1M, connected in parallel, over the first 5 days (see Figure 4.4). This allowed for exaggerated corrosion in one beam, and reduced corrosion in the other. This trend was also true for each situation where crack

propagation occurred very quickly on only one side of a beam. In these cases crack propagation occurred more slowly in the opposite steel reinforcing bar.

Also observed in each bar that underwent prolonged corrosion (Groups 2 and 3) was a stage of plateau in the crack width, which held constant for several days without widening. This plateau began when crack widths were approximately 0.5 to 0.6mm (around days 10 to 17) and lasted about 3-5 days.. A theory on this phenomenon is that at this stage corrosion had begun to spread to the painted areas of the reinforcing steel. Corrosion continued but the evidence was not in crack widening, but rather in crack lengthening, which was not addressed in this research. Once the beam had cracked continuously in the longitudinal direction, corrosion continued throughout the bar and the cracks continued to widen. Figure 4.6, 4.7 and 4.8 show the crack width propagation each corrosion group.

As expected, the beam specimens that were exposed to the accelerated corrosion process the longest exhibited the widest crack widths. Table 4.1 provides a brief visual description of each beam following the accelerated corrosion process. Cracking is rated as light, significant, major or severe (the most advanced). A comparative analysis between crack width and mass loss is performed later in this chapter.

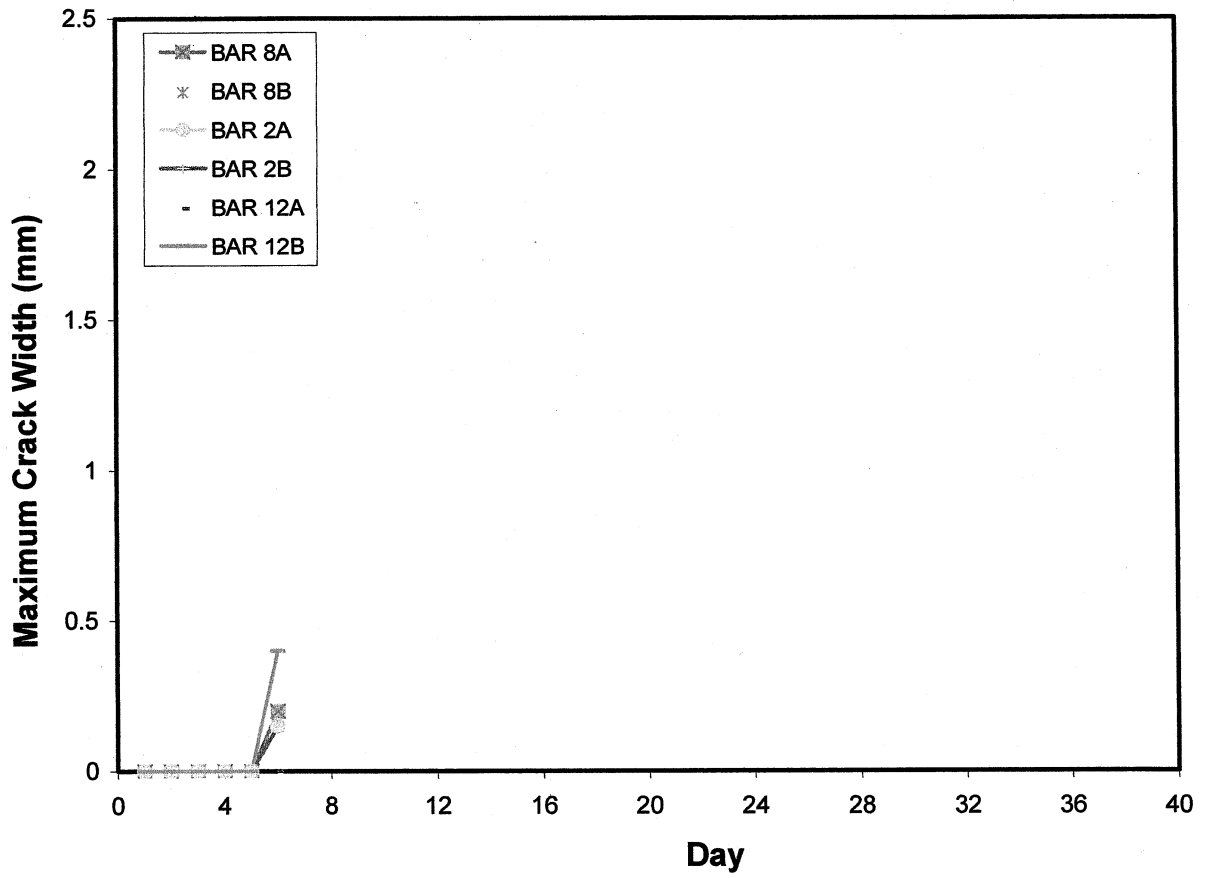


**Figure 4.6: Crack propagation for lowest level corrosion group**

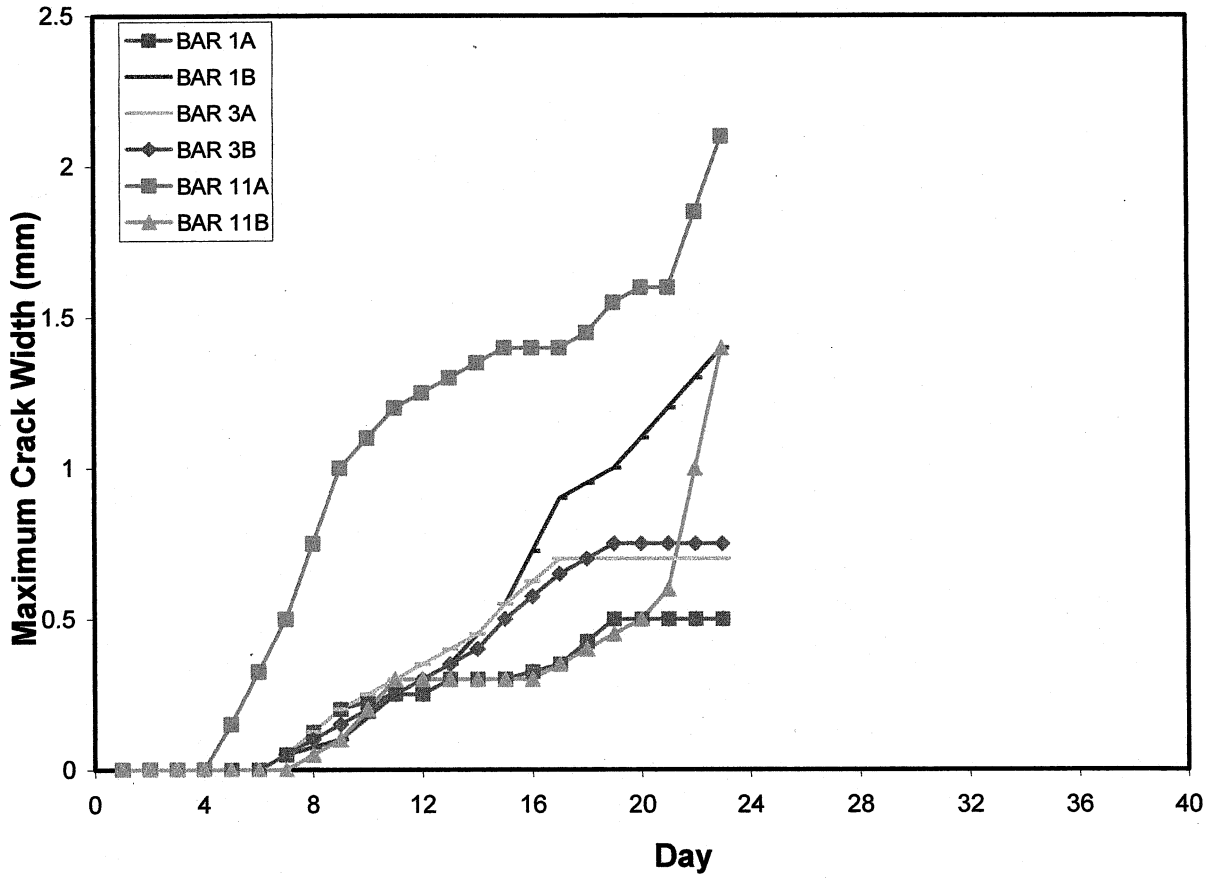


**Figure 4.7: Crack propagation for mid-level corrosion group**

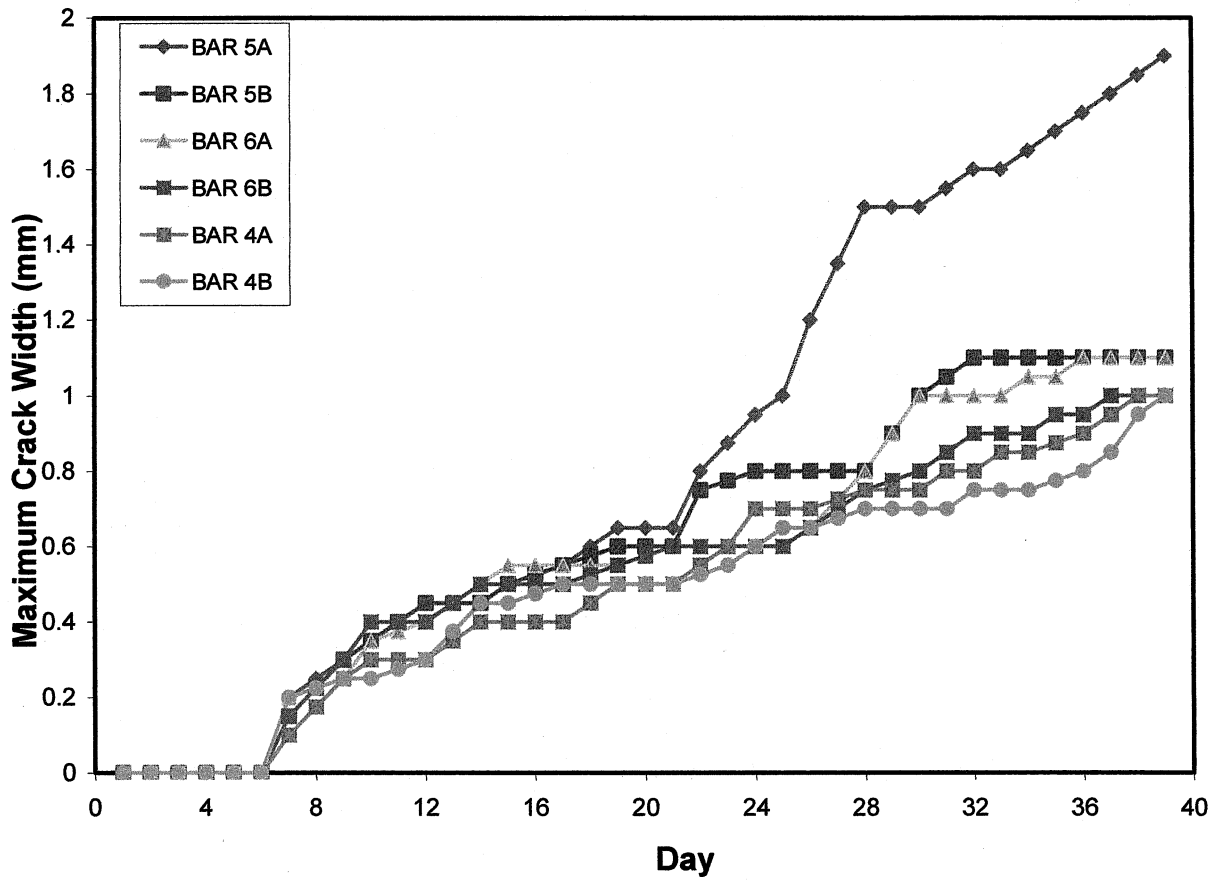


Figure 4.8: Crack propagation for highest level corrosion group

**Table 4.1 Visual descriptions of corroded beam specimens**

Corrosion Group	Beam No.	Visual Description
Lowest Level Corrosion Group	2L	Light longitudinal cracking on bottom face only, central area Light transverse cracking at central stirrups, Side A and B
	8L	Significant longitudinal cracking on bottom face only, central area Significant transverse cracking bottom face, central area
	12L	Light longitudinal cracking on Side A only, central area Light transverse cracking at central stirrups, Side A
Mid-Level Corrosion Group	1M	Major longitudinal cracking entire length, Side B Major longitudinal cracking entire length, bottom face Significant Transverse cracking on Side A and b and top face
	3M	Major longitudinal cracking, entire length Side A and B Significant transverse cracking on four faces, central area Light transverse cracking outside central area
	11M	Major longitudinal cracking entire length, Side A Significant longitudinal cracking entire length, bottom face Significant transverse cracking all faces, central area
Highest Level Corrosion Group	4H	Severe longitudinal cracking on Side A, entire length Severe longitudinal cracking on bottom face, entire length Significant transverse cracking at most stirrup locations, all faces
	5H	Severe longitudinal cracking Side A and B, entire length Significant cracking on bottom face, entire length Significant transverse cracking at most stirrup locations, all faces
	6H	Severe longitudinal cracking Side B, entire length Major longitudinal cracking Side A, entire length Significant transverse cracking at most stirrup locations, all faces

#### 4.2.3.1 Lowest Level Corrosion Group

At this lowest stage of corrosion, cracking was only noticeable on one face of the beam. As expected, cracking began at the centre portion along the flexural reinforcement that was unpainted. Corrosion had not advanced at other areas of the beam enough to cause cracking. An example of the extent of the cracking on one face is seen in Figure 4.9, showing one side of Beam 11M.

Despite cracking being confined to only one face of the beam for the lowest corrosion stage, crack width had advanced to a maximum of 0.3mm. This was observed to be a rapid progression following first cracking, and was attributed to the relatively high current density that was applied to the reinforcing steel.

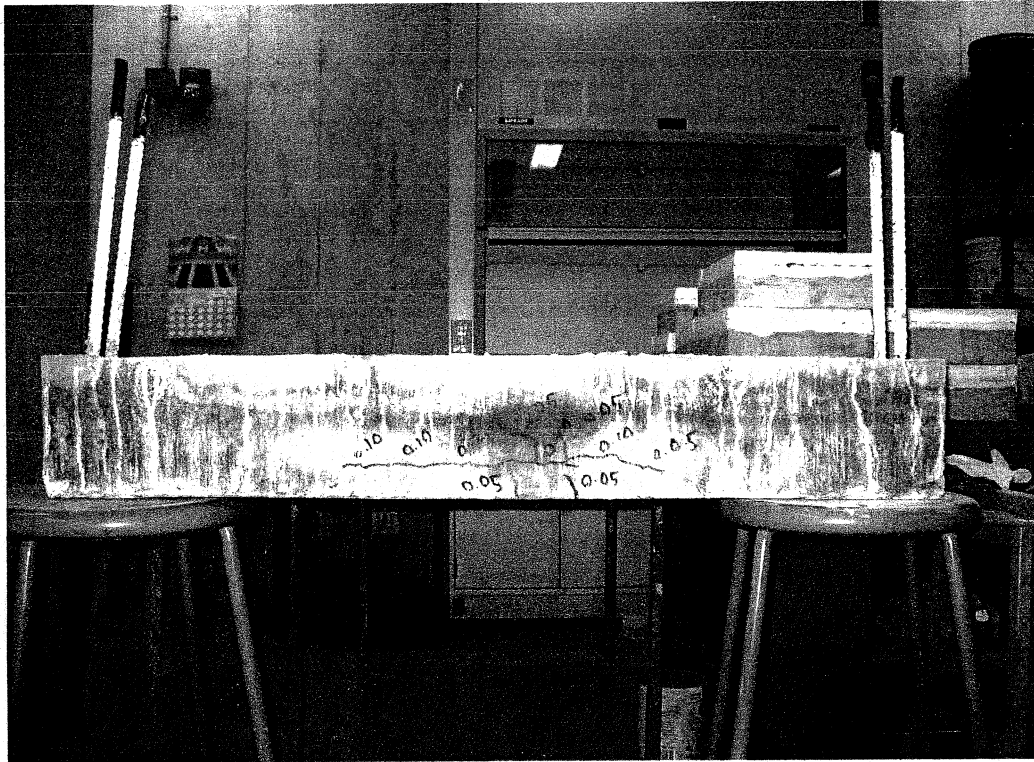


**Figure 4.9: Cracking on only Side B of Beam 11M**

#### **4.2.3.2 Mid-Level Corrosion Group**

In the mid-level corrosion group, cracking had advanced past the unpainted middle section of the beam. Longitudinal cracks had spread the whole length of the beam and signs of cracking along some of the stirrups were evident. However, in spite of the cracking apparent outside of the

central zone, cracking near midspan of the beams continued to propagate. The average crack width for the 17 days corrosion stage was 2.32mm, as opposed to 0.30mm at the earlier stage.

The extent of cracking outside the central unpainted zone was likely due to the loss of paint in these areas. As the corrosion process developed, paint was dislodged by the adjacent corrosion taking place and corrosion continued to progress down the bar length. While crack length was not reported in this study, the qualitative evidence gathered supports this hypothesis, in particular the crack progression from centre towards the ends of the beam.

#### **4.2.3.3 Highest Level Corrosion Group**

In the final stage of corrosion, the corrosion cracking was even less confined to the desired central area. At this stage, cracking was evident at most stirrups, and considerable cracking had taken place where the tensile reinforcement exited vertically from the top of the beam. Cracking was very prominent on all faces of the beams, including the ends of each beam.

In addition to the widespread cracking, the crack width at midspan widened at a lower rate. The average crack width at this stage was equal to 2.75mm, which was not proportional to the length of corrosion exposure. This was likely due to the fact that corrosion was taking place elsewhere along the beam, where the paint had been cracked in the manner explained above. Thus, corrosion at midspan failed to continue at the same rate as before. This risk of this behaviour is that enough corrosion and cracking took place outside of the central area to vary the behaviour of the beams in flexural testing.

### 4.3 Mechanical testing

Following the accelerated corrosion process and mapping the corrosion cracks, the beam specimens were mechanically loaded according to the method described in Section 3.3. After observing a bearing failure in the first beam tested, a small bearing plate was installed on top of the roller in order to spread the load. Due to the bearing failure, Beam 7 (a potential control beam) was eliminated from the study. This new bearing plate method was successful and the following tests proceeded without incident. A photo of the bearing failure can be seen in Figure 4.10.

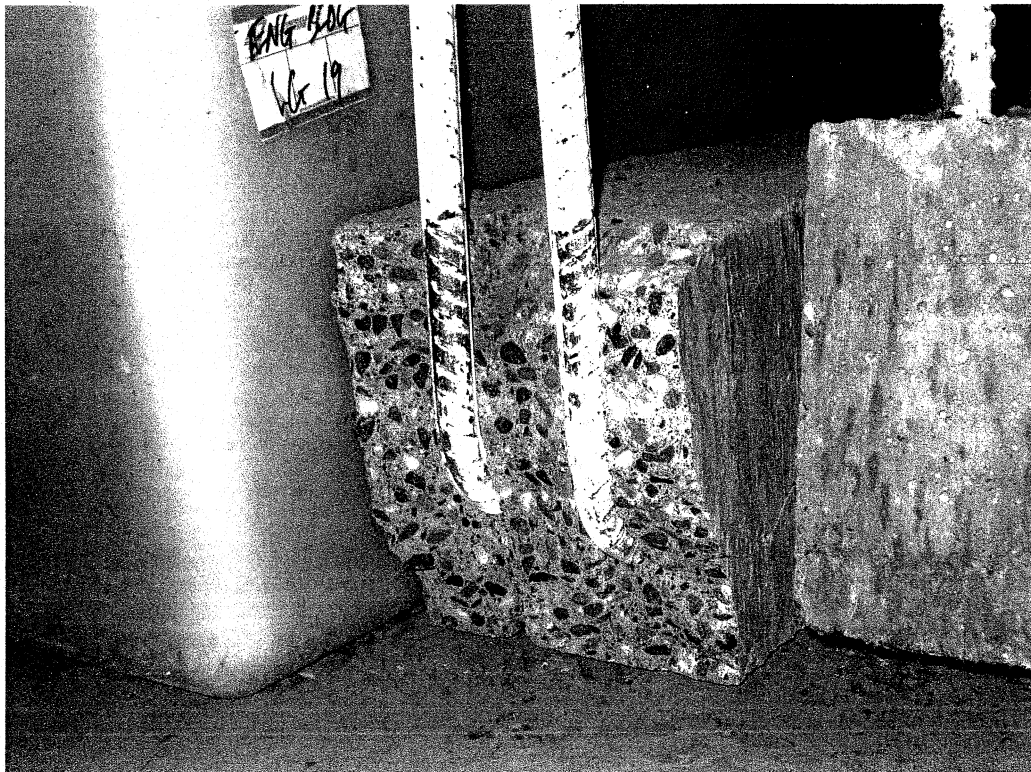


**Figure 4.10: Bearing failure of Beam 7**

The flexure test was conducted as shown in Figure 3.3. The load and midspan deflection data for each specimen was recorded at pre-determined load intervals up to failure. The data generated was utilized to plot load-deflection curves for each of the tested specimens. The ultimate load and the corresponding midspan deflections for the beam specimens are presented in Table 4.2.

**Table 4.2: Ultimate Loads and Corresponding Midspan Deflections**

Beam No.	Ultimate Load	Midspan Deflection
	kN	mm
9C	152.1	5.7
10C	150.6	5.4
2L	132.0	7.4
8L	142.6	7.1
1M	131.5	7.6
3M	127.8	8.4
11M	118.1	9.7
4H	115.9	8.4
5H	120.5	7.0
6H	114.1	6.5

### 4.3.1 Effect of Corrosion on Load deflection Behaviour

#### 4.3.1.1 Control Specimens Group

The two control beams were tested for determining the reference flexural strength. They both failed in flexure, as expected. The failure was first characterised by the formation of several bending cracks, followed by the yielding of the bars, followed by few shear cracks and finally concrete crushing. Upon observation of their load-deflection behaviour, we can see that their curves were

almost identical to one another. This provided much confidence in the setup and testing equipment. Figure 4.11 shows the load-deflection curves for the control beams.

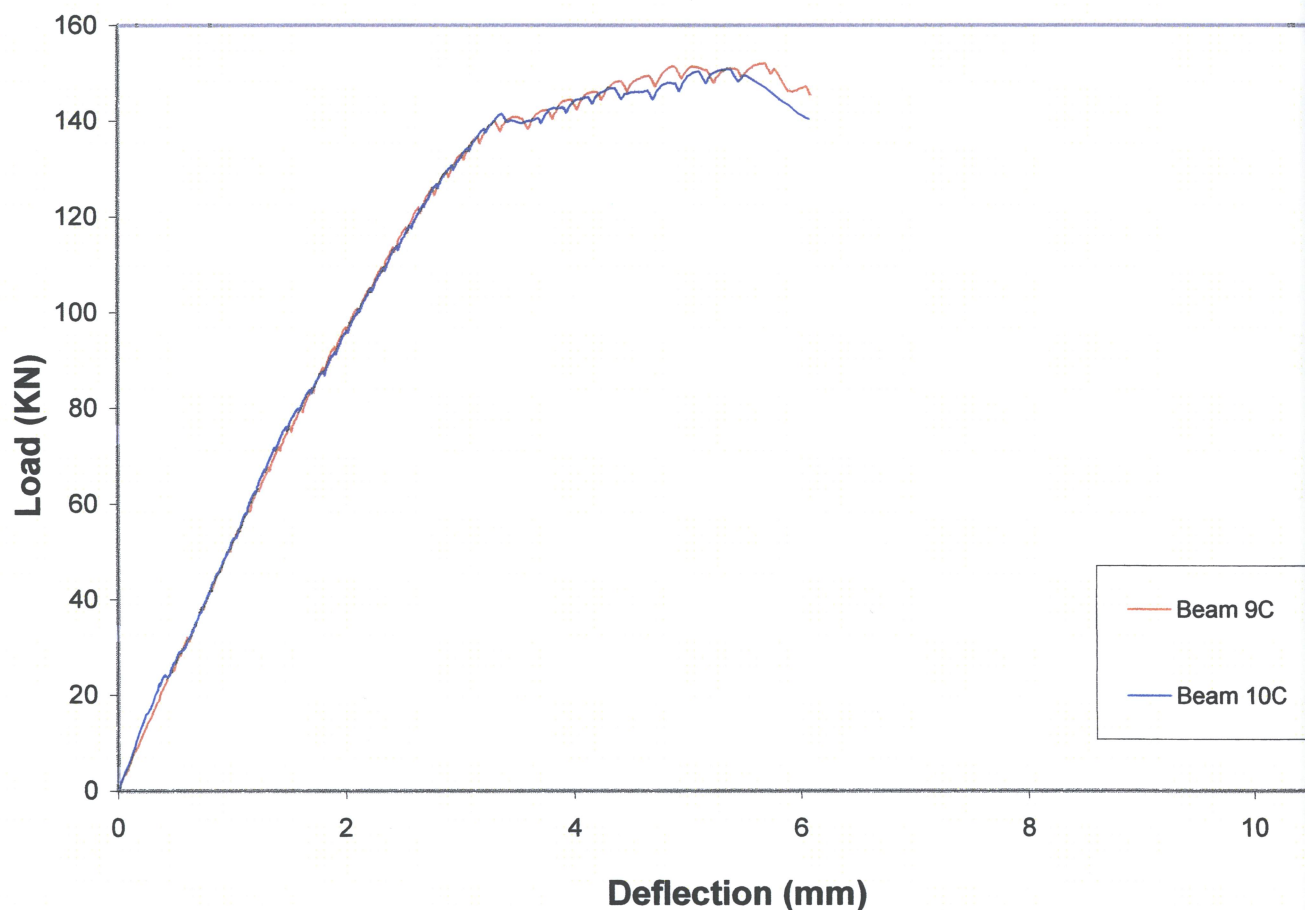


**Figure 4.11: Load deflection behaviour of control specimens**

#### **4.3.1.2 Corroded Specimens**

Load-deflection curves for both control and the corroded beam specimens are shown in Figure 4.10. This data indicates that reinforcement corrosion has a strong influence on the flexural behaviour of the concrete beam specimen. As expected the corroded beams had higher deflection than the corresponding control beams due to the degradation of stiffness of the corroded beams.

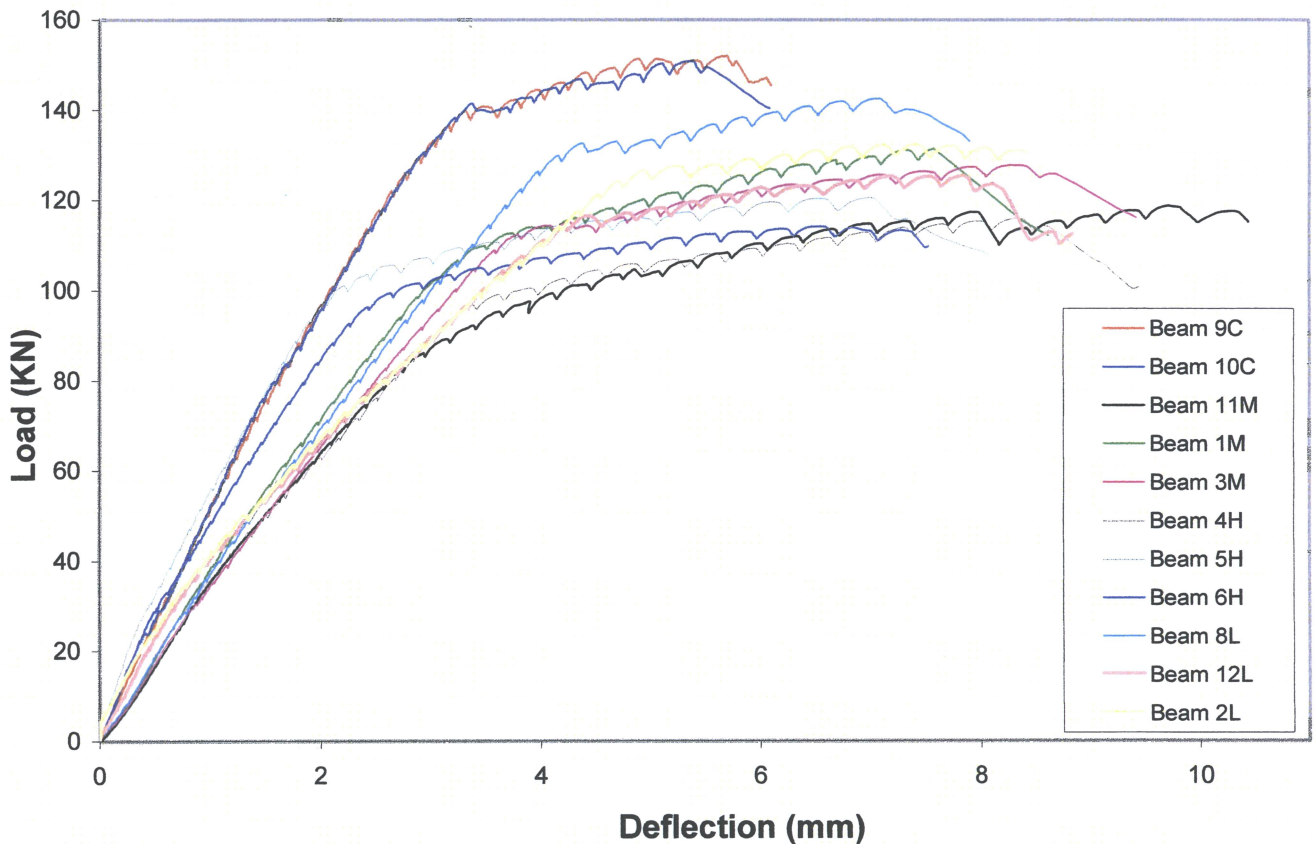


**Figure 4.12: Load deflection behaviour for all beam specimens**

#### 4.3.1.2.1 Lowest-Level Corrosion Group

**Beam 2L:** Beam 2L performed as anticipated. While the initial cracking was entirely confined to the bottom face of the beam, the failure of the beam was flexure. Similarly to Beam 8L, shear cracking was evident but the main cracks were still the flexural failure cracks.

The ultimate load carried by Beam 2L was equal to 132.3kN and the corresponding deflection at this load was 7mm. This result is similar to that found with Beam 8L and fits well with the trends of this study. More insight will be given to the topics of load-deflection behaviour when it is discussed with respect to mass loss, crack width and chloride ion content.

Shear cracking appeared in the lightly corroded beams since enough steel remained to reach the shear cracking stage. The more highly corroded beam specimens yielded prior to shear cracking taking place. This was evidenced in the failure of the control beams as well, where shear cracking was evident but the failure mode was ultimately flexure.

**Beam 8L:** The ultimate load for Beam 8L was 142.6kN and the corresponding deflection was equal to 7.1mm. In spite of the cracking that took place at the bottom of the beam, this is approximately what was expected for this level of corrosion. Observed was a loss in ultimate load and an increase of deflection at ultimate load. This type of result is supported in similar studies (Almusallam et al., 1996; Cabrera, 1996).

Beam 8L failed in flexure; however pronounced shear cracking was observed as shown in Figure 4.13 and 4.14. Shear cracking was also observed in the control specimens. Corrosion cracking was light, with the exception of the bottom of the beam, where it was quite pronounced. It can be deduced from the Figure 4.13 that corrosion cracking played a major role in the failure of this beam. Of all the beams, Beam 8L was one of the few to have its primary longitudinal cracking located primarily on the bottom face. This led to more pronounced lateral cracking and consequently a reduced load carrying capacity. This reinforces the point of the variability seen in corroded beams, where corrosion cracking can lead to unexpected results.



**Beam 12L:** Beam 12L failed in shear. This was unexpected and was likely to due a problem within the steel reinforcing cage, and the spacing of the stirrups. If stirrups within the cage had been slightly misaligned, a shear crack could have propagated through the beam without hitting any stirrups. Another potential problem could have been poor concrete contact to the steel cage due to inadequate vibration. The light corrosion cracking pattern did not suggest that large losses in load carrying capacity should have been expected. The ultimate load reached was 125.5kN with a corresponding deflection of 8.0mm. While a loss in serviceability was expected even at low levels of corrosion, it was not anticipated to this degree. In addition, the ultimate load is significantly lower than was anticipated.

#### **4.3.1.2.2 Mid-Level Corrosion Group**

**Beam 11M:** Beam 11M failed in flexure as expected. A significant loss of ultimate strength was observed, corresponding to a strength loss of 13%. The behaviour of Beam 11M was unique in that it peaked very late, after an initial drop.

This change in behaviour was accompanied with much higher deflections at ultimate load. For Beam 11M the deflection at ultimate load was equal to 9.7mm. This corresponds to a deflection  $L/90$  where the control beam deflection at ultimate load was equal to  $L/180$ . This is a significant loss in serviceability.

It did not appear as though failure occurred specifically through any of the pre-existing corrosion cracks. In fact, it appeared as if most of the failure cracks were completely independent of the

corrosion cracks. On Side A however, it did appear as if one of the main flexural cracks began at one of the small vertical/transverse corrosion cracks, shown in Figure 4.15. However, this was not evidenced on side B.

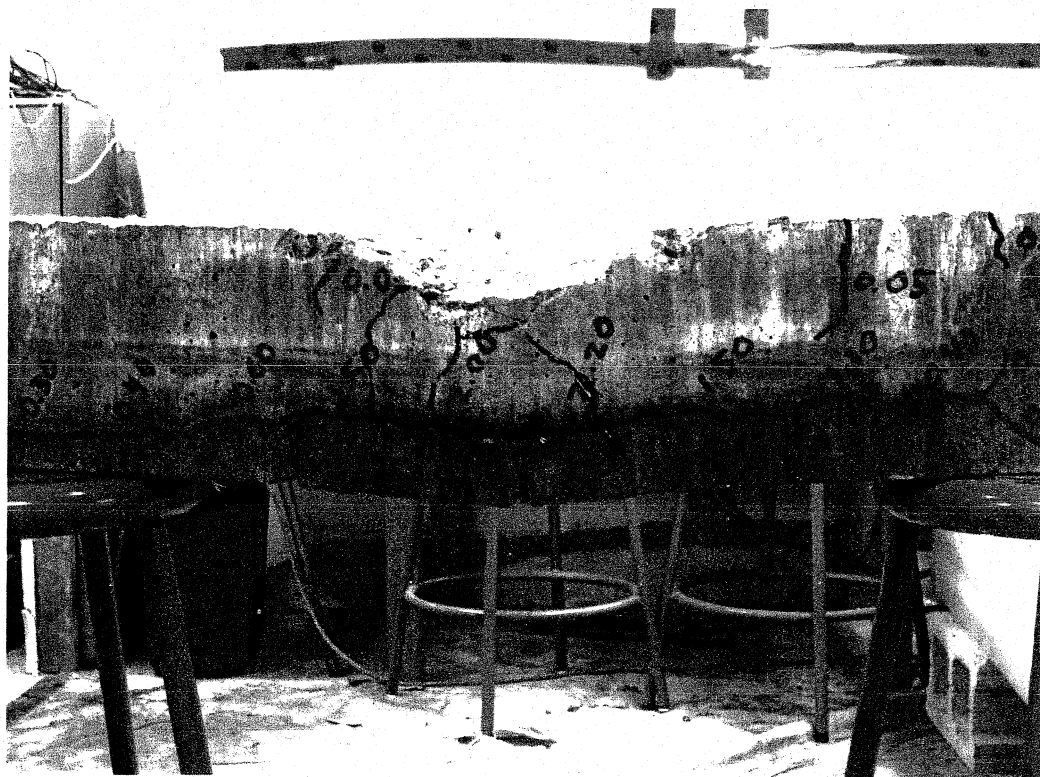


**Figure 4.15: Failure through Corrosion Cracks on Beam 11M**

Of course, it is very difficult to detect microcracking with only a crackscope and therefore difficult to understand the full extent of the corrosion damage of each beam. It is likely that microcracks played a role in ultimate failure.

**Beam 1M:** Beam 1M failed in flexure. No transverse cracks were visible prior to testing and therefore visible transverse cracking did not appear to play a role in the failure mechanism. Again, it is difficult to determine the contribution of microcracking to the failure.

Ultimate load carried by Beam 1M was 131.5kN, with a corresponding deflection of 7.6mm. This fit well with the other data collected, as well as with the other specimens of similar corrosion level.

**Beam 3M:** In Beam 3M there was evidence of longitudinal cracking due to corrosion playing a role in flexural failure. As anticipated the beam failed in flexure. The evidence gathered from the bottom face of the beam is of particular interest. Prior to testing, a small crack large enough to measure (0.05mm) was noted on the bottom of the beam, running perpendicular to the tensile reinforcing steel, shown in Figure 4.16. Due to its' position, this crack is very likely due to the corrosion of the tensile reinforcing bars located above it. As Figure 4.16 shows, failure cracks propagated directly through this existing crack. Despite longitudinal cracks appearing to have little effect on failure, secondary cracking in the transverse direction appears to play a significant role.

Beam 3M reached an ultimate load of 127.8kN and a corresponding deflection of 8.4mm. This again fits with the principle that corroded beams will exhibit excessive deflections when compared to uncorroded beams of similar proportions.

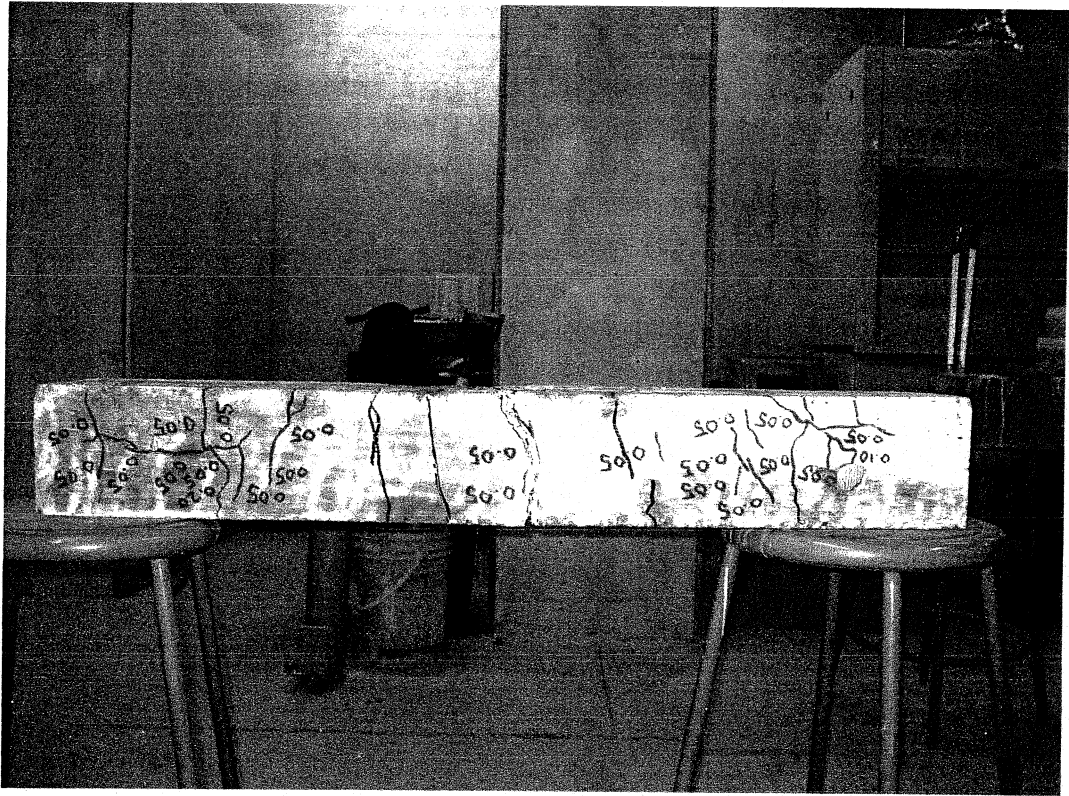


**Figure 4.16: Failure cracking on bottom face of Beam 3M**

#### **4.3.1.2.3 Highest-Level Corrosion Group**

**Beam 4H:** Beam 4H was severely cracked prior to testing. However, very little of the serious cracking was perpendicular to the longitudinal reinforcement, towards the centre of the beam. Correspondingly, photos of the failed beam show that pre-existing cracks did not play a major role in the flexural failure of this beam. In fact, the cracks that appeared to have played the most significant role are the cracks at the first stirrups.

One effect of the corrosion was that a portion of the steel cover concrete was dislodged during testing. This is shown in Figure 4.17. While spalling is unsightly over the service life of concrete structures, it can also affect the moment of inertia of the section and therefore the stiffness.

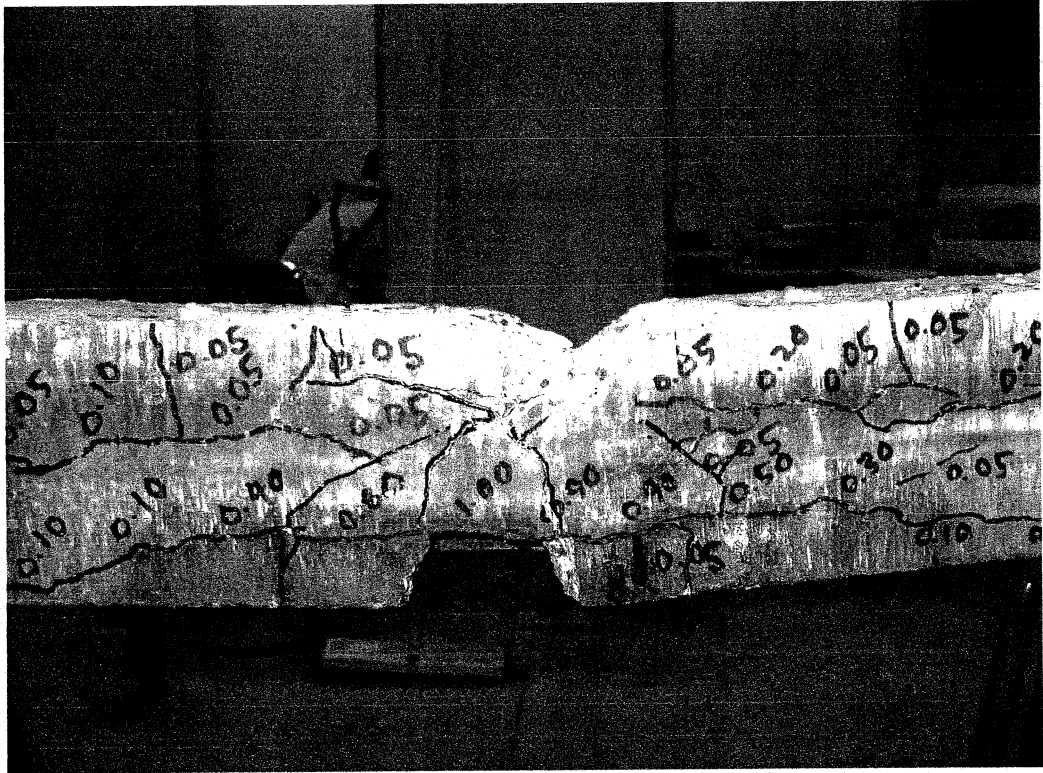


**Figure 4.17: Concrete spalling following testing of Beam 4H**

The ultimate load at failure was equal to 115.9kN, a loss of 23.3%. This relationship will be studied more closely in the discussion sections to follow. The deflection corresponding to this ultimate load was 8.4mm. Again, this was a considerable increase from the 5mm indicated by the control beams.

**Beam 5H:** With Beam 5H, again there was evidence of longitudinal corrosion cracking playing a role in flexural failure. It was observed that the main flexural vertical crack at the bottom of the beam passes through the pre-existing crack due to the corrosion of the longitudinal steel. As with Beams 11M and 3M, it did not appear to be the wider longitudinal cracks which played a major role, but the secondary vertical cracks that seemed to accelerate the failure. Once the flexural cracks reach the longitudinal cracks they may propagate in the longitudinal direction and locate planes of weakness in the concrete. This was evidenced on both sides of the beam and can be seen prominently in Figure 4.18.

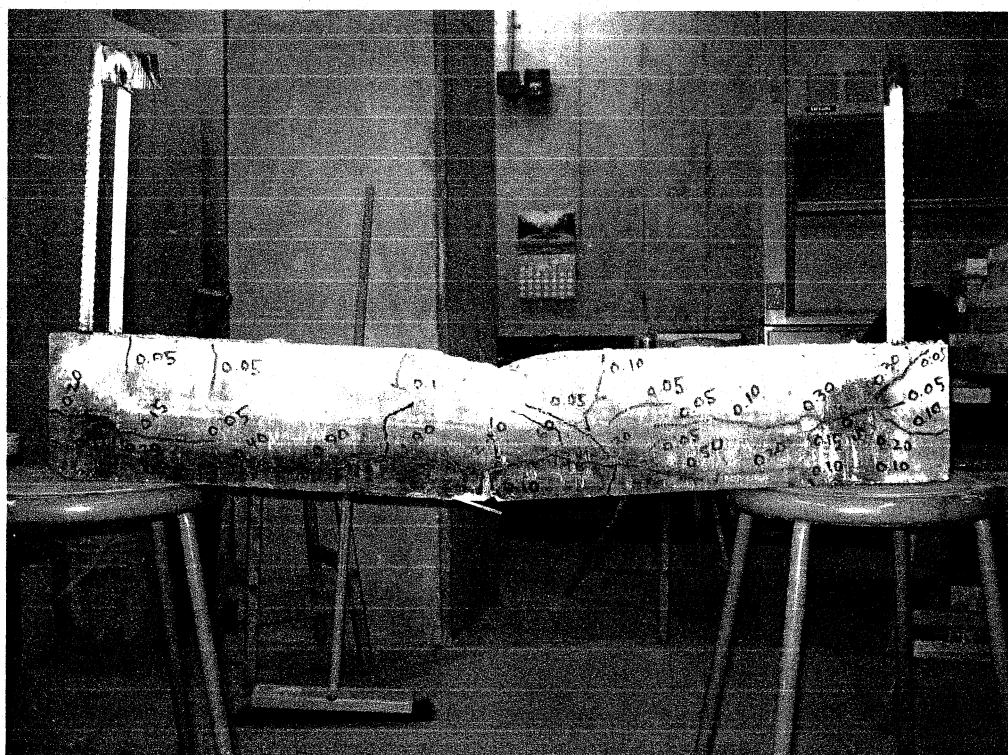


**Figure 4.18: Propagation of failure cracks of Beam 5H**

Beam 5H had a ultimate load of 120.5kN and a corresponding deflection at ultimate load of 7.0mm. While this is certainly a significant drop in ultimate load carrying capacity and a

noticeable drop in serviceability, it is perhaps not as much as expected for a beam that was subjected to such long-term accelerated corrosion.

**Beam 6H:** Beam 6H also failed in flexure. The ultimate load reached during testing was 114.1kN. This large strength loss was expected from the beams of higher corrosion levels, when compared to the results of Beam 5H. The corresponding deflection at peak load was equal to 6.5mm. This deflection was slightly surprising compared to some of the other results obtained but further investigation, in Section 4.4, will reveal why these two beams (5H and 6H) behaved in this surprising manner, with respect to their deflections.

No vertical cracks were observed with the crackscope prior to testing, and therefore it is difficult to determine how much of a role the pre-existing corrosion cracks played in the flexural failure of the beam. If any, we can assume it was a secondary role by weakening the concrete cover and allowing the faster propagation of the cracks during testing. Loss of cover leads to a loss of stiffness that is apparent in the summary graph, Figure 4.12.

## **4.4 Collection and Interpretation of Data**

This phase consisted of the collection of data following the testing of the specimens. Many indicators of performance and behaviour were contained within the failed specimens and it required considerable effort to extract as much data as possible.

There were two goals of this phase. One, to collect the mass loss of each reinforcing bar and compute to the average mass loss of each beam; and two, to extract the chloride ion content at each bar and compute the average chloride ion content for each beam. These parameters, along with the crack width measured earlier, would be essential as indicators of degree of corrosion.

#### **4.4.1 Mass Loss**

The observations and measurements of the changes in the reinforcing bar diameter, strength, and the extent of corrosion pitting, have been evaluated to determine the effect of the corrosion attack after exposure of the test specimen to the aggressive environment for varied periods of time. Loss of metal relative to the original reinforcing steel bar weight was evaluated. For this purpose, the specimens were broken open to retrieve the reinforcing bar after the completion of the test. Preparation, cleaning and evaluation of weight loss were carried out in accordance with ASTM G1. This process was performed as outlined in the section 3.4.1 of Experimental Procedure.

Each reinforcing bar was carefully examined for its general condition as a result of the corrosion effects in terms of pitting, rib degradation, and then weighed to determine the percentage weight loss. A sample of a corroded rebar after evaluating the actual mass loss is shown in Figure. 4.19. The qualitative evidence collected reaffirms the general perception that corrosion is not expected to be uniform throughout the length of the bar. The loss of mass at some sections of the reinforcing steel is higher than at other sections. The original masses and the corroded masses are summarized in Table 4.3. In addition, a visual description of all corroded bars is presented in Table 4.4.



**Figure 4.19: Corrosion at midspan of Bar 5B**

**Table 4.3: Mass Loss for Corroded Bars**

Bar No.	Original Mass (g)	Corroded Mass (g)	Mass Loss (g)	Total Mass Loss (g)	Mass Loss (%)
1A	2.968	2.864	0.104		
1B	2.944	2.848	0.096	0.2	17.78
2A	2.947	2.921	0.026		
2B	2.948	2.93	0.018	0.044	3.91
3A	2.956	2.869	0.087		
3B	2.949	2.868	0.081	0.168	14.93
4A	2.95	2.791	0.159		
4B	2.96	2.827	0.133	0.292	25.96
5A	2.939	2.765	0.174		
5B	2.942	2.81	0.132	0.306	27.2
6A	2.939	2.781	0.158		
6B	2.942	2.813	0.129	0.287	25.51
8A	2.952	2.928	0.024		
8B	2.947	2.921	0.026	0.05	4.44
11A	2.947	2.814	0.133		
11B	2.987	2.903	0.084	0.217	19.29
12A	3.023	2.995	0.028		
12B	3.014	2.978	0.036	0.064	5.69

**Table 4.4: Visual descriptions of corroded reinforcing bars**

Corrosion Group	Beam No.	Bar	Visual Description
Lowest Level Corrosion Group	2	A	Light general corrosion, confined to central area Significant pitting near midspan
		B	Light general corrosion, confined to central area Significant pitting near midspan
	8	A	Light general corrosion, confined to central area Light pitting near midspan
		B	Light general corrosion, confined to central area Light pitting near midspan
	12	A	Light general corrosion, confined to central area Light pitting near midspan
		B	Light general corrosion, confined to central area Light pitting near midspan
Mid-Level Corrosion Group	1	A	Major general corrosion on central area, significant pitting Light general corrosion and pitting outside central area
		B	Major general corrosion on central area, significant pitting Significant general corrosion and pitting outside central area
	3	A	Major general corrosion on central area, significant pitting Significant general corrosion and pitting outside central area
		B	Major general corrosion on central area, significant pitting Significant general corrosion outside central area
	11	A	Major general corrosion on central area, significant pitting Light general corrosion and pitting outside central area
		B	Major general corrosion on central area, significant pitting Light general corrosion and pitting outside central area
Highest Level Corrosion Group	4	A	Severe general corrosion and pitting within central area Major general corrosion and pitting outside central area
		B	Severe general corrosion and pitting within central area Major general corrosion and pitting outside central area
	5	A	Severe general corrosion and pitting within central area Severe general corrosion and pitting outside central area
		B	Severe general corrosion and pitting within central area Severe general corrosion and pitting outside central area
	6	A	Severe general corrosion and pitting within central area Major general corrosion and pitting outside central area
		B	Severe general corrosion and pitting within central area Major general corrosion and pitting outside central area

#### 4.4.1.1 Ultimate Load versus Mass Loss: Figures and Discussion

Table 4.5 lists the ultimate load of the corroded beams with respect to the control beams for varying degrees of corrosion (% mass loss). It is clear that the degree of corrosion has a distinct influence on the load carrying capacity of the beam specimens

**Table 4.5: Relative strength and mass loss for each beam**

Beam No.	Relative Strength	Mass Loss
	%	%
9C	100	0.0
10C	100	0.0
2L	87	3.9
8L	94	4.4
1M	87	17.8
3M	84	14.9
11M	78	19.3
4H	77	26.0
5H	80	27.2
6H	75	25.5

Upon observation of the ultimate load vs. mass loss curve, Figure 4.12, the distinct downward trend is immediately evident. This trend was anticipated at the outset of this experiment. A combination of the loss of bond between steel and concrete at midspan, and the loss in cross-sectional diameter of the steel bars accounts for this drop. The linear trend for ultimate load,  $P_{ult}$ , can be approximated by the equation:

$$P_{ult} = 151.45 - 1.4\Delta m$$

(4.1)

where  $\Delta m$  is the steel mass loss in percentage (%)

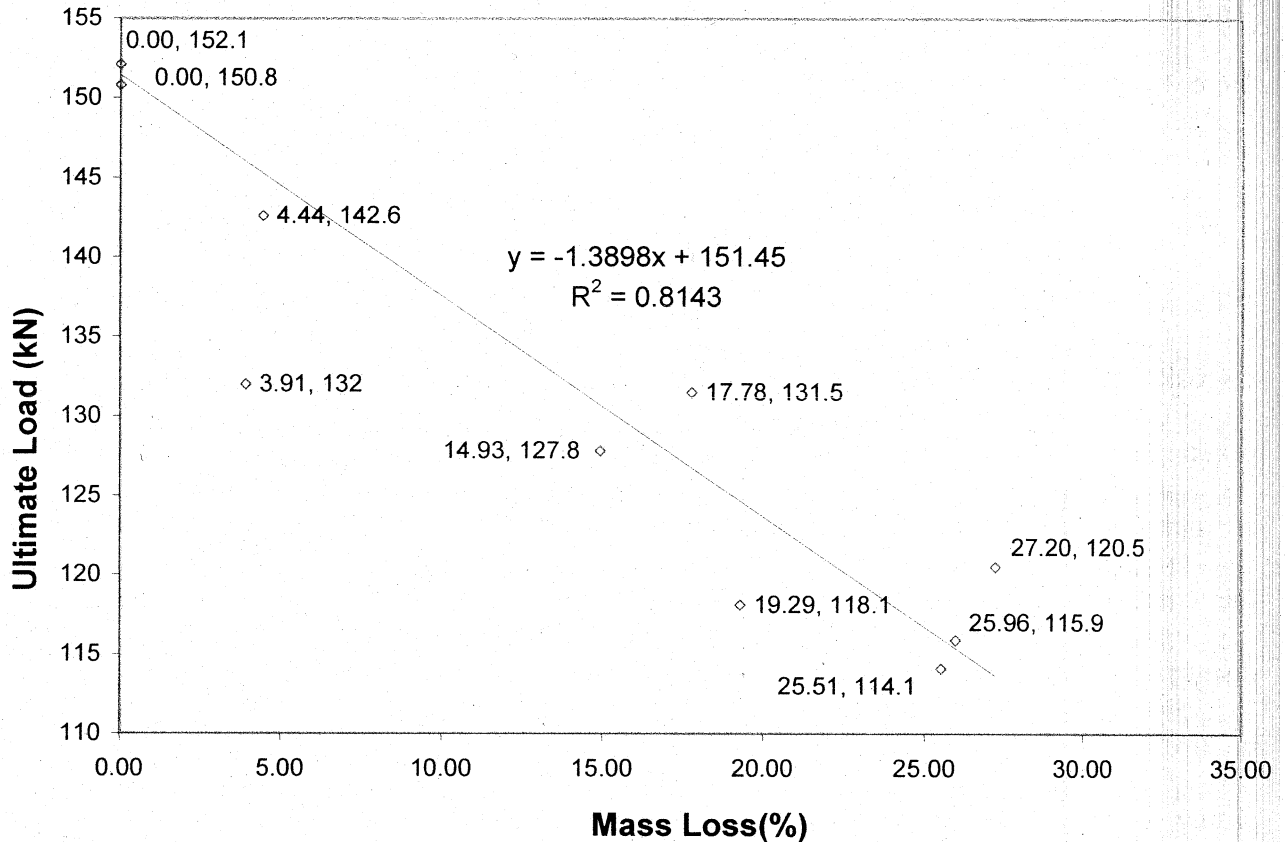


Figure 4.20: Ultimate load versus mass loss

The loss in bond associated with corrosion causes a limited transfer of tensile stresses to the steel (Rodriguez et al., 1997) and the loss in cross-sectional area of the reinforcing steel is equivalent to losing reinforcing steel area. This results in a smaller yield force in the tensile bars and a correspondingly smaller compression block in the beam during flexure, and consequently a smaller resisting couple between the tensile and compressive forces. It has been shown that the loss of bond plays a significant role in the behaviour of beams with corroded reinforcement.

Results have shown that the decrease in ultimate strength is not proportional to the loss of reinforcing steel area, it is significantly larger (Mangat & Elgarf, 1999).

The one data point diverges most significantly from the trend line is Beam 2L (mass loss = 3.91). Here, there is a distinct loss of strength corresponding to a relatively small mass loss, less than 5%.

With respect to Beam 2L, observations from the cracking showed nothing unusual. Stirrup corrosion had likely begun on the first stirrups, but this was not unique amongst its corrosion group and a flexural failure was still observed. This was confirmed upon extraction of the stirrups, light corrosion had begun on the first and second stirrups on each side. Observations of the corroded reinforcing bars did show significant levels of pitting near midspan. If a disproportionate amount of pitting takes place in one area, a weakness is created. As specimens in flexure are most sensitive at midspan, this accounts for a premature failure. Some of the pitting occurred at points very close to one another; this could have created a local weakness. Other specimens within the same corrosion group did not show such significant pitting. Other specimens showed light pitting and a more general corrosion. Again, there is evidence that the behaviour of reinforced concrete beams becomes much less predictable as reinforcement corrosion progresses.

There are other possibilities to explain why Beam 2L had a 13% loss in ultimate load with only a 3.91% loss in tensile steel reinforcing mass. It was observed that Beam 2 showed the weakest cylinder strength in testing. If it happened that this mix was in fact weaker, then it could account

for the poor results in mechanical testing. A small drop in compressive strength could sway the results slightly; however such a large drop is unlikely. It has been observed that the bond loss between the steel and concrete is a major factor with respect to flexural strength, and a small loss in concrete compressive strength would not affect this very much. The loss in steel area would be likewise unaffected. It is more likely that cylinder results variations were result of being from the tail end of the mix, as discussed in Section 4.2.1. In addition, results could have been swayed by entrapped air due to inadequate compaction during casting.

Examining the trend from Eq. 4.1, the results can be compared with those of other researchers. It should be remarked, however, that this trend is only a indicator for this study, and that a large degree of variation was generally encountered. At any rate, it warrants comparing these results with other research. At 9.7% mass loss Ahmed et al. (2006) observed a 13% strength loss. Using the trend created, the same mass loss produced a corresponding strength loss of 9.1% with respect to the control beams for this study. El-Maaddawy et al. (2005) found that with 8.9% and 22.2% mass loss, strength losses of 6.4% and 20.0% were observed, respectively. This study showed strength losses of 8.2% and 20.4% for the same mass losses. As anticipated, these results compare quite well.

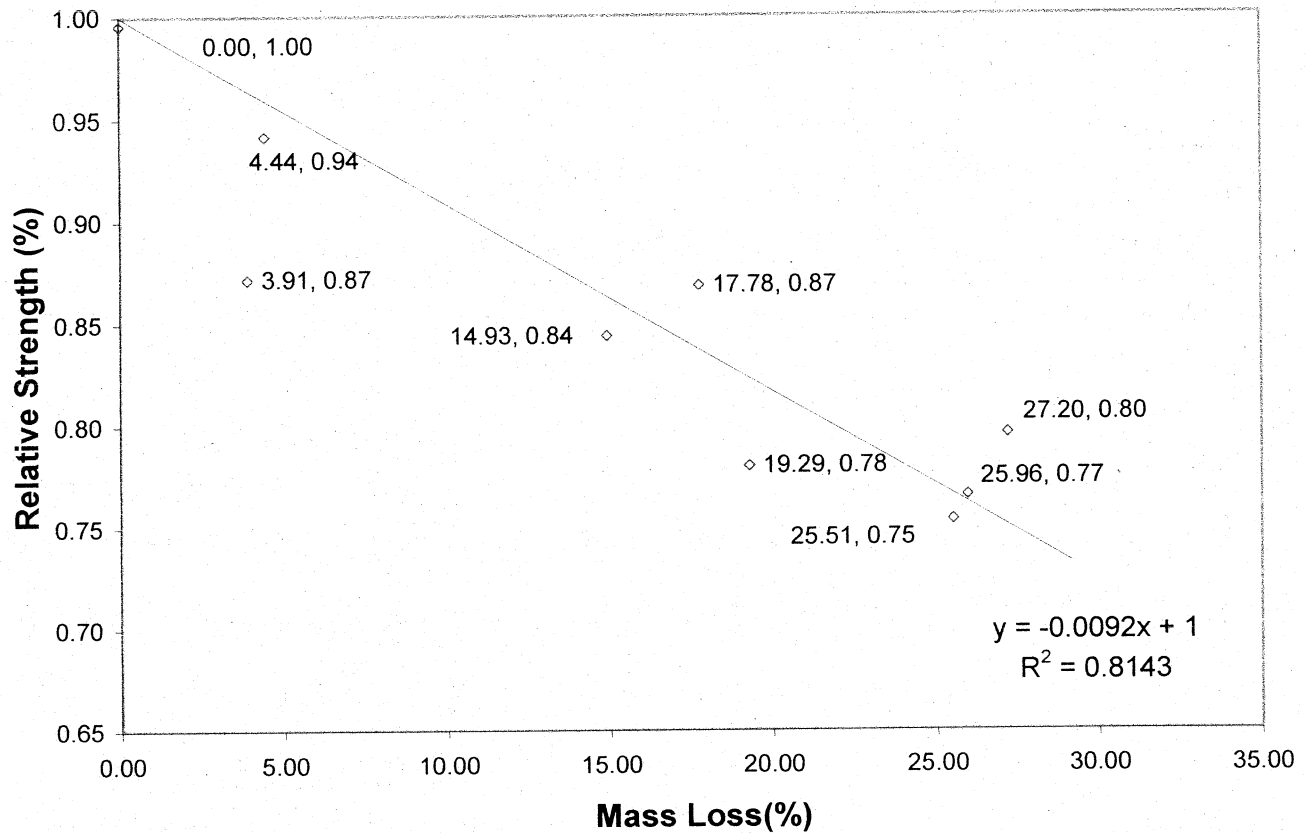


**Figure 4.21: Relative strength versus mass loss**

Introducing the relative strength values observed in Table 4.5 it is possible to derive a new relationship. Figure 4.21 allows the results of this experiment to be compared effectively with the results of other researchers. Figure 4.21 shows a linear trendline of approximate equation:

$$RS = 1 - 0.01 \Delta m \quad (4.1)$$

where RS is the relative strength in %, and  $\Delta m$  is the degree of mass loss in %.

Again, this trend is an indicator of the performance of the beams for this study. Throughout the study a high degree of variability was encountered amongst the corroded specimens and it not accounted for within Eq. 4.1.

#### **4.4.1.2 Stiffness versus Mass Loss: Figures and Discussion**

As discussed in Chapter 2, corrosion of reinforcing steel has been associated with a loss in serviceability, namely with higher than expected deflections. In this study, the stiffness of corroded beams was observed in order to determine to what extent changes in deflection should be expected over the service life of reinforced concrete members. Stiffness was calculated from the slope of the load-deflection graphs within the elastic range, in kN/mm.

As shown in the stiffness vs. mass loss graph, Figure 4.22, there is a significant loss of stiffness, even within the lowest level corrosion group. The trend is not a gradual decline in stiffness but a quick drop at mass losses of lower than 5%, followed by a slower, linear decline. These results vary from what was observed in the ultimate load analysis, where a more gradual decline was observed. This quick rapid stiffness loss was true with the exception of Beam 5H and 6H, which exhibited surprising stiffness at high levels of corrosion. Beam 5H showed no loss in stiffness with a mass loss of 25.51% and Beam 6H exhibited a stiffness loss of only 13% with a mass loss of 24.7%.

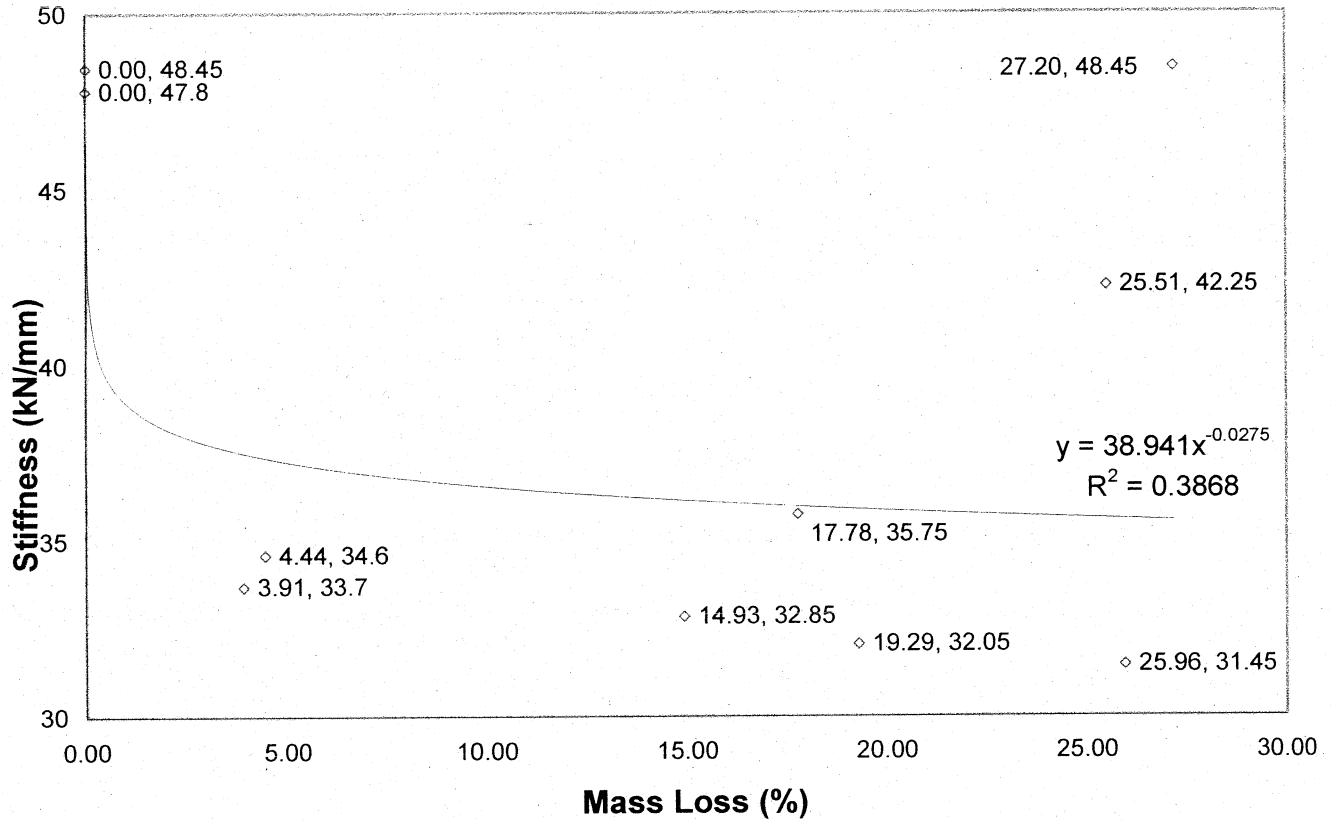


**Figure 4.22: Stiffness versus mass loss**

One explanation for higher stiffness in Beams 5H and 6H is that while both had a large total mass loss, 27.2% and 24.7% respectively, the distribution of each was detrimental to the expected result. Upon observation of the recovered reinforcing steel it was evident that there were several locations of heavy pitting outside of the main flexural region. This was true with all the highly corroded samples, but was most pronounced in Beams 5H and 6H. This was also evidenced by the observations of the corrosion cracking prior to testing, where cracking was very pronounced outside the central zone.

In one study by Torres-Acosta (2004) a loss of stiffness of 32% was observed with a 14% loss in reinforcement radius. This corresponds to an average mass loss of 20%. These results compare

very well with those observed in this study, where for a similar mass loss of 20% a loss of stiffness of 33% was observed. At an equivalent mass loss of 26%, an accompanying stiffness loss of 25% was observed. Again, this conformed fairly well to the results of this study where a stiffness loss of 32% was observed for the same mass loss.

Eliminating the two points that deviate significantly from the trend, Beam 5H and 6H, a more pronounced trend is observed. There is a sharp decrease in stiffness at relatively low corrosion levels, followed by a linear downward trend. This can be observed in Figure 4.23. From this figure, it is clear that the stiffness of the reinforced beam is reduced abruptly at low corrosion levels. This drop can be attributed to the formation of cracks due to corrosion, the associated resulting reduction in bond between steel and concrete by the reduction in confinement. After a certain degree of corrosion, the effect of corrosion on stiffness of the beam decreases, and beyond certain level (approximately 4%), it does not affect the stiffness significantly. Due to the prior formation of many internal cracks, the reinforced concrete beam has already lost much of its stiffness, and a further increase in corrosion does not cause any further reduction in the stiffness.

We can also observe the relative beam deflections with respect to the control beams. This makes the results applicable to all beams and more easily compared with similar research. Observing Figures 4.24 and 4.25, it is remarked that the relative deflections are significantly larger as the loading progresses from 80kN to 110kN. Again the serviceability of corroded beams is called into question, as significantly greater deflections are observed at even moderate loading.

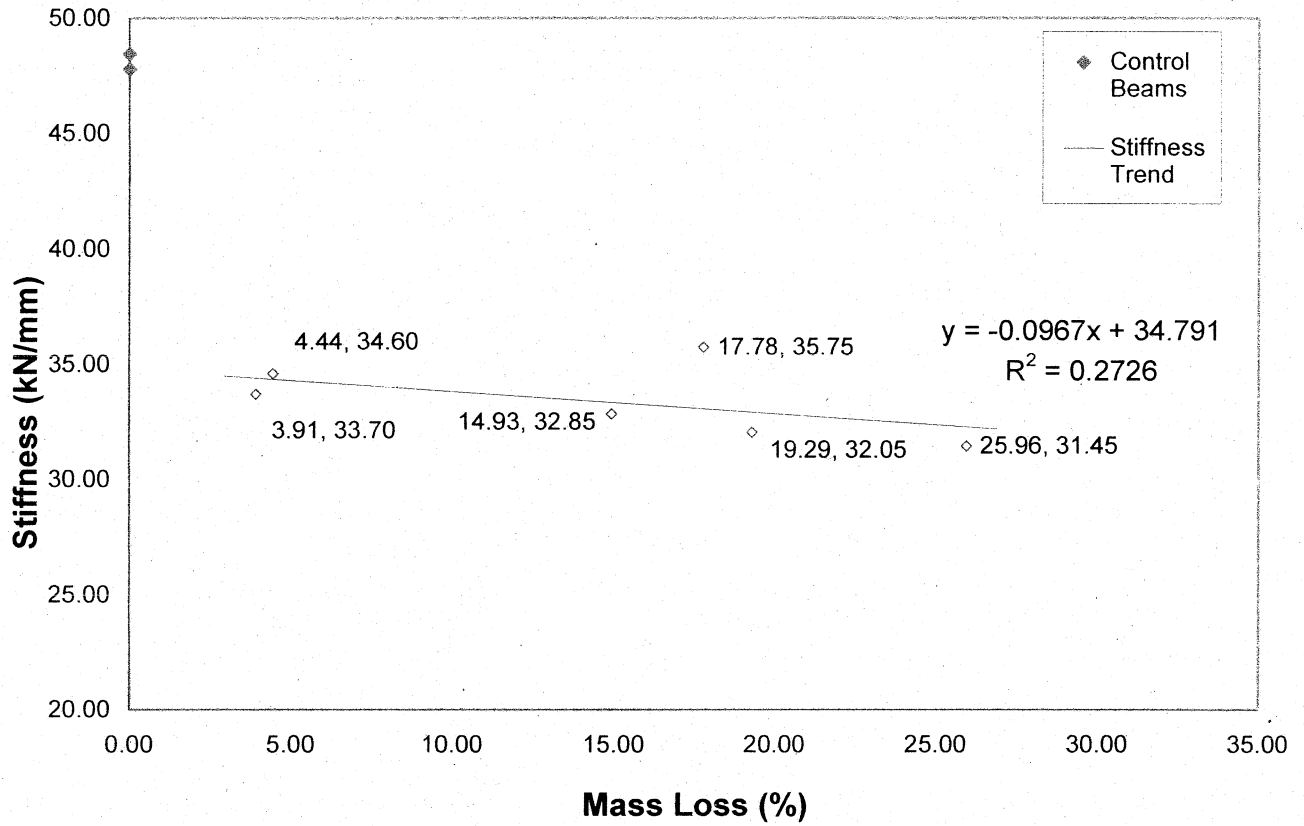


**Figure 4.23: Corrected stiffness versus mass loss**

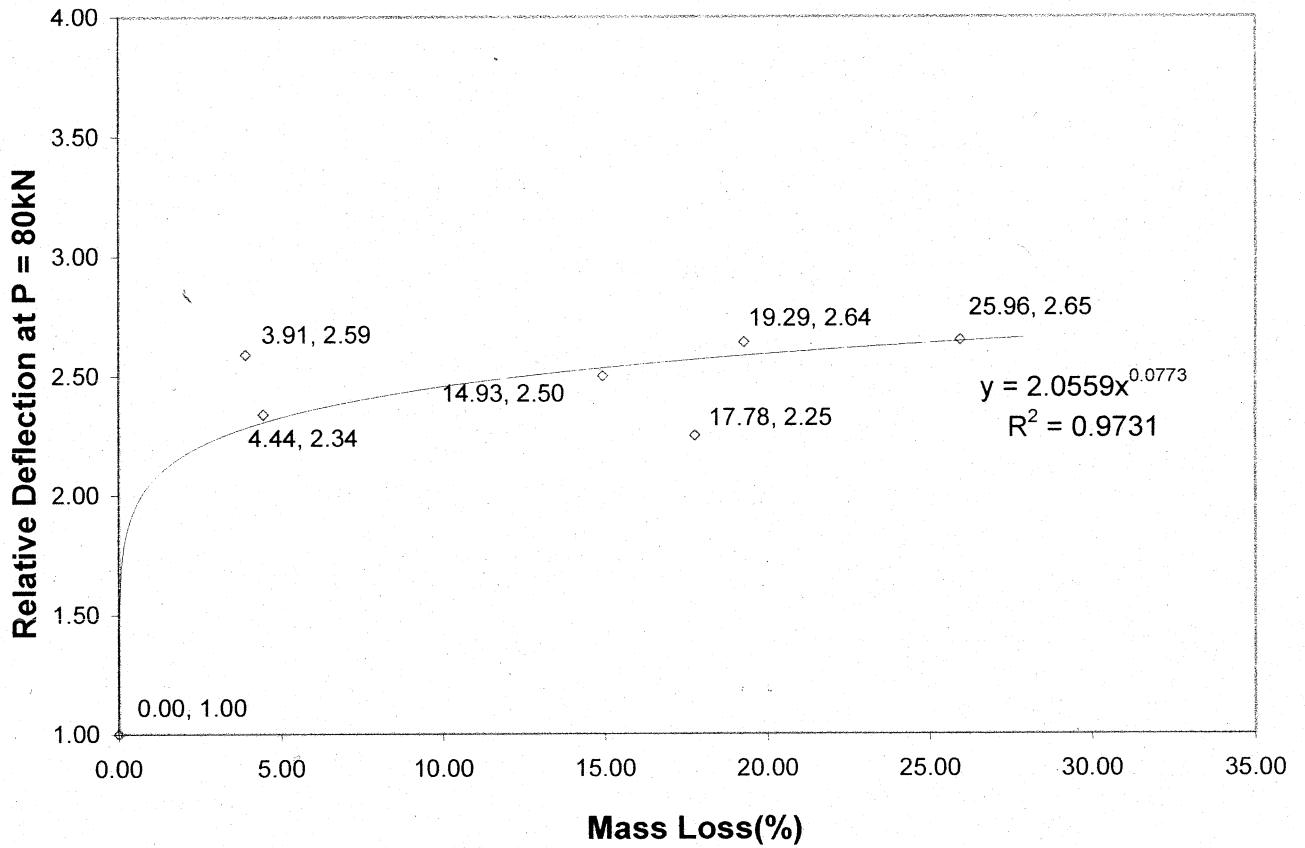
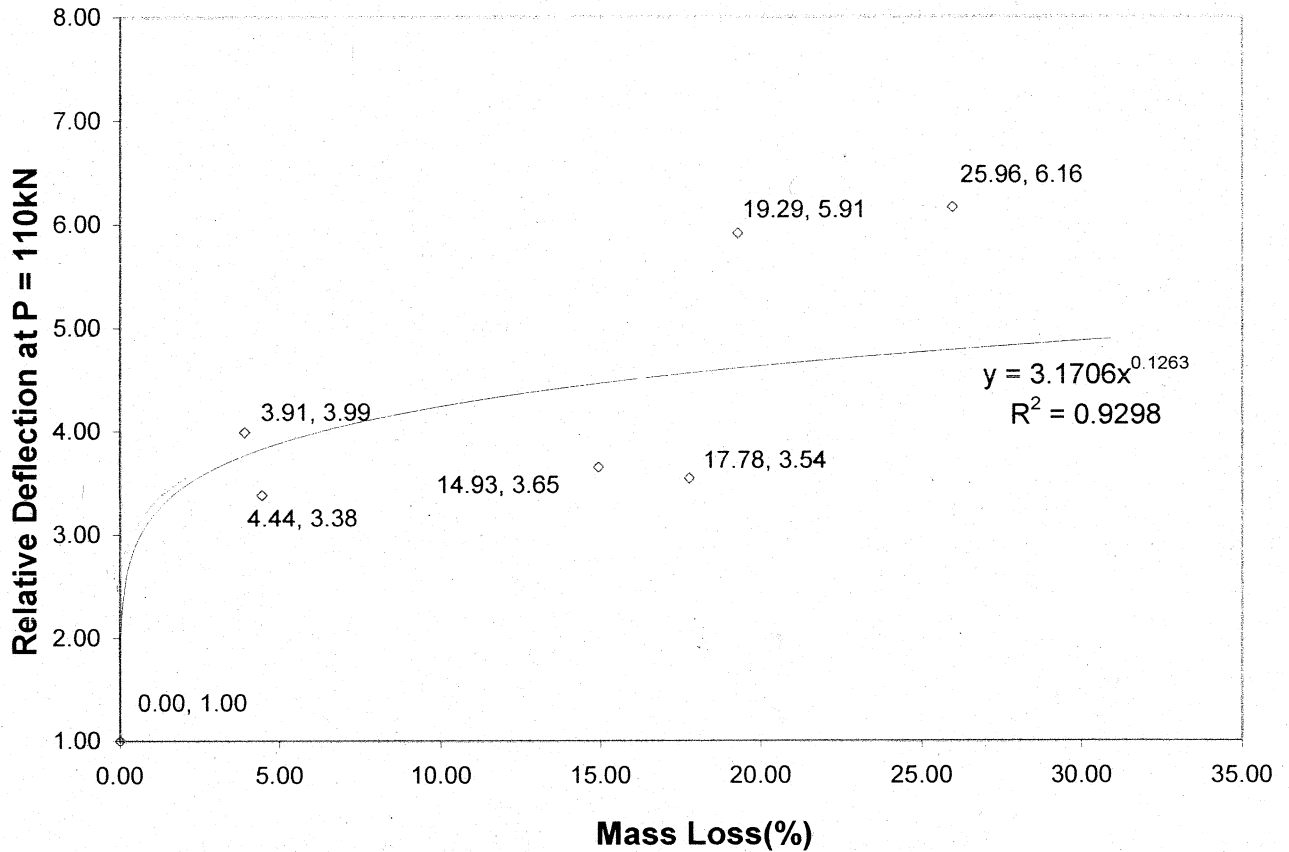


Figure 4.24: Relative deflection at P = 80kN vs. mass loss



**Figure 4.25: Relative deflection at P = 110kN vs. mass loss**

#### 4.4.2 Chloride Ion Content

The chloride ion content of concrete is critical to the life of the reinforcement, because small amounts of chloride can disrupt the passive layer that protects the steel from corrosion. This was examined in detail in Chapter 2. Therefore, to assess the condition of the deteriorating concrete, it is essential to determine the concentration of chloride in the concrete.

The variation of the chloride ion content across the concrete cover thickness was obtained according to the procedure that was presented in Chapter 3, explaining how the chloride content changes with depth.

A chloride ion selective probe was used to determine the chloride ion profile for each specimen according to ASTM standard C1152-90 method, as described in Chapter 3. The chloride ion content was extracted from the drilled concrete dust as outlined in Chapter 3. The data from each bar was collected at bar depth (30mm), at mid-cover (15mm deep) and at the surface of the beam. The complete results can be seen in Table 4.4. Despite collecting data at each depth for each bar, it was determined that the chloride ion content data collected at the bar depth provided the most accurate results. This stands to reason since the corrosion process is active at the depth of the bar, not within the concrete cover. These results were then averaged between the two bars to obtain the average chloride ion content value for the entire beam.

One aim of collecting the chloride ion content data was to determine its use as an indicator of degree of corrosion, and therefore strength loss as well as serviceability loss. For this reason the chloride ion content values have been compared directly to the mass loss data, as well as the crack width data.

**Table 4.6 Chloride Ion Content Results**

Sample Location		Chloride Ion Content	Average CIC per Bar
Bar No.	Location	(%)	(%)
1A	SURFACE	0.36	0.37
	15mm	0.40	
	AT BAR	0.36	
1B	SURFACE	0.98	0.83
	15mm	0.86	
	AT BAR	0.66	
2A	SURFACE	0.21	0.26
	15mm	0.22	
	AT BAR	0.35	
2B	SURFACE	0.22	0.24
	15mm	0.21	
	AT BAR	0.29	
3A	SURFACE	0.45	0.42
	15mm	0.40	
	AT BAR	0.40	
3B	SURFACE	0.33	0.31
	15mm	0.36	
	AT BAR	0.23	
4A	SURFACE	0.54	0.52
	15mm	0.50	
	AT BAR	0.52	
4B	SURFACE	0.80	0.69
	15mm	0.50	
	AT BAR	0.76	
5A	SURFACE	0.78	0.65
	15mm	0.72	
	AT BAR	0.45	
5B	SURFACE	0.80	0.64
	15mm	0.33	
	AT BAR	0.78	
6A	SURFACE	0.90	0.76
	15mm	0.76	
	AT BAR	0.62	
6B	SURFACE	0.78	0.62
	15mm	0.70	
	AT BAR	0.39	
8A	SURFACE	0.26	0.23
	15mm	0.22	
	AT BAR	0.20	
8B	SURFACE	0.24	0.21
	15mm	0.19	
	AT BAR	0.20	
11A	SURFACE	0.96	0.98
	15mm	0.98	
	AT BAR	1.00	
11B	SURFACE	0.44	0.38
	15mm	0.34	
	AT BAR	0.35	
12A	SURFACE	0.22	0.29
	15mm	0.32	
	AT BAR	0.33	
12B	SURFACE	0.29	0.26
	15mm	0.20	
	AT BAR	0.29	

#### 4.4.2.1 Ultimate Load versus Chloride Ion Content: Figures and Discussion

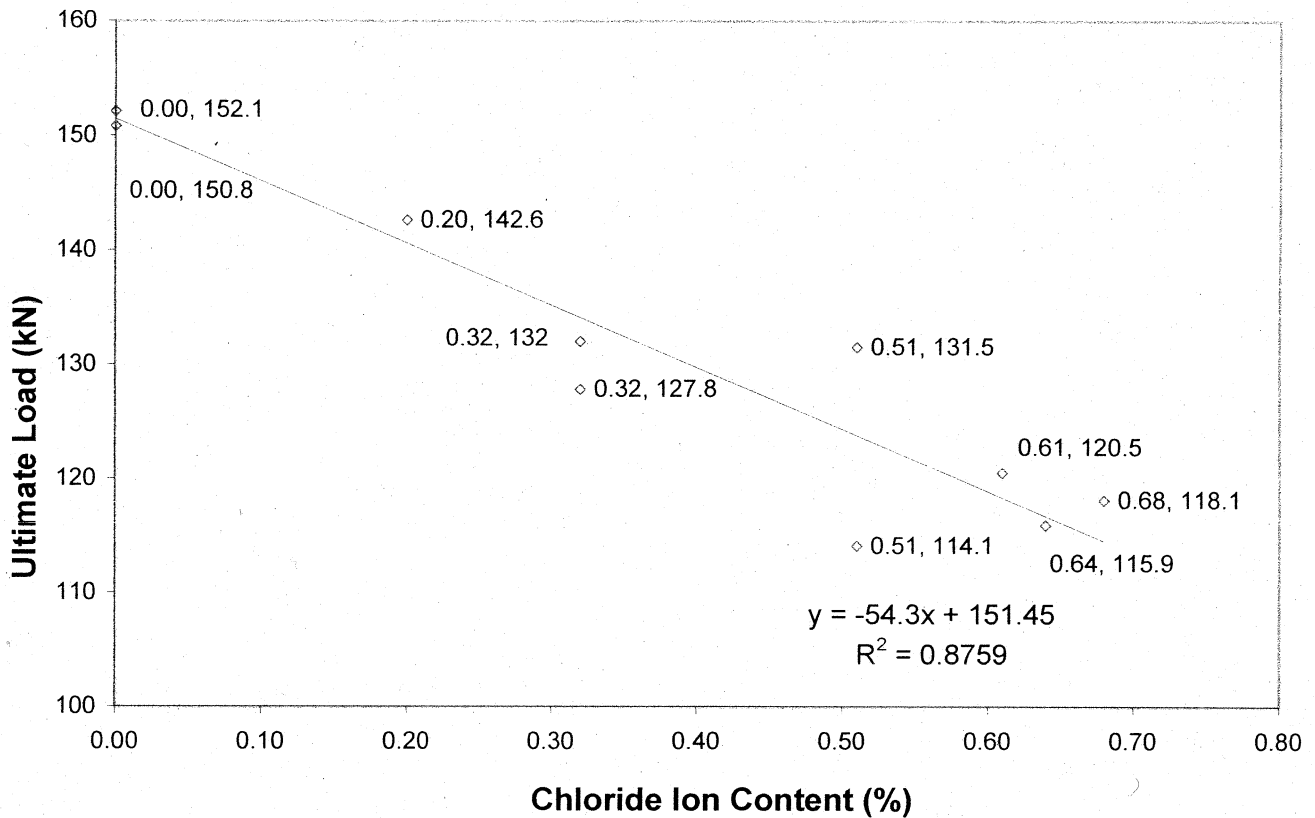


**Figure 4.26: Ultimate load versus chloride ion content**

The Ultimate Load vs. Chloride Ion Content (CIC) produces another very similar trend to the mass loss data: a gradual linear decline in strength with increasing CIC. As compared to the crack width and mass loss parameters, the chloride ion content data showed the least deviation from the linear trend line. Even Beam 2L, which had remained an outlier on both previous graphs, fit much better in terms of chloride ion content. This is observed in Figure 4.26.

If pitting was occurring near midspan of Beam 2L (CIC = 0.32%), chloride ion levels would have been elevated and would be accounted for using this parameter. In fact the only data point that did not fit well was from Beam 1M, which had a chloride ion content of 0.60%. This outlier

could have been produced by drilling too much dust directly on top of a crack, where chloride will accumulate in higher proportions. Overall, chloride ion content proved to be a very effective indicator of ultimate load capacity and potential strength loss.

#### 4.4.2.2 Stiffness versus Chloride Ion Content: Figures and Discussion

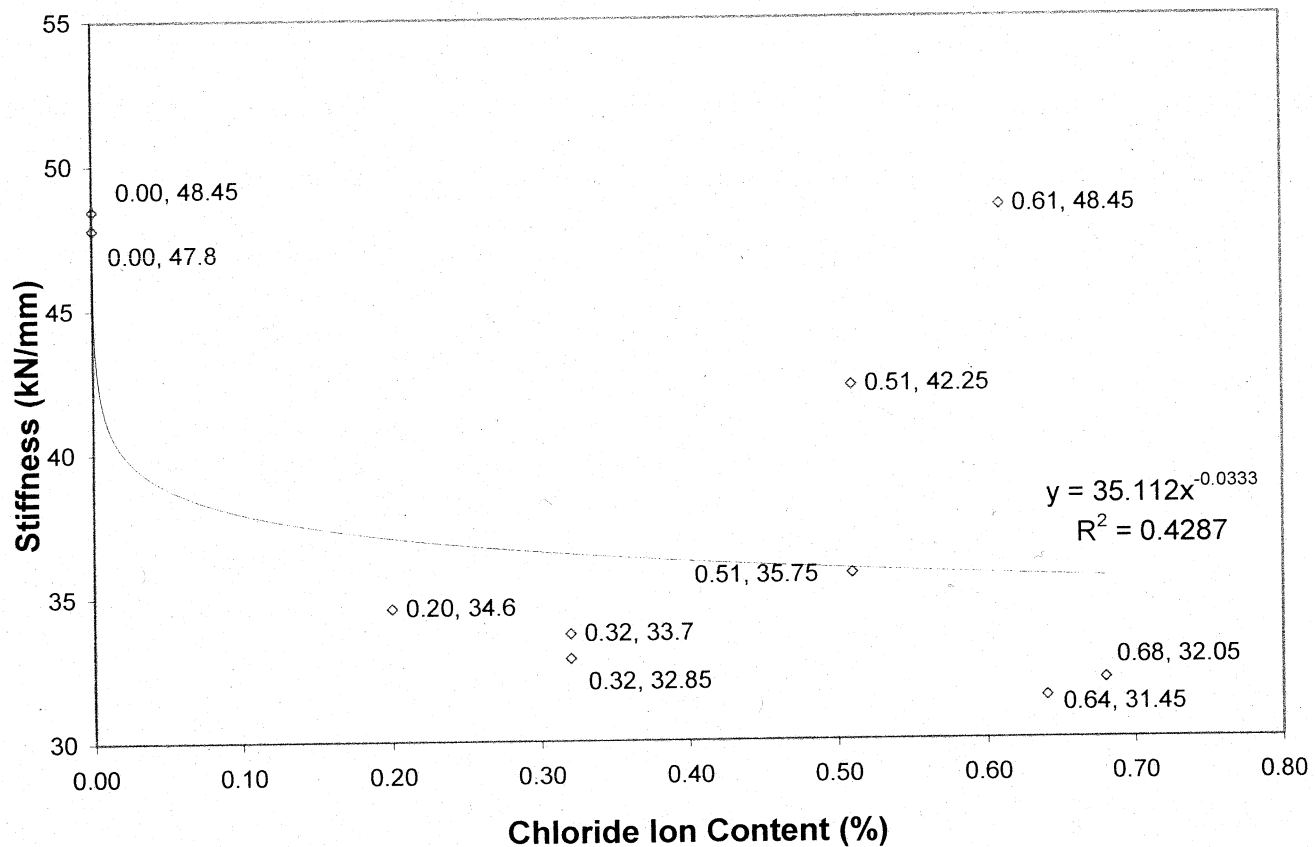
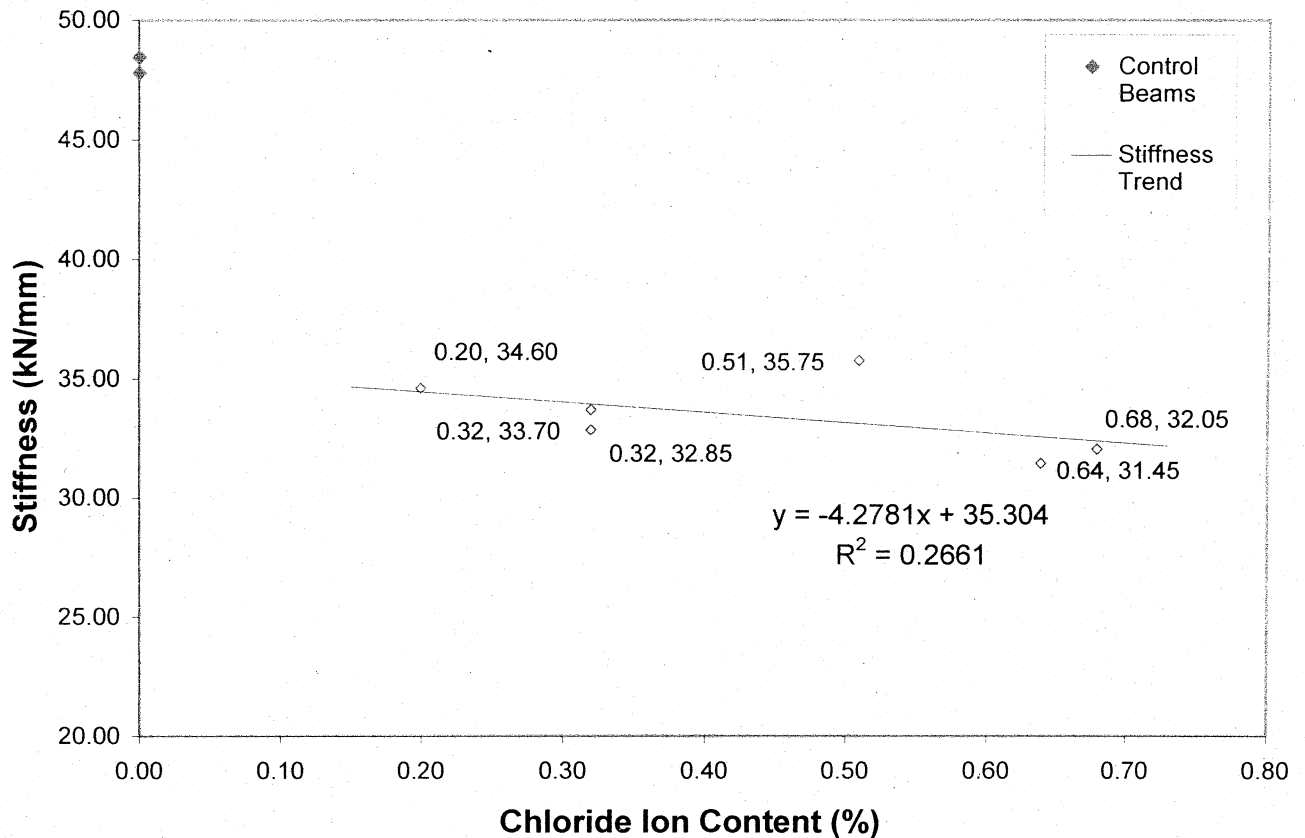


Figure 4.27: Stiffness versus chloride ion content

With respect to chloride ion content, seen in Figure 4.27, the trend is observed again, with the outliers remaining Beam 5H and Beam 6H. Concrete dust samples were taken from a range of locations but when cracks are closely spaced the dust is often extracted next to a crack, where chloride values are elevated. This could account for small deviations in the chloride ion content values, but likely not the large deviation of Beam 5H.



**Figure 4.28: Corrected stiffness versus chloride ion content**

With the elimination of the outliers, Beam 5H and 6H, there is a similar trend observed again: a large loss at low CIC followed by a gradual decline. This can be observed in Figure 4.28. When the stiffness is observed with respect to the chloride ion content it is seen that the drop in stiffness is not as abrupt as it appears in the crack width and mass loss graphs. The levels of chloride required to produce a significant drop in stiffness are actually quite high. The lowest level, 0.2% (by mass of sample), is double what is believed to be the threshold level for corrosion initiation, 0.1%, (Dekoster et al., 2003). Other studies have shown that at 0.05% chloride ion content there is zero probability of corrosion and at 0.2% chloride ion content there is a 100% chance of reinforcement corrosion (Nygaard and Geiker, 2005). When viewed in this

light, the drop in stiffness is not as surprising. Even at chloride ion contents as low as 0.2%, considerable corrosion had already taken place.

### 4.4.3 Crack Width

#### 4.4.3.1 Ultimate Load versus Crack Width: Figures and Discussion

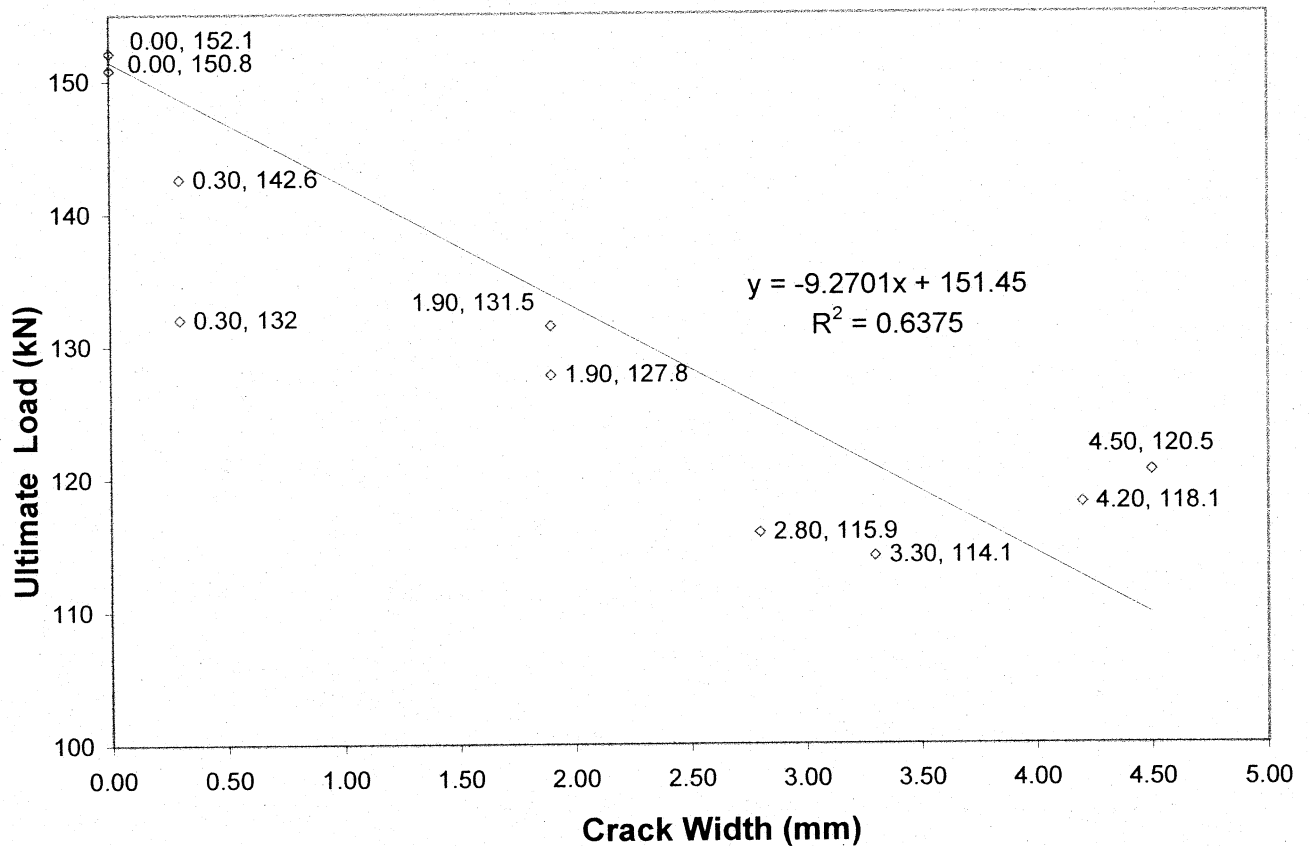


Figure 4.29: Ultimate load versus crack width

When the ultimate load vs. crack width figure is observed, (Figure 4.29), a similar trend is observed to that of the mass loss data. The main difference between the ultimate load vs. crack width and the ultimate load vs. mass loss is that the deviation from the trend line is much greater within the crack width data. Again there is a large deviation with Beam 2L, for the same reasons

as discussed in Section 4.4.1.1. With Beam 2L one would expect a higher loss in ultimate load to be associated with the observed crack width, 0.3mm. It is likely that general corrosion plays the most significant role in crack width due to a higher accumulation of corrosion products, and since pitting was the likely cause of the early failure, crack width did not prove to be a good indicator for Beam 2L. Despite the deviations associated with the crack width graph, it still produces a similar trend. In the face of no other options, measurement of crack width remains a reasonable method to estimate the degree of corrosion, and potential beam performance.

#### 4.4.3.2 Stiffness versus Crack Width: Figures and Discussion

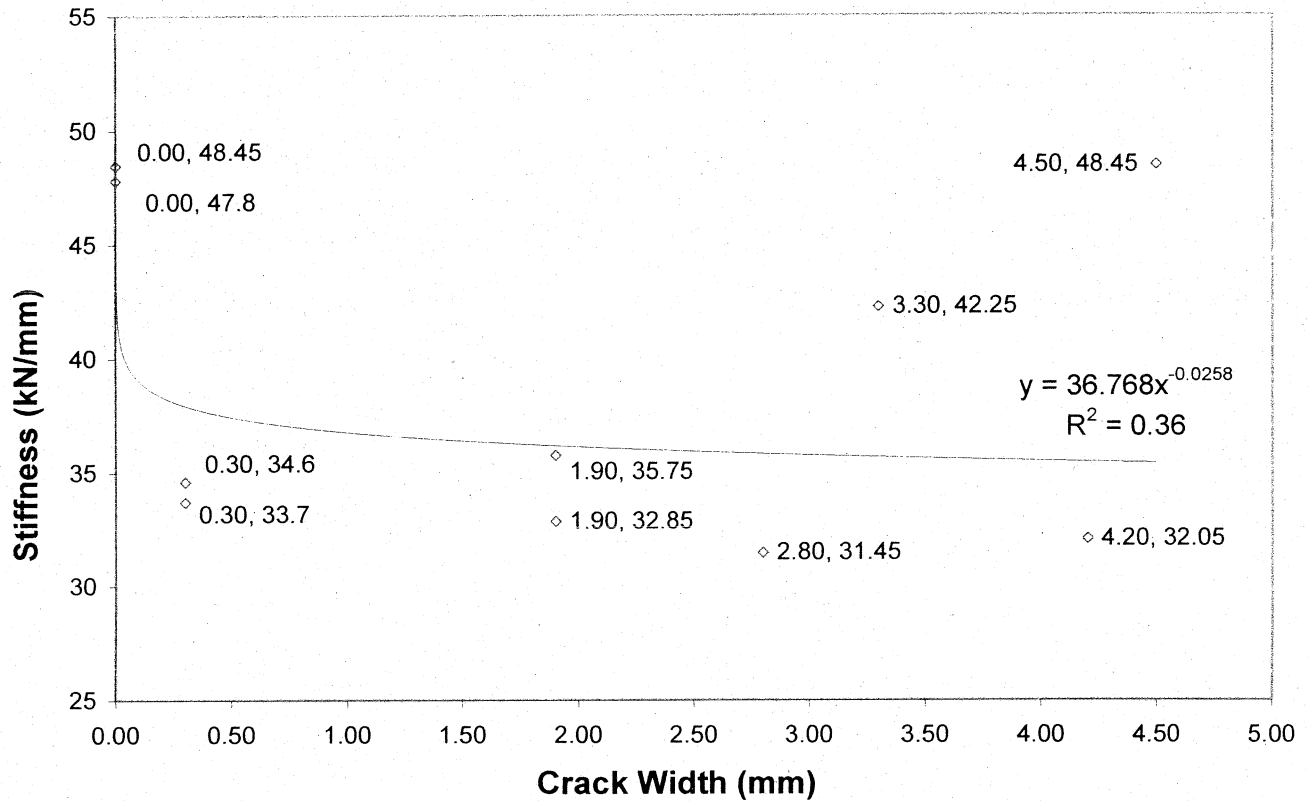
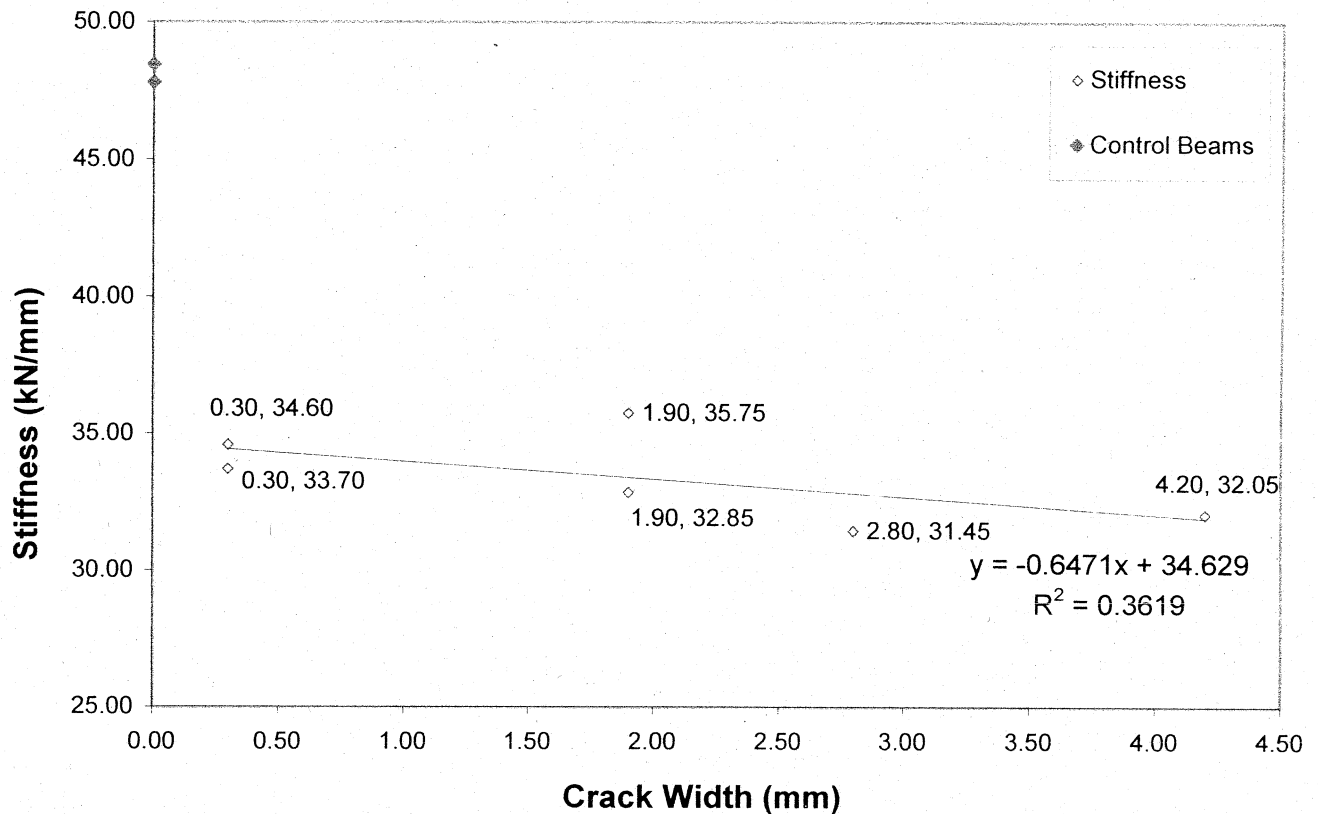


Figure 4.30: Stiffness versus crack width

When the stiffness results are observed in terms of crack width (Figure 4.30), Beam 5H (crack width = 4.50mm) remains an outlier. In addition to Beam 5H, Beam 6H (crack width = 3.30mm) again contradicts the general trend. Beam 5H and 6H deviate since at higher corrosion levels the cracks did not propagate as quickly; corrosion was taking place all along the beams, not just in the flexural region. However, the trend remains the same, a rapid drop in stiffness followed by a gradual linear decline.



**Figure 4.31: Corrected stiffness versus crack width**

Again, the major trend becomes more apparent when Beams 5H and 6H are eliminated. This can be observed from Figure 4.31. Here, the sharp drop and steady decline are more clearly observed.

#### 4.4.5 Parameter Comparison for Corroded Beam Performance

As discussed earlier, chloride ion content gave the most reliable results in terms of strength and stiffness loss due to reinforcement corrosion. This shows the chloride ion content is a direct indicator of the amount of corrosion taking place in the location of interest. Crack width provides

similar benefits, but without the precision. Crack widths at very small thicknesses cannot be seen with the naked eye, and therefore it is difficult to know when significant strength loss is likely to occur. By the time cracks are visible to the naked eye, corrosion is already affecting the behaviour of the reinforced concrete element significantly, as shown in this study. Also, in the field there is a difficulty seeing all cracks present, on all faces of the beam, in order to gain a complete picture prior to analysis. With chloride ion content, this is not a concern, samples can be drilled to any depth and any angle required.

Mass loss alone will not give an accurate portrayal of the state of corrosion within a reinforced concrete element. In addition, reliable mass loss predictions can be difficult to obtain on the field. Crack width and chloride ion content offer two viable alternatives to predict degree of corrosion in the field. In combination with each other, an accurate prediction of corrosion levels can certainly be achieved.

The benefits to using chloride ion content as a corrosion indicator are clear. One dust sample will give the relative severity of the corrosion at that specific location. Likewise, multiple samples will give the severity of the corrosion taking place at specific lengths along the beam or member. While the laboratory work associated with each sample can take time, the field samples are relatively easily obtained and do not require significant space to move or ship. Ultimately, as the results of this investigation show, chloride ion content can also give more reliable results. In Figures 4.32 and 4.33 the relationships of crack width and chloride ion content are related to the mass loss for this study.

The relationship between chloride ion content and mass loss is consistent. There are some small variations but in general, it appears as if the chloride ion content of a concrete is a good indicator of the mass loss that has taken place. The two points that stand out are the two at relatively low mass loss (44g and 55g). This can be explained since in order for mass loss to initiate, chloride concentrations must build up in order to break down the protective passive layer. This means that there can be higher chloride concentrations with relatively low mass losses, since in this case mass loss has just begun. At higher mass losses we see a greater consistency.

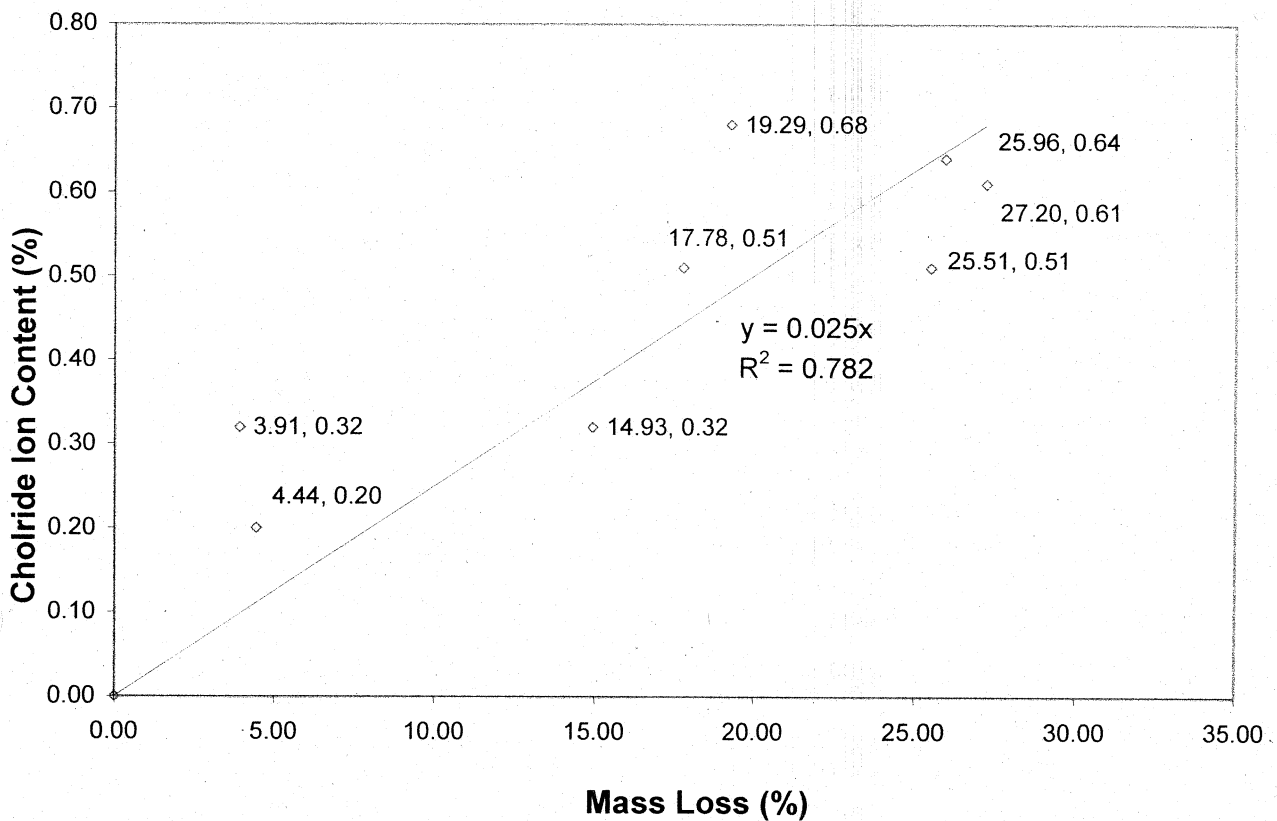
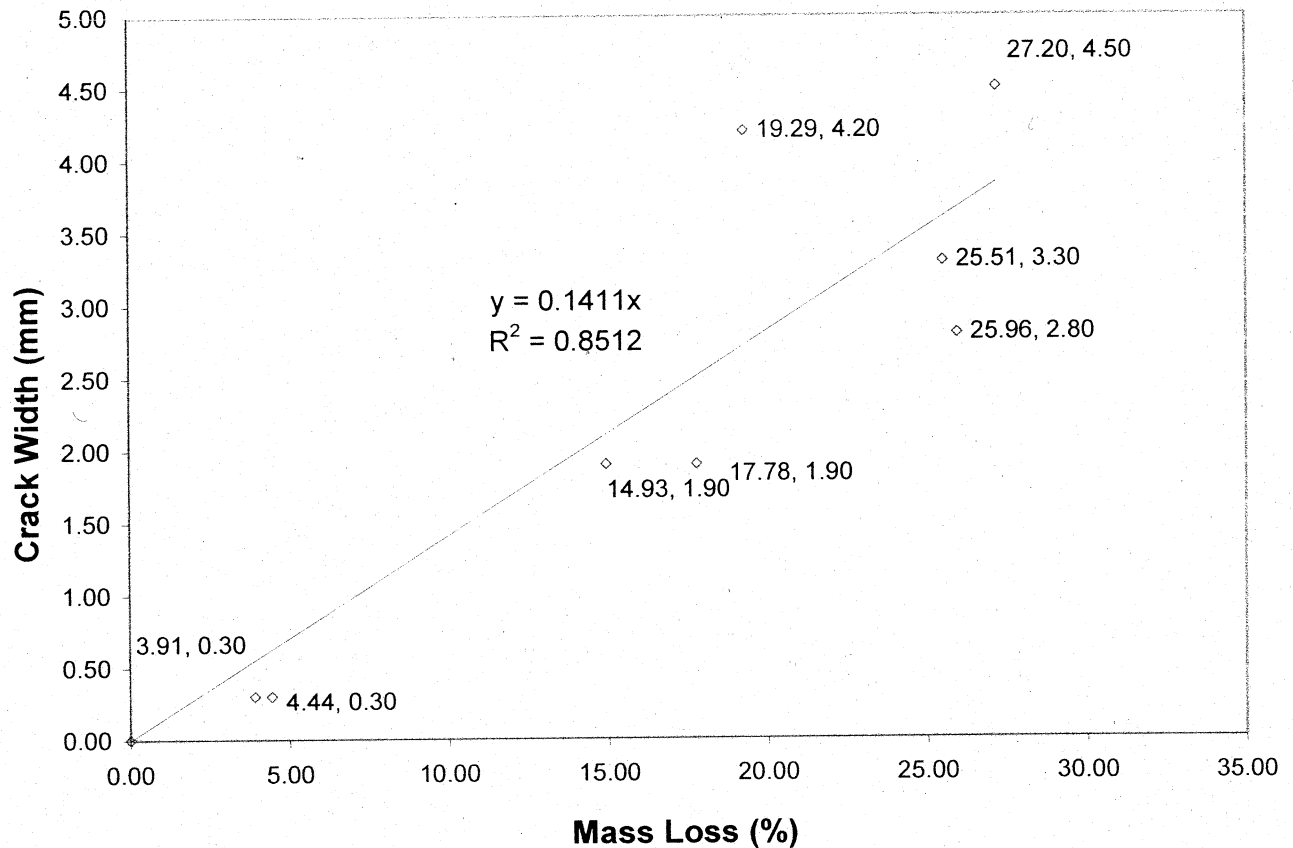


Figure 4.32: Chloride ion content versus mass loss



**Figure 4.33: Crack width versus mass loss**

#### 4.4.6 Discussion Summary

In general, the chloride ion content produced the most reliable trends with respect to ultimate load. Pitting of the bars created uncertainty with respect to mass loss and the locations of the pitting created a high sensitivity. If the degree and location of pitting could be quantified, then mass loss would prove to be a more reliable parameter. Similar problems are encountered with the use of crack width. It remains a question of where one considers the crack width, and if the transverse cracks are considered in conjunction with the longitudinal cracks. From the observations of this study, the transverse cracks may play a greater role in the premature failure of beams, but they can be hard to see and require a greater degree of interpretation. Chloride ion

content proves to be a reliable indicator of strength loss. If care is taken to spread out the dust samples and avoid areas of potential chloride build-up (such as cracks locations), then as shown above it can be a very useful tool for investigators.

Research has shown that at low corrosion levels, the effect of bond loss can be ignored and that the ultimate load carrying capacity of the beam is affected only by the loss on steel reinforcement (El Maaddawy et al., 2005). At higher levels of corrosion the loss in bond can no longer be discounted and plays a role in the ultimate strength. (Aza et al., 2007). Research varies with respect to what level of corrosion is required to affect the bond strength.

The general trend seen in all the stiffness graphs is intriguing. Why does the stiffness drop so suddenly, at mass losses as low as 4%? For the answer it is important to analyze the mechanics of the composite materials.

Concrete gains its stiffness from both reinforcing steel and the surrounding concrete. The total stiffness,  $EI$ , is a function of the composite material. An uncorroded beam is fairly easily analysed in the manner, assuming a good bond between the steel and the concrete. However, when the bond between the steel and the concrete begins to break down, the tensile stresses that cannot be transferred to the steel from the concrete cannot effectively, leading to larger deflections than expected and a loss of stiffness. In the respect it is believed that it isn't the loss of steel that is the main contributor to stiffness loss, but the loss of bond between steel and concrete. In this experiment, the tensile bars were well anchored at each end so the tensile

stresses could still be transferred; only this occurred out of the midspan area, creating a loss of stiffness, but not a loss of ultimate load.

The loss in stiffness is more apparent when the load deflection graph is examined once the outliers of Beams 5H and 6H have been removed. If the elastic range is then observed the stiffness trend is apparent. This can be seen in Figure 4.34.

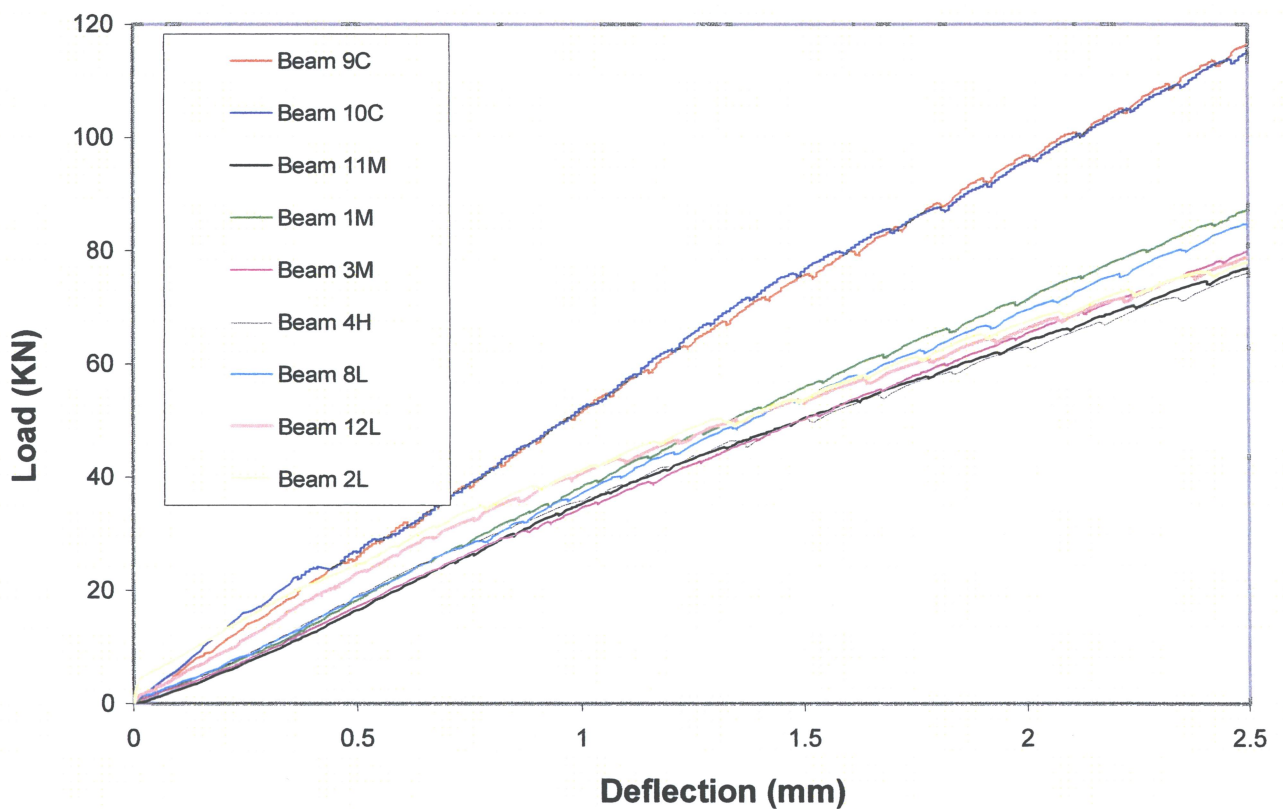


**Figure 4.34: Summary of load deflection behaviour within the elastic range**

# 5 CONCLUSIONS

This chapter summarizes the findings of the experimental studies on the influence of corrosion on the flexural behaviour of a reinforced concrete beams, chloride ion content and cracking of the reinforced concrete element due to corrosion.

## 5.1 Summary and Conclusions

The primary objective of this research program was to determine the effect of corrosion of tensile steel reinforcement on the performance of reinforced concrete beams. This was accomplished through a preliminary analysis of the load deflection results, the stiffness and ultimate load behaviour of reinforced concrete beams at various corrosion levels. In general, the results found corresponded well with those of other researchers, and added to the pool of data that will be necessary to predict the performance of corroded beams in the future.

It was also determined that chloride ion content at the depth of the steel is a very reliable corrosion indicator. It can be used not only as an indicator as to whether the passive layer has broken down and corrosion has begun, but also as an indicator of the degree to which corrosion has advanced. At this point there is sufficient concurrence between this study and those performed by other researchers to predict the amount of strength loss and stiffness loss that has taken place at a given level of corrosion. This will prove to be a very effective tool in the future, when evaluation of existing corroded concrete structures will be of paramount importance.

Based on the data developed in this study, the following conclusions are drawn:

1. The ultimate load ( $P_{ult}$ ) of corroded reinforced concrete beams decreases in a linear fashion as degree of corrosion increases. This decrease is due to a combination of loss of steel area and loss of bond strength between the reinforcing steel and concrete. The relationship that was derived for the ultimate capacity of the beams for this study with respect to mass loss ( $\Delta m$ ), by percentage, is given by:

$$P_{ult} = 151.45 - 1.4\Delta m \quad (6.1)$$

This result compared well to the results of other researchers studying beams of similar proportions. Further study is required in order to show that a similar relationship exists in beams of larger or full-scale proportions.

With respect to relative strength (RS) the relationship derived was:

$$RS = 1 - 0.01\Delta m \quad (6.2)$$

This result compared favourably with similar research. The steady linear decline was typical for similar studies. These equations represent observed trends within the specimens studied; further investigation is required to determine if these trends can be more widely applied. In addition, a wide range of variability was observed within this study, amongst the corroded specimens.

2. Stiffness is of critical importance from the standpoint of residual beam capacity. Very modest corrosion is required to reduce the steel reinforced beam stiffness to an unacceptable level. The stiffness of corroded reinforced concrete beams exhibited a sharp drop in stiffness at mass losses as low as 3.9%. This sharp drop was likely caused by microcracking within the concrete cover, and the subsequent loss of contribution of the bottom cover to the total inertia of the beam, even at relatively low degrees of corrosion. Loss of bond transfer to the reinforcing steel at midspan due to the corrosion was also a likely contributor to the stiffness loss. Even at the first visible cracking on the beam surface, microcracking had likely advanced enough that the bottom cover portion of the concrete was ineffective. Following the initial drop in stiffness, the stiffness continued to decrease gradually with an increasing degree of corrosion. This is likely due the continued loss of steel area within the reinforced concrete as well as worsening bond strength as degree of corrosion increased.

It was proposed that excessive deflection might serve as a good indicator of advancing corrosion among in-service reinforced concrete structure.

3. Crack width and chloride ion content were examined as indicators of degree of corrosion, in particular when compared to mass loss. Traditionally, mass loss has been the main indicator of degree of corrosion of corroded reinforced concrete beams. Overall, chloride ion content showed to be a very effective indicator of corrosion. In some cases, chloride

ion content might be a more effective indicator than mass loss due to its ability to pinpoint high localized concentrations of chloride ions and therefore the possibility of pitting in this area.

Crack width proved to be another possible indicator of degree of corrosion although less reliable than chloride ion content. In the absence of other alternatives crack width can be used to evaluate the condition of corroded structures.

## **5.2 Suggestions for Future Research**

This study has illuminated the need for research in several areas. Hence, it is suggested that a similar study of the influence of corrosion on flexural behaviour be undertaken using similar tests covered by this investigation to cover the following experimental parametric studies:

1. The effect of stirrup corrosion on beam shear behaviour should be examined. With a large number of studies already relating the effects of corrosion on bond strength and pullout strength there is a need to examine the combined effects of tensile steel corrosion, reinforcement corrosion and bond loss. Some researchers have remarked a change in failure mode towards a less ductile failure but this requires further research.
2. In the present study, accelerated corrosion of reinforcement was used by the impressed current, and then tests were carried out on the corroded specimens to study its effects on flexural strength. In existing structures, the corrosion of reinforcement takes place while

being under load. Hence, tests should be carried out to study the simultaneous effect of applied load and reinforcement corrosion on the flexural strength.

3. This study highlights the effects of tensile steel corrosion on flexural behaviour. In the future, the large pool of data on corroded concrete elements should be used to develop evaluation guidelines for the engineer, so that they might effectively evaluate in-service corroded concrete structures. One of the points that continued to surface was that corroded reinforced concrete members behaved a less predictable manner than non-corroded equivalents. This is due to the effects of localized corrosion such as pitting as well as a bond loss in the corroded areas. While a tested system is required to evaluate in-service corroded concrete elements, it must also take into account this added variability. Efforts in the research industry should be directed towards creating these evaluation guidelines that will become more and more necessary as our infrastructure continues to degrade before our eyes.



# REFERENCES

- Ahmed, S. F. U., Maalej, M., Paramasivam, P., & Mihashi, H. (2006). Assessment of corrosion-induced damage and its effect on the structural behaviour of RC beams containing supplementary cementitious materials. *Prog. Struct. Engng Mater.*, 8, 69-77.
- Akgul, F., & Frangopol, D. (2005). Lifetime performance analysis of existing reinforced concrete bridges. I: Theory. *Journal of Infrastructure Systems*, 11(2), 122-128.
- Aldulaimy, Z. (2007) "Optimization of the effect of corrosion on bond behaviour between steel and concrete". M.ASc Thesis, Ryerson University
- Almusallam, A. A., Al-Gahtani, A. S., Aziz, A. R., & Rasheeduzzafar. (1996). Effect of reinforcement corrosion on bond strength. *Construction and Building Materials*, 10(2), 123-129.
- Almusallam, A., Al-Gahtani, A., Aziz, A., Dakhil, F., & Rasheeduzzafar. (1996). Effect of reinforcement corrosion on flexural behavior of concrete slabs. *Journal of Materials in Civil Engineering*, 8(3), 123-127.
- Alonso, C., Andrade, C., Rodriguez, J., & Diez, J. (1998). Factors controlling cracking of concrete affected by reinforcement corrosion. *Materials and Structures*, 31(7), 435-441.

- Al-Saadoun, S. S., Rasheeduzzafar, , & Al-Gahtani, A. S. (1993). Corrosion of reinforcing steel in fly ash blended cement concrete. *Journal of Materials in Civil Engineering*, 5(3), 356-371.
- Al-Sulaimani, G. J., Kaleemullah, M., Basunbul, I. A., & Rasheeduzzafar. (1990). Influence of corrosion and cracking on bond behavior and strength of reinforced concrete members. *ACI Structural Journal (American Concrete Institute)*, 87(2), 220-231.
- Amleh, L., & Ghosh, A. K. (2006). Modeling the effect of corrosion on bond strength at the steel-concrete interface with finite-element analysis. *Canadian Journal of Civil Engineering*, 33(6), 673-682.
- Amleh, L., & Mirza, M. S. (2004). Corrosion response of a decommissioned deteriorated bridge deck. *Journal of Performance of Constructed Facilities*, 18(4), 185-194.
- Amleh, L., (2000), "Bond Deterioration of Reinforcing Steel in Concrete due to Corrosion," PhD Thesis, McGill University.
- Amleh, L., & Mirza, S. (1999). Corrosion influence on bond between steel and concrete. *ACI Structural Journal*, 96(3), 415.
- Amleh, L., Mirza, S., Rajamane, N. P., & Kalyanasundaram, P. (2000). Corrosion influence on bond between steel and concrete. *ACI Structural Journal*, 97(2), 353.
- Azad, A., Ahmad, S., & Azher, S. (2007). Residual strength of corrosion-damaged reinforced concrete beams. *ACI Materials Journal*, 104(1), 40.

- Bhargava, K., Ghosh, A. K., Mori, Y., & Ramanujam, S. (2007). Models for corrosion - induced bond strength degradation in reinforced concrete. *ACI Materials Journal*, 104(6), 594-603.
- Borgard, B., Warren, C., Somayagi, S., & Heidersbach, R. (1990). Mechanisms of corrosion of steel in concrete. In N. S. Berke, V. Chaker & D. Whitmore (Eds.), *Corrosion rates of steel in concrete* (STP 1065 ed., pp. 174-178). Philadelphia, Pa.: American Society for Testing and Materials.
- Cabrera, J. G. (1996). Deterioration of concrete due to reinforcement steel corrosion. *Cement & Concrete Composites*, 18(1), 47-59.
- Cabrera, J. G., & Ghaddoussi, P. (1992). The effect of reinforcement corrosion on the strength of the steel/concrete bond.
- Cairns, J., & Millard, S. Section 13.2: Reinforcement corrosion and its effects on residual strength of concrete structures. *Proc., 8th Int'l Conf. on Structure Faults and Repair*, Edinburgh, UK.
- Canadian Society for Civil Engineering. (2003). *The technology roadmap (online)*. Retrieved 06/27, 2008, from <http://www.ccpe.ca/e/files/trmreporteng.pdf>
- Coronelli, D. (2002). Corrosion cracking and bond strength modeling for corroded bars in reinforced concrete. *ACI Structural Journal*, 99(3), 267-276.
- Corrosion in reinforced concrete structures*(2005). Bohni H. (Ed.), Cambridge, England: Woodhead; Boca Raton :CRC Press.

- Corrosion of steel in concrete: Prevention, diagnosis, repair.* (2004). In Bertolini L. (Ed.), .  
Weinheim, Germany: Wiley-VCH.
- Dekoster, M., Buyle-Bodin, F., Maurel, O., & Delmas, Y. (2003). Modelling of the flexural behaviour of RC beams subjected to localised and uniform corrosion. *Engineering Structures*,
- Du, Y., Clark, L. A., & Chan, A. (2007). Impact of reinforcement corrosion on ductile behaviour of reinforced concrete beams. *ACI Structural Journal*, 104(3), 285.
- El Maaddawy, T., Soudki, K., & Topper, T. (2005). Long-term performance of corrosion-damaged reinforced concrete beams. *ACI Structural Journal*, 102(5), 649-656.
- El Maaddawy, T., & Topper, T. (2005). Long-term performance of corrosion-damaged reinforced concrete beams. *ACI Structural Journal*, 102(5), 649.
- ElMaaddawy, T., & Soudki, K. (2003). Effectiveness of impressed current technique to simulate corrosion of steel reinforcement in concrete. *Journal of Materials in Civil Engineering*, 15(1), 41-47.
- Hassan, A., (2003) "Bond Of Reinforcement In Concrete With Different Types Of Corroded Bars" MSc. Thesis, Ryerson University.
- Higgins, C., & Farrow III, William C. (2006). Tests of reinforced concrete beams with corrosion damaged stirrups. *ACI Structural Journal*, 103(1), 133.
- Huang, R., & Yang, C. C. (1997). Condition assessment of reinforced concrete beams relative to reinforcement corrosion. *Cement and Concrete Composites*, 19(2), 131-137.

- Isecke, B. (1982). Collapse of the berlin congress hall prestressed concrete roof. *Materials Performance*, 21(12), 36-39.
- Khedr, S., & Idriss, A. (1995). Resistance of silica-fume concrete to corrosion-related damage. *Journal of Materials in Civil Engineering*, 7(2), 102-107.
- Li, C. Q. (2003). Life cycle modeling of corrosion affected concrete structures - initiation. *Journal of Materials in Civil Engineering*, 15(6), 594-601.
- Li, C. Q., Lawanwisut, W., & Zheng, J. J. (2005). Time-dependent reliability method to assess the serviceability of corrosion-affected concrete structures. *Journal of Structural Engineering*, 131(11), 1674-1680.
- Li, C. (2004). Reliability based service life prediction of corrosion affected concrete structures. *Journal of Structural Engineering*, 130(10), 1570-1577.
- Liang, M., Lin, L., & Liang, C. (2002). Service life prediction of existing reinforced concrete bridges exposed to chloride environment. *Journal of Infrastructure Systems*, 8(3), 76-85.
- Mangat, P. S., & Elgarf, M. S. (1999). Flexural strength of beams with corroding reinforcement. *ACI Structural Journal*, 96(1), 149-158.
- Mindess, S. (2003). In Darwin D., Young J. F. (Eds.), *Concrete* (2nd ed. ed.). Upper Saddle River, NJ: Prentice Hall.
- Mirza, M. S. (2006). Durability and sustainability of infrastructure - A state-of-the-art report. *Canadian Journal of Civil Engineering*, 33(6), 639-649.

- Mirza, M. S., & Amleh, L. (2002). Sustainable infrastructure and civil engineering education. *Canadian Society for Civil Engineering - 30th Annual Conference: 2002 Challenges Ahead*, 2002 857-863.
- Neville, A. M. (1975). *Properties of concrete*. London: Pitman.
- Nygaard, P., & Geiker, M. (2005). A method for measuring the chloride threshold level required to initiate reinforcement corrosion in concrete. *Materials and Structures*, 38(4), 489-494.
- Oh, B. H., Jang, S. Y., & Shin, Y. S. (2003). Experimental investigation of the threshold chloride concentration for corrosion initiation in reinforced concrete structures. *Magazine of Concrete Research*, 55(2), 117-124.
- Oh, B., Lew, Y., & Choi, Y. (2007). Realistic assessment for safety and service life of reinforced concrete decks in girder bridges. *Journal of Bridge Engineering*, 12(4), 410-418.
- Prediction of concrete durability: Proceedings of STATS 21st anniversary conference(1997)*. In Glanville J., Neville A. M. and STATS (Firm) (Eds.), (1st ed. ed.). New York: E & FN Spon.
- Rodriguez, J., Ortega, L. M., & Garcia, A. (1994). Corrosion of reinforcing bars and service life of R/C structures: Corrosion and bond deterioration. *Proc. Int. Conf. on Concrete Across Borders*, 2 315-326.
- Rodriguez, J., Ortega, L., & Casal, J. (1997). Load carrying capacity of concrete structures with corroded reinforcement. *Construction and Building Materials*, 11(4), 239-248.

- Rostam, S. (2003). Reinforced concrete structures - shall concrete remain the dominating means of corrosion prevention? *Materials and Corrosion*, 54(6), 369-378.
- Spellman, D. L., & Stratfull, R. F. (1973). Concrete variables and corrosion testing. *Highway Research Record*, (423), 27.
- Stern, M., & Geary, A. L. (1957). Electrochemical polarization: I. A theoretical analysis of the shape of polarization curves. *Journal of the Electrochemical Society*, 104(1), 56-63.
- Stratfull, R. F. (1973). Half-Cell potentials and the corrosion of steel in concrete. *Highway Research Record*, (433), 12-35.
- Smith, R., (2007), " The effects of corrosion on the performance of reinforced concrete beams" M.ASc. Thesis, Ryerson University.
- Torres-Acosta, A., Fabel-Gallegos, M. J., Vazquez-Vega, D., Hernandez-jiminez, J. R., & Martínez-Madrid, M. (2004). Influence of corrosion on the structural stiffness of reinforced concrete beams. *Wilson Applied Science & Technology Abstracts*, 9(60), 862-872.
- Trejo, D., & Reinschmidt, K. (2007). Justifying materials selection for reinforced concrete structures. II: Economic analysis. *Journal of Bridge Engineering*, 12(1), 38-44.
- Tuutti, K. (1982). Corrosion of steel in concrete. *Swedish Cement and Concrete Institute*, , 17-21.
- Uomoto, T. (1984). Deterioration mechanism of concrete structures casued by corrosion of reinforcing bars. *Translations of the Japan Concrete Institute*, 6

- Val, D. (2007). Factors affecting life-cycle cost analysis of RC structures in chloride contaminated environments. *Journal of Infrastructure Systems*, 13(2), 135-143.
- Vu, K. T., & Stewart, M. (2005). Predicting the likelihood and extent of reinforced concrete corrosion-induced cracking. *Journal of Structural Engineering*, 131(11), 1681-1689.
- Yoon, D., Weiss, W. J., & Shah, S. (2000). Assessing damage in corroded reinforced concrete using acoustic emission. *Journal of Engineering Mechanics*, 126(3), 273-283.

④  
R-27-87

